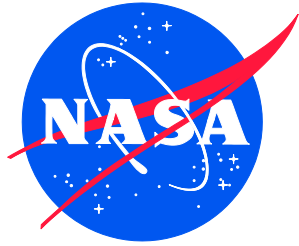


NASA/TM-2017-219666/Volume I  
NESC-RP-14-00965



# Independent Assessment of the Backshell Pressure Field for Mars Entry, Descent, and Landing Instrumentation 2 (MEDLI2)

*Jill L. Prince/NESC  
Langley Research Center, Hampton, Virginia*

*Mark Shoenenberger  
Langley Research Center, Hampton, Virginia*

## NASA STI Program . . . in Profile

Since its founding, NASA has been dedicated to the advancement of aeronautics and space science. The NASA scientific and technical information (STI) program plays a key part in helping NASA maintain this important role.

The NASA STI program operates under the auspices of the Agency Chief Information Officer. It collects, organizes, provides for archiving, and disseminates NASA's STI. The NASA STI program provides access to the NTRS Registered and its public interface, the NASA Technical Reports Server, thus providing one of the largest collections of aeronautical and space science STI in the world. Results are published in both non-NASA channels and by NASA in the NASA STI Report Series, which includes the following report types:

- **TECHNICAL PUBLICATION.** Reports of completed research or a major significant phase of research that present the results of NASA Programs and include extensive data or theoretical analysis. Includes compilations of significant scientific and technical data and information deemed to be of continuing reference value. NASA counter-part of peer-reviewed formal professional papers but has less stringent limitations on manuscript length and extent of graphic presentations.
- **TECHNICAL MEMORANDUM.** Scientific and technical findings that are preliminary or of specialized interest, e.g., quick release reports, working papers, and bibliographies that contain minimal annotation. Does not contain extensive analysis.
- **CONTRACTOR REPORT.** Scientific and technical findings by NASA-sponsored contractors and grantees.

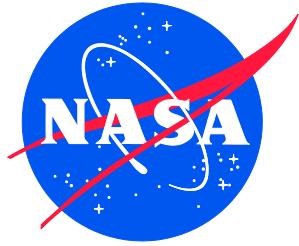
- **CONFERENCE PUBLICATION.** Collected papers from scientific and technical conferences, symposia, seminars, or other meetings sponsored or co-sponsored by NASA.
- **SPECIAL PUBLICATION.** Scientific, technical, or historical information from NASA programs, projects, and missions, often concerned with subjects having substantial public interest.
- **TECHNICAL TRANSLATION.** English-language translations of foreign scientific and technical material pertinent to NASA's mission.

Specialized services also include organizing and publishing research results, distributing specialized research announcements and feeds, providing information desk and personal search support, and enabling data exchange services.

For more information about the NASA STI program, see the following:

- Access the NASA STI program home page at <http://www.sti.nasa.gov>
- E-mail your question to [help@sti.nasa.gov](mailto:help@sti.nasa.gov)
- Phone the NASA STI Information Desk at 757-864-9658
- Write to:  
NASA STI Information Desk  
Mail Stop 148  
NASA Langley Research Center  
Hampton, VA 23681-2199

NASA/TM-2017-219666/Volume I  
NESC-RP-14-00965



# Independent Assessment of the Backshell Pressure Field for Mars Entry, Descent, and Landing Instrumentation 2 (MEDLI2)

*Jill L. Prince/NESC  
Langley Research Center, Hampton, Virginia*

*Mark Shoenenberger  
Langley Research Center, Hampton, Virginia*

National Aeronautics and  
Space Administration

Langley Research Center  
Hampton, Virginia 23681-2199

September 2017


## **Acknowledgments**

The NESC assessment team would like to acknowledge the efforts of Ms. Kathryn A. Kuykendoll of the NASA LaRC quality assurance (QA) laboratory (now retired). Her extensive experience and knowledge was critical to successfully measuring the mass properties of the ballistic range models with sufficient confidence that they would fly straight down the range to be recovered. Ms. Kuykendoll made key contributions in the design of the fixtures used for mass property measurements and the development of the measurement types and procedures to accurately show that the model centers of gravity (CGs) were within required tolerances. Ms. Kuykendoll's efforts were crucial to the successful completion of this assessment.

The use of trademarks or names of manufacturers in the report is for accurate reporting and does not constitute an official endorsement, either expressed or implied, of such products or manufacturers by the National Aeronautics and Space Administration.
---

Available from:


NASA STI Program / Mail Stop 148  
NASA Langley Research Center  
Hampton, VA 23681-2199  
Fax: 757-864-6500

	<b>NASA Engineering and Safety Center Technical Assessment Report</b>	Document #: <b>NESC-RP- 14-00965</b>	Version: <b>1.0</b>
Title:	<b>Independent Assessment of the Backshell Pressure Field for MEDLI2 (Mars 2020)</b>		Page #: 1 of 74

# **Independent Assessment of the Backshell Pressure Field for Mars Entry, Descent, and Landing Instrumentation 2 (MEDLI2)**

**Volume 1**

**March 9, 2017**


	<b>NASA Engineering and Safety Center Technical Assessment Report</b>	Document #: <b>NESC-RP-14-00965</b>	Version: <b>1.0</b>
Title: <b>Independent Assessment of the Backshell Pressure Field for MEDLI2</b>			Page #: 2 of 74

## Report Approval and Revision History

NOTE: This document was approved at the March 9, 2017, NRB. This document was submitted to the NESC Director on September 5, 2017, for configuration control.


Approved:	<i>Original Signature on File</i>	<i>9/7/17</i>
	NESC Director	Date

Version	Description of Revision	Office of Primary Responsibility	Effective Date
1.0	Initial Release	Jill L. Prince, Manager, NIO, LaRC	3/9/17

	<b>NASA Engineering and Safety Center Technical Assessment Report</b>	Document #: <b>NESC-RP- 14-00965</b>	Version: <b>1.0</b>
Title: <b>Independent Assessment of the Backshell Pressure Field for MEDLI2</b>			Page #: 3 of 74

## Table of Contents

<b>Technical Assessment Report .....</b>	<b>7</b>
<b>1.0 Notification and Authorization.....</b>	<b>7</b>
<b>2.0 Signature Page.....</b>	<b>8</b>
<b>3.0 Team List .....</b>	<b>9</b>
3.1 Acknowledgements.....	9
<b>4.0 Executive Summary .....</b>	<b>10</b>
<b>5.0 Assessment Plan .....</b>	<b>12</b>
<b>6.0 Problem Description .....</b>	<b>13</b>
<b>7.0 Data Analysis.....</b>	<b>15</b>
7.1 Test Facility and Methods.....	15
7.1.1 Transonic Experimental Facility.....	15
7.1.2 Ballistic Range Model Geometry.....	18
7.1.3 Model Design and Surface Pressure Instrumentation .....	18
7.1.4 Pressure Transducer Calibration.....	21
7.1.5 Mass Properties Measurements .....	25
7.1.6 Test Matrix.....	28
7.1.7 Data Recording .....	30
7.1.8 Data Reduction .....	31
7.2 Results .....	34
7.2.1 Data-recording Anomalies .....	34
7.2.2 Pressure Histories .....	36
7.3 Pretest CFD Summary .....	41
7.3.1 US3D .....	41
7.3.2 OVERFLOW .....	45
7.3.3 Pretest Dynamic CFD Analysis .....	48
7.4 Posttest Results using OVERFLOW .....	50
7.4.1 Posttest CFD Matrix .....	50
7.4.2 Forced Oscillation CFD Simulation Results.....	50
7.4.3 6-DOF CFD Simulation Results .....	55
7.5 Posttest Results using US3D.....	59
7.5.1 Posttest CFD Matrix .....	59
7.5.2 Comparison of US3D and OVERFLOW, Mach = 2.8, 20-degree Forced Oscillation .....	59
7.5.3 Effect of Atmosphere on the Backshell Pressure Profile .....	63
7.6 Comparison of Ballistic Range Data and CFD .....	65
<b>8.0 Findings, Observations, and NESC Recommendations.....</b>	<b>69</b>
8.1 Findings .....	69
8.2 Observations .....	70
8.3 NESC Recommendations .....	71

	<b>NASA Engineering and Safety Center</b> <b>Technical Assessment Report</b>	Document #: <b>NESC-RP-14-00965</b>	Version: <b>1.0</b>
Title: <b>Independent Assessment of the Backshell Pressure Field for MEDLI2</b>			Page #: 4 of 74

<b>9.0</b>	<b>Alternate Viewpoint.....</b>	<b>71</b>
<b>10.0</b>	<b>Other Deliverables .....</b>	<b>71</b>
<b>11.0</b>	<b>Lessons Learned.....</b>	<b>71</b>
<b>12.0</b>	<b>Recommendations for NASA Standards and Specifications.....</b>	<b>72</b>
<b>13.0</b>	<b>Definition of Terms.....</b>	<b>72</b>
<b>14.0</b>	<b>Acronym List.....</b>	<b>73</b>
<b>15.0</b>	<b>References.....</b>	<b>74</b>
<b>16.0</b>	<b>Appendices (separate volume) .....</b>	<b>74</b>

### List of Figures

Figure 7.1.1-1.	Exterior and Interior Views of USARL TEF.....	16
Figure 7.1.1-2.	USARL TEF Ballistic Range Layout.....	16
Figure 7.1.1-3.	Catcher Box Arrangement.....	17
Figure 7.1.2-1.	Mars 2020 Ballistic Range Model Geometry .....	18
Figure 7.1.3-1.	Ballistic Range Model Pressure Port Locations .....	19
Figure 7.1.3-2.	Model Assembly Components and Instrumentation.....	20
Figure 7.1.3-3.	Example of As-built Model (#2) .....	20
Figure 7.1.4-1.	Model-Installed Pressure Transducer Calibration Setup .....	22
Figure 7.1.4-2.	Model #2 Linear Model Fit through Calibration Points .....	23
Figure 7.1.4-3.	Model #2 Linear Model Fit through Calibration Points .....	24
Figure 7.1.5-1.	Model Installed in Longitudinal MOI Measurement Fixture at Space Electronics LLC.....	26
Figure 7.1.5-2.	Model Orientation Measurements in NASA LaRC QA Lab .....	27
Figure 7.1.6-1.	Loading Instrumented Model in 10-degree Sabot .....	30
Figure 7.1.7-1.	Setup for Onboard Data Recording Initiation and Download .....	31
Figure 7.1.8-1.	Shadowgraph Geometry for Model Position/Orientation Measurement .....	32
Figure 7.1.8-2.	Examples of Ballistic Range Shadowgraphs .....	33
Figure 7.1.8-3.	Examples of Ballistic Range Shadowgraphs (Shot 40021) .....	34
Figure 7.2.2-1.	Pressure History from Shot 40018.....	37
Figure 7.2.2-2.	Pressure History from Shot 40021.....	38
Figure 7.2.2-3.	Complete Pressure History and Detail from Shot 40023.....	40
Figure 7.3.1.3-1.	Mach Contours, 0-degree Angle of Attack.....	43
Figure 7.3.1.3-2.	Mach Contours, 20-degree Angle of Attack.....	43
Figure 7.3.1.3-3.	Nominal Mesh, 0-degree Angle of Attack.....	44
Figure 7.3.1.3-4.	Deformed Mesh, 20-degree Angle of Attack .....	44
Figure 7.3.2.3-1.	Mach Contours and Mesh, 0-degree Angle of Attack .....	47
Figure 7.3.2.3-2.	Mach Contours and Mesh, 20-degree Angle of Attack .....	47
Figure 7.3.3.1-1.	Pressure Measurement Locations from Pretest CFD.....	48






	<b>NASA Engineering and Safety Center Technical Assessment Report</b>	Document #: <b>NESC-RP- 14-00965</b>	Version: <b>1.0</b>
Title: <b>Independent Assessment of the Backshell Pressure Field for MEDLI2</b>			Page #: 5 of 74

Figure 7.3.3.1-2.	Computed Pressures on Second Backshell Conic for Free to Pitch Simulations having Initial Amplitude of 30 degrees and Mach 3 .....	49
Figure 7.3.3.1-3.	Computed Pressures on Second Backshell Conic for Free to Pitch Simulations having Initial Amplitude of 30 degrees and Mach 1.5 .....	49
Figure 7.4.2-1.	Unfiltered Pitching Moment Coefficient from Forced Oscillation Simulations.....	50
Figure 7.4.2-2.	Filtered Pitching Moment Coefficient from Forced Oscillation Simulations.....	51
Figure 7.4.2-3.	Comparison of Static Aerodynamics between Forced Oscillations and Unmoving CFD .....	51
Figure 7.4.2-4.	Comparison of Dynamic Aerodynamic Coefficients between Forced Oscillation CFD and 65-mm Ballistic Range Data .....	52
Figure 7.4.2-5.	Pressure Measurement Location for CFD Simulations .....	53
Figure 7.4.2-6.	Pressure Measurements from 20-degree Pitch Amplitude Simulation .....	54
Figure 7.4.2-7.	Pressure Measurements from 10-degree Pitch Amplitude Simulation .....	54
Figure 7.4.2-8.	Pressure Measurements from 2-degree Pitch Amplitude Simulation .....	55
Figure 7.4.2-9.	$\alpha$ and $\beta$ for 6-DOF Simulations .....	56
Figure 7.4.2-10.	Mach-number Variation during 6-DOF Simulations.....	56
Figure 7.4.2-11.	Comparison of Static Aerodynamics between Fixed, Forced Oscillation, and 6-DOF CFD Simulations .....	57
Figure 7.4.2-12.	Comparison of Dynamic Aerodynamic Coefficients between Forced Oscillation CFD, 6-DOF CFD, and 65-mm Ballistic Range Data .....	57
Figure 7.4.2-13.	Mach-number Variation in CFD versus Shot 40018 .....	58
Figure 7.4.2-14.	$\alpha_{Total}$ Growth in CFD versus Shot 40018 .....	59
Figure 7.5.2-1.	OVERFLOW and US3D Pressure Coefficient Contours along Pitch Plane, 20-degree Angle of Attack .....	60
Figure 7.5.2-2.	OVERFLOW Wake Pressure along Pitch Plane, Captured at Different Angles of Attack .....	61
Figure 7.5.2-3.	Comparison OVERFLOW and US3D Predictions of Wake Pressure Coefficient along Pitch Plane .....	62
Figure 7.5.2-4.	OVERFLOW/US3D Wake Pressure Coefficient Comparison, Stretched y-axis .....	63
Figure 7.5.3-1.	Comparison of Pressure Coefficient in Pitch Plane for Earth and Mars Atmospheres .....	64
Figure 7.5.3-2.	Zoomed View of Pressure Coefficient on Backshell for Earth and Mars Atmospheres .....	65
Figure 7.6-1.	Shot 40018, Comparison of Measured Pressure Coefficients with CFD Calculations .....	66
Figure 7.6-2.	Shot 40023, Comparison of Measured Pressure Coefficients with CFD Calculations .....	68

	<b>NASA Engineering and Safety Center Technical Assessment Report</b>	Document #: <b>NESC-RP- 14-00965</b>	Version: <b>1.0</b>
Title: <b>Independent Assessment of the Backshell Pressure Field for MEDLI2</b>			Page #: 6 of 74

### List of Tables

Table 7.1.5-1.	Mass Properties of Models for Each Data Shot.....	27
Table 7.1.6-1.	Ballistic Range Test Matrix .....	29
Table 7.1.6-2.	Ambient Conditions for Ballistic Range Shots.....	30
Table 7.3.3.1-1.	Pressure Probe Locations with Origin at Nose of Model .....	48
Table 7.4.2-1.	Pressure Probe Locations with Origin at Nose of Model .....	53

	<b>NASA Engineering and Safety Center Technical Assessment Report</b>	Document #: <b>NESC-RP- 14-00965</b>	Version: <b>1.0</b>
Title: <b>Independent Assessment of the Backshell Pressure Field for MEDLI2</b>			Page #: 7 of 74


## Technical Assessment Report

### 1.0 Notification and Authorization

The Mars Entry, Descent, and Landing Instrumentation 2 (MEDLI2) project requested that the NASA Engineering and Safety Center (NESC) support a ballistic range test to measure backshell pressures on scale models of the Mars 2020 entry capsule. The MEDLI2 project needed the test to provide important dynamic pressure data to help select a backshell pressure port, quantify drag coefficient reconstruction uncertainties, and design the data acquisition hardware.

Ms. Jill Prince, Manager of the NESC Integration Office (NIO) at the NASA Langley Research Center (LaRC), was selected to lead this assessment. Mr. Mark Schoenenberger was selected as the technical lead.

The key stakeholders for this assessment were Mr. Henry Wright, Project Manager for the MEDLI2 project, and the MEDLI2 project team.

	<b>NASA Engineering and Safety Center Technical Assessment Report</b>	Document #: <b>NESC-RP- 14-00965</b>	Version: <b>1.0</b>
Title: <b>Independent Assessment of the Backshell Pressure Field for MEDLI2</b>			Page #: 8 of 74

## 2.0 Signature Page

Submitted by:

*Team Signature Page on File – 9/11/17*

---

Ms. Jill L. Prince

Date


Significant Contributors:

---

Mr. Mark Schoenenberger

Date

Signatories declare the findings, observations, and NESC recommendations compiled in the report are factually based from data extracted from program/project documents, contractor reports, and open literature, and/or generated from independently conducted tests, analyses, and inspections.


	<b>NASA Engineering and Safety Center Technical Assessment Report</b>	Document #: <b>NESC-RP-14-00965</b>	Version: <b>1.0</b>
Title: <b>Independent Assessment of the Backshell Pressure Field for MEDLI2</b>			Page #: 9 of 74

### 3.0 Team List

Name	Discipline	Organization
<b>Core Team</b>		
Jill Prince	NESC Lead	LaRC
Mark Schoenenberger	Technical Lead	LaRC
Roy Savage	MTSO Program Analyst	LaRC
Helen Hwang	MEDLI2 Principal Investigator	ARC
Gordon Brown	USARL Representative	USARL
Wayne Hathaway	Data Analysis	Arrow Tech Associates
Chris Karlgaard	Data Analysis	LaRC/AMA
Alan Schwing	CFD Analysis	JSC
Scott Sealey	Pressure Calibration	LaRC
Eric Stern	CFD Analysis	ARC
John Van Norman	Aerodynamics	LaRC/AMA
Gregorio Villar	Mars 2020 Integration	JPL
Todd White	Aerothermodynamics	ARC
Leslie Yates	Data Analysis	ARC/Aerospace Computing, Inc.
<b>Administrative Support</b>		
Linda Burgess	Planning and Control Analyst	LaRC/AMA
Jonay Campbell	Technical Writer	LaRC/NGC
Diane Sarrizin	Project Coordinator	LaRC/AMA

### 3.1 Acknowledgements

The NESC assessment team would like to acknowledge the efforts of Ms. Kathryn A. Kuykendoll of the NASA LaRC quality assurance (QA) laboratory (now retired). Her extensive experience and knowledge was critical to successfully measuring the mass properties of the ballistic range models with sufficient confidence that they would fly straight down the range to be recovered. Ms. Kuykendoll made key contributions in the design of the fixtures used for mass property measurements and the development of the measurement types and procedures to accurately show that the model centers of gravity (CGs) were within required tolerances. Ms. Kuykendoll's efforts were crucial to the successful completion of this assessment.

	<b>NASA Engineering and Safety Center Technical Assessment Report</b>	Document #: <b>NESC-RP- 14-00965</b>	Version: <b>1.0</b>
Title: <b>Independent Assessment of the Backshell Pressure Field for MEDLI2</b>			Page #: 10 of 74


## 4.0 Executive Summary

As part of its science package, the Mars Entry, Descent, and Landing Instrumentation 2 (MEDLI2) project will be installing a single pressure transducer on the backshell of the Mars 2020 entry capsule. The transducer will record surface pressure to help determine the backshell contribution to the axial force coefficient of the capsule during entry at Mars. The MEDLI2 project requested assistance from the NASA Engineering and Safety Center (NESC) in obtaining experimental data to inform its selection of the location of the pressure port. It was proposed by the MEDLI2 project that a ballistic range test with onboard pressure instrumentation would provide data to confirm that flow is generally separated on the backshell and that there are no significant pressure variations that would warrant additional transducers to resolve the wake contribution to the axial force coefficient.


The NESC approved the assessment plan, and a ballistic range test was conducted in March and April 2016 in the Transonic Experimental Facility (TEF) at the Aberdeen Proving Grounds Transonic Range in Aberdeen, Maryland, to obtain backshell surface pressure measurements on 2-percent scale models of the Mars 2020 entry capsule. Ninety-millimeter (mm) diameter models were launched from a smooth-bore 120-mm powder charge gun at velocities near Mach 3.0 through quiescent air down the TEF range. Shadowgraph images were taken at 15 data stations along the range to determine the velocity and attitude histories of the models. An onboard data system recorded up to four surface pressures, which were downloaded after recovery at the end of the range. Stagnation pressure was measured to anchor the vehicle Mach number to attitude and position histories determined by fitting 6-degree-of-freedom (DOF) trajectories through the shadowgraph data points. The test measured pressure and trajectory data from several successful shots. Multiple backshell pressures were correlated with the vehicle attitude histories. These data show that to first order the wake pressure is uniform and varies primarily with total angle of attack.

Computational fluid dynamics (CFD) analyses, using the unsteady codes US3D and OVERFLOW, were run to help interpret the ballistic range pressure data and estimate the Earth-based test validity at Mars flight conditions. Both codes were generally in good agreement with ballistic range data, showing separated flow of near-constant pressure over most of the backshell. US3D predictions showed similar separated wake behavior at Mars flight conditions.

Based on the results of the ballistic range test and supported by CFD results, the NESC recommends the pressure port be located on the leeward side of the backshell in the middle of the second cone section. This location should be at the same radius from the vehicle axis of symmetry as the baseline location selected by the MEDLI2 project, but 180 degrees to the opposite side of the vehicle. Data show that either location would measure separated flow, which varies nearly uniformly over the backshell with angle of attack. However, at the large angles of attack that will be experienced by the entry capsule at its nominal trim attitude, there appears to be flow attachment on the first cone upstream of the original port location. The surface pressure on the leeward side of the backshell should be more uniform at all angles of

	<b>NASA Engineering and Safety Center Technical Assessment Report</b>	Document #: <b>NESC-RP- 14-00965</b>	Version: <b>1.0</b>
Title: <b>Independent Assessment of the Backshell Pressure Field for MEDLI2</b>			Page #: 11 of 74

attack, and the risk of ambiguous or anomalous pressure readings due to local flow features is reduced.

	<b>NASA Engineering and Safety Center Technical Assessment Report</b>	Document #: <b>NESC-RP-14-00965</b>	Version: <b>1.0</b>
Title: <b>Independent Assessment of the Backshell Pressure Field for MEDLI2</b>			Page #: 12 of 74

## 5.0 Assessment Plan


The test conducted for this assessment was executed almost exactly as proposed. The test campaign, including model design, calibration, sabot development and verification testing, and the final instrumented ballistic range test execution, is essentially the same as proposed in the assessment plan. There are two notable deviations from the plan:

1. At the assessment plan acceptance review, the NESC Review Board (NRB) added a requirement that an early career engineer be assigned to support the assessment. The NESC assessment team added Alan Schwing from NASA Johnson Space Center (JSC) and Eric Stern from NASA Ames Research Center (ARC) to perform CFD analysis in support of the ballistic range test. The CFD results proved useful in interpreting the ballistic range results and providing estimates of the validity of the Earth-based data at Mars flight conditions.
2. The other notable deviation from the assessment plan was the slip in schedule. The original NRB acceptance review of the final assessment report was scheduled for September 2015. There were three reasons for the schedule slip:
  - a. A number of technical problems were encountered that resulted in additional development testing and verification measurements of the instrumented ballistic range models. The personnel of the United States Army Research Laboratory (USARL) added testing and development work required to complete a successful test campaign.
    - i. The instrumented models had to be recovered to download pressure data recorded to non-volatile memory onboard. The first test shots of uninstrumented models swerved significantly and saw large oscillation amplitudes due to sabot separation at launch.<sup>1</sup> The sabots required a redesign and additional certification testing.
    - ii. After the sabot redesign, preliminary testing continued to show model swerve problems. It was found that small asymmetries (i.e., outer mold line (OML) and CG offset) could result in swerving flight down the range such that models would miss the model catcher system. Model recovery was necessary for data download. QA measurements of the instrumented model as-built geometries were performed at the NASA LaRC QA lab. Mass properties measurements of the instrumented models were performed by a commercial vendor, Space Electronics LLC in Berlin, Connecticut.
    - iii. Additional development testing of uninstrumented models was performed to determine the best configuration and location of the catcher boxes. The initial

---

<sup>1</sup> Sabots hold the models in the launch gun and seal against the gases that accelerate the model to the desired velocity.




	<b>NASA Engineering and Safety Center Technical Assessment Report</b>	Document #: <b>NESC-RP- 14-00965</b>	Version: <b>1.0</b>
Title: <b>Independent Assessment of the Backshell Pressure Field for MEDLI2</b>			Page #: 13 of 74

launch velocity, downrange catcher position, and model fabrication quality were determined through a combination of test and analysis.

- b. The instrumented models were shot in March and April 2016. A problem was encountered with the onboard data recording system. In some instances, the onboard data recorder stopped during flight. Other models did not power-up after recovery so that data could be downloaded. Key data from one model were retrieved by machining away material to gain direct physical access to the onboard memory chip. The data recorded during this one critical shot were downloaded and delivered to NASA LaRC in August 2016, which was approximately 4 months after the test was conducted.
- c. The CFD analysis added by the NRB resulted in a schedule slip. Preliminary ballistic range results were required to provide conditions for the posttest CFD analysis; therefore, key CFD solutions could not be started until after the test program and preliminary data reduction was complete. Unsteady CFD can be computationally expensive. Final results were completed in December 2016.

## 6.0 Problem Description

The Mars 2020 mission will fly a blunt entry capsule nearly identical to the Mars Science Laboratory (MSL) entry vehicle [ref. 1]. The vehicle will deliver an MSL-class rover to the surface of Mars in early 2021 to search for rock samples that include signs of Mars' watery past and perhaps signs of ancient life. The MSL capsule flew the MEDLI experiment on the entry capsule's aeroshell. The MEDLI experiment consisted of aeroheating measurements and surface pressure measurements. The surface pressure measurement experiment was called the Mars Entry Air Data System experiment (MEADS). MEADS consisted of seven pressure transducers located at the stagnation point and across the capsule forebody to measure stagnation pressure and pressures sensitive to angle of attack and sideslip variation. These pressure measurements were used to reconstruct the dynamic pressure and the wind-relative attitude of the vehicle as it decelerated through the hypersonic and high-supersonic flight regimes. The experiment was successful and helped reconstruct a complete description of the flight trajectory and aerodynamic performance at dynamic pressures above 850 Pascal (Pa). The full-scale range of the pressure transducers was 34473.8 Pa (5.0 pounds per square inch (psi)), which was slightly greater than the peak stagnation pressure experienced during entry. As the capsule decelerated, dynamic pressure dropped significantly. By approximately Mach 3.1, the dynamic pressure had dropped to a level where the MEADS system could not meet the desired attitude and dynamic pressure measurement accuracies. The MEADS measurements were used with the onboard inertial measurement unit (IMU) to reconstruct the static aerodynamic coefficients. Results indicated that the preflight predictions of axial force coefficient ( $C_A$ ) and pitching moment ( $C_m$ ) were in close agreement with preflight predictions. However, as the capsule slowed to dynamic pressures below the minimum design condition (i.e.,  $q_\infty = 850$  Pa), the reconstructed  $C_A$  departed


	<b>NASA Engineering and Safety Center Technical Assessment Report</b>	Document #: <b>NESC-RP-14-00965</b>	Version: <b>1.0</b>
Title: <b>Independent Assessment of the Backshell Pressure Field for MEDLI2</b>			Page #: 14 of 74

from predictions. At the point of supersonic parachute deployment (near Mach 2.0), the reconstructed  $C_A$  was 10 percent higher than preflight predictions. This discrepancy is equal to the +3 standard-deviation dispersion level of  $C_A$  in the MSL aerodynamic database used in preflight Monte Carlo simulations. However, the large  $C_A$  discrepancies were measured when the vehicle was flying at dynamic pressures below the design operational envelope of the MEDLI pressure instrumentation. The uncertainties on the reconstructed  $C_A$  history were large in this supersonic region; the accuracy of the MEDLI pressure instrumentation was not sufficient to definitively confirm that supersonic  $C_A$  was significantly higher than preflight predictions.

Entry capsules like MSL and Mars 2020 have high ballistic coefficients with terminal velocities near the supersonic parachute deploy conditions. Therefore, the capsules spend a significant portion of the trajectory decelerating through low supersonic conditions before reaching safe conditions for parachute deployment (i.e., Mach 2.3 or below). Therefore, errors in predicting supersonic  $C_A$  can result in large errors in downrange landing accuracy.

The Mars 2020 capsule will fly the MEDLI2 experiment on its aeroshell. One of MEDLI2's objectives is to measure the  $C_A$  during low supersonic flight to better improve landing ellipse predictions of future missions. The MEDLI2 instrumentation will be similar to that of MEDLI, with some key changes. Six of the seven forebody pressure transducers have a reduced full-scale range of 6894.8 Pa (1.0 psi) to better resolve dynamic pressure and other flight parameters at supersonic speeds. At low supersonic conditions, the pressure on the capsule backshell is a significant contributor to  $C_A$ . Therefore, MEDLI2 will include a backshell pressure measurement to help interpret the forebody pressures, reconcile them with the onboard IMU, and determine the partial contributions of forebody and backshell to the total  $C_A$ . This data set will be used to reconstruct  $C_A$  to an accuracy of 2 percent at supersonic speeds down to parachute deploy conditions. The reconstructed trajectory and vehicle performance will validate preflight predictions and enable better predictive capabilities for future flights.

Due to mechanical design and project budgetary constraints, there will be only one backshell pressure transducer on Mars 2020. It is imperative that the backshell transducer is located where the pressure measurements can be interpreted clearly. In other words, the MEDLI2 project wants to ensure that the single backshell transducer measures a pressure that is representative of the separated wake region that extends over a majority of the backshell. There have been surface pressure experiments conducted by the Viking and MSL Programs; however, sting effects alter the wake pressure environment significantly. CFD codes can have problems predicting wake pressures; therefore, the MEDLI2 project solicited help from the NESC to conduct a free-flight ballistic range test with onboard pressure transducers. The results of this test are reported here. The test recorded backshell and stagnation pressures at various angles of attack as scale models of the Mars 2020 vehicle decelerated from Mach 3.0 to below approximately Mach 1.75. The pressure histories were anchored to shadowgraph measurements recorded at 15 stations along the test range. The variation of pressure with angle of attack and Mach number was determined explicitly for several candidate port locations. The test program encountered a number of

	<b>NASA Engineering and Safety Center Technical Assessment Report</b>	Document #: <b>NESC-RP- 14-00965</b>	Version: <b>1.0</b>
Title: <b>Independent Assessment of the Backshell Pressure Field for MEDLI2</b>			Page #: 15 of 74

complications but, ultimately, successfully recorded data and helped determine the MEDLI2 backshell pressure port location.

## 7.0 Data Analysis


### 7.1 Test Facility and Methods

The test development was accomplished through a partnership between NASA LaRC and the USARL at the Aberdeen Proving Grounds, Maryland. Sponsored by the NESC in support of the MEDLI2 project, NASA served as principle investigator. The USARL led the development of the ballistic range models, including instrumentation and test procedures, then conducted the tests at the TEF on the USARL Transonic Range. Onboard data were downloaded upon recovery of the instrumented models, and data were correlated with velocity and attitude histories determined by fitting 6-DOF trajectories through position/orientation data measured from orthogonal shadowgraphs taken at 15 stations along the TEF. The trajectory reconstructions were performed by Aerospace Computing, Inc.

#### 7.1.1 Transonic Experimental Facility

The TEF is a 200-meter (m) indoor range operated by the USARL. The range has five instrumented pits, each populated with five orthogonal shadowgraph stations. Models are fired from powder-charge artillery guns mounted approximately 32 m uprange of the indoor facility. For this test program, a 120-mm smooth-bore gun was used. The models were launched within four-petal sabots (see Figure 7.1.6-1). The sabots hold the models at the desired initial angle of attack and seal the projectile so the launch gases accelerate the model effectively. As the projectile package exits the gun, dynamic pressure causes the sabot petals to separate from the projectile, which proceeds into the range through a small aperture ( $\sim 0.5 \text{ m} \times 0.5 \text{ m}$ ). The petals separate and deviate from the projectile flight path, impacting on a stripper plate outside the range. Within the range, cameras capture orthogonal shadowgraph images of the model at up to 25 data stations. The exterior of the TEF, as well as the shadowgraph stations and pit cameras inside the range, are shown in Figure 7.1.1-1.

The shadowgraphs are digitized, and the model position and orientation are measured as a function of time relative to a common coordinate frame within the range. Details of how the images are captured and processed to determine the model position and orientation are provided in the following sections. Six-DOF trajectories are fit through these data points to calculate a reconstruction of the capsule position, velocity, and attitude down the range. As shown in Section 7.2.2, the trajectory data could be extrapolated upstream to the gun barrel exit to provide velocity and attitude information before entry into the range. For these tests, it was decided to determine the roll angle of the models relative to the range coordinate frame. Roll attitude is required to determine angle of attack and sideslip histories relative to a coordinate frame defined on the models. Determining the attitude history for each shot with roll information allows the surface pressure measurements to be located relative to the defined pitch and yaw planes. To

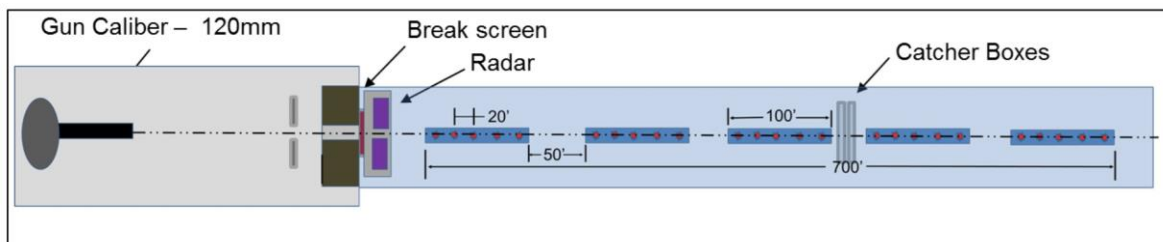
	<b>NASA Engineering and Safety Center Technical Assessment Report</b>	Document #: <b>NESC-RP-14-00965</b>	Version: <b>1.0</b>
Title: <b>Independent Assessment of the Backshell Pressure Field for MEDLI2</b>			Page #: 16 of 74

determine roll, each model had a roll pin that protruded from the aft-most surface. The pin was offset from the model axis of symmetry. The offset allowed the roll angle to be determined from the orthogonal shadowgraphs.



**Figure 7.1.1-1. Exterior and Interior Views of USARL TEF (interior view (looking uprange) shows camera stations and reflective screens)**


The layout and arrangement of the launcher gun, aperture, and shadowgraph pits in the TEF range are described in Figure 7.1.1-2. The onboard instrumentation was recorded to non-volatile memory located on a circuit board within each model. To retrieve data, the models must be captured intact. An extensive test program was conducted prior to the instrumented test series to determine the methodology that best enabled the safe capture of each model. It was determined that the models had to be fabricated symmetrically with the CG close to the spin axis of the vehicle OML. Testing showed that variability in the initial flight path exiting the gun (i.e., due primarily to whipping or kicking of the gun barrel and aerodynamic jump due to sabot separation) resulted in significant deviations from the initial bore-sited target points. An outdoor test program was conducted to determine the catcher location, size, and layout.



**Figure 7.1.1-2. USARL TEF Ballistic Range Layout**

A modular system of catcher boxes was developed for this test. The catchers were fabricated from plywood boxes and filled with sheets of Homasote® fiberboard or bundles of corrugated




	<b>NASA Engineering and Safety Center Technical Assessment Report</b>	Document #: <b>NESC-RP- 14-00965</b>	Version: <b>1.0</b>
Title: <b>Independent Assessment of the Backshell Pressure Field for MEDLI2</b>			Page #: 17 of 74

cardboard (see Figure 7.1.1-3). The boxes were built on site and designed so that they could be stacked and rearranged quickly with facility assets (i.e., two fork lifts). Repeated shots into the same box could damage the catchers, making the stack unstable and reducing their stopping power if a subsequent model entered an area where previous shots had penetrated. This modular system allowed expended catcher boxes to be replaced easily so testing could resume quickly.



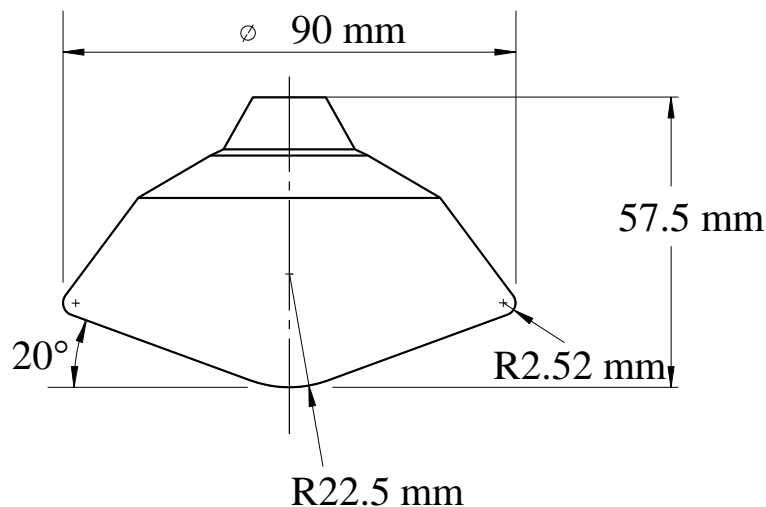
**Figure 7.1.1-3. Catcher Box Arrangement (dark circles are holes from prior shot penetrations)**

Measurements of the model OML and mass properties taken before the test program provided data for estimating the expected impact zone (due to model asymmetry) as a function of downrange position. Equations were developed to estimate the swerve due to an offset CG or asymmetric OML. This model was used to define tolerances for CG position. Those equations and their application in defining CG tolerances are presented in Appendix B. The mass properties measurement process is described in the Section 7.1.5. In addition to model measurements, the scatter pattern measured from a test series of uninstrumented models fired at an outside range, and the limitations on how the catcher boxes could be stacked within the range, established that the catcher system should be located between pits 3 and 4 (the position of the catcher box is shown in Figure 7.1.1-2), approximately 165 m from the gun barrel exit. This extensive preflight measurement and test program resulted in a successful instrumented test program. Each instrumented model was recovered from the catcher boxes.

	<b>NASA Engineering and Safety Center Technical Assessment Report</b>	Document #: <b>NESC-RP-14-00965</b>	Version: <b>1.0</b>
Title: <b>Independent Assessment of the Backshell Pressure Field for MEDLI2</b>			Page #: 18 of 74

### 7.1.2 Ballistic Range Model Geometry

The ballistic range models were 2-percent scale models of the 4.5-m diameter Mars 2020 entry capsule. The Mars 2020 aeroshell is a near “build-to-print” copy of the MSL entry vehicle [ref. 1] that successfully flew through the atmosphere in 2012 to deliver the *Curiosity* rover to the Martian surface. Key dimensions of the 90-mm-diameter ballistic range model are shown in Figure 7.1.2-1. The mass of each model was approximately 1.37 kilograms (kg).




**Figure 7.1.2-1. Mars 2020 Ballistic Range Model Geometry**

### 7.1.3 Model Design and Surface Pressure Instrumentation

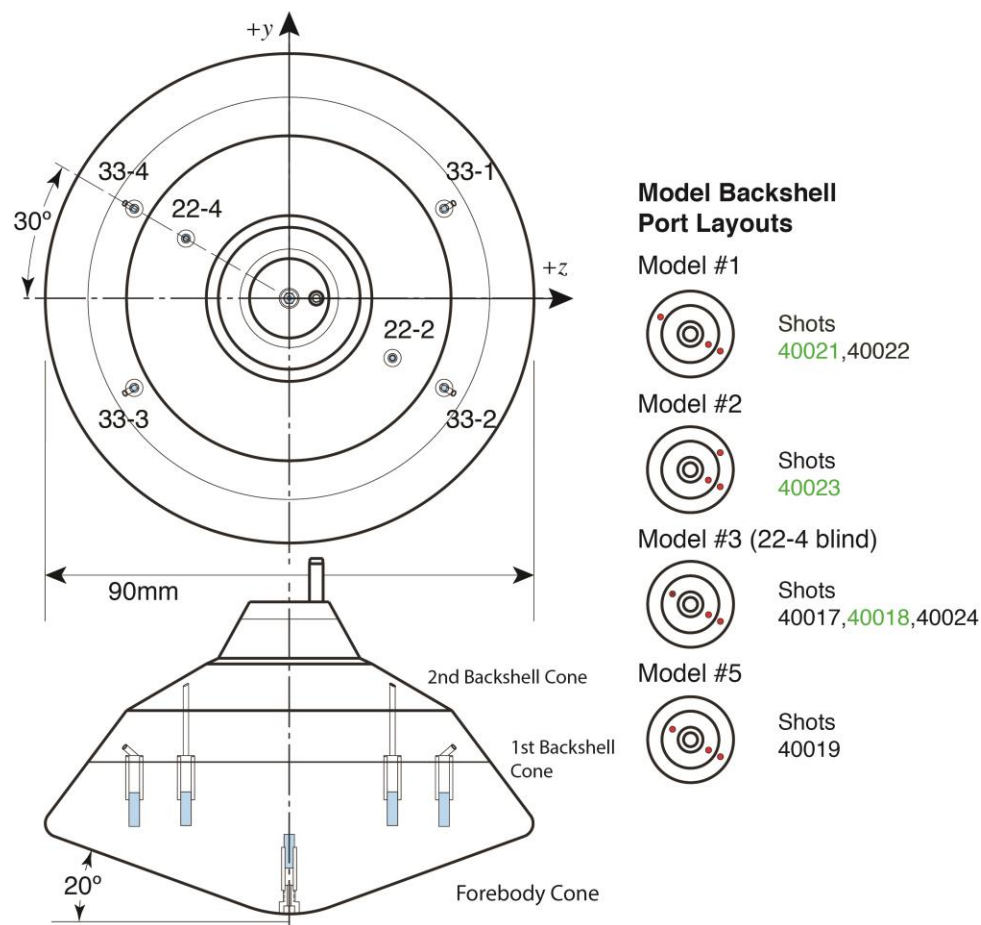
Each model was machined with a stagnation port on the nose and six ports on the backshell. The available port locations are shown in Figure 7.1.3-1 with diagrams showing the populated port locations for each model built for the test. The port nomenclature denotes first the radial distance from the model centerline in mm (i.e., 22 or 33 mm) and then a clock-angle index number (i.e., 1 through 4). All pressures were measured with Kulite® XCEL-072 transducers. The forebody transducer had a full-scale range of 3.45 MPa (500 psi), and the backshell transducers had a full-scale range of 172.4 kPa (25 psi). These off-the-shelf transducers provided the accuracy to resolve the stagnation and wake pressures across the expected Mach range the models would see during free flight. All transducers could survive pressures to 6.9 MPa (1000 psi), which is greater than the pressures experienced during launch within the gun barrel.

Five models were fabricated for this test program. Model #4 had a firmware problem that was discovered after the onboard electronics were potted, so only four models were used during the

	<b>NASA Engineering and Safety Center Technical Assessment Report</b>	Document #: <b>NESC-RP- 14-00965</b>	Version: <b>1.0</b>
Title: <b>Independent Assessment of the Backshell Pressure Field for MEDLI2</b>			Page #: 19 of 74


test program. The onboard data recording system could record up to four pressure channels. Therefore, each model was instrumented with four pressure transducers.

Each model measured stagnation pressure, and different combinations of three port locations on the backshell were selected for the four instrumented models (see Figure 7.1.3-1). The different port arrangements were selected to measure, as the capsule oscillated during flight, pressure variations on opposite sides of the model, adjacent backshell cone surfaces, and variations with clock angle.

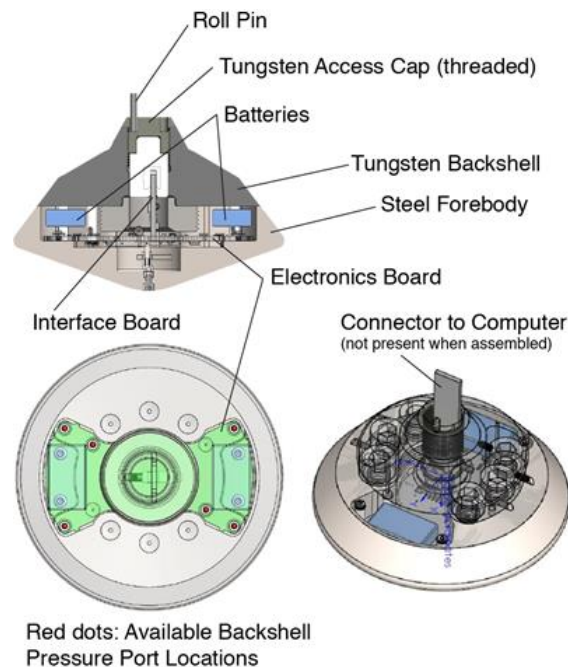


**Figure 7.1.3-1. Ballistic Range Model Pressure Port Locations**  
(green numbers indicate shots with successful data measurements)

Cutaway views showing the model assembly and internal instrumentation are shown in Figure 7.1.3-2. The completed Model #2 is shown in Figure 7.1.3-3. The body of the model was made in two main pieces. The forebody was made of steel, and the aft body and threaded data access cap were made of tungsten. The model sections of different densities were selected to locate the CG at the proper axial location, matching the MSL and Mars 2020 reentry capsules.

	<b>NASA Engineering and Safety Center Technical Assessment Report</b>	Document #: <b>NESC-RP-14-00965</b>	Version: <b>1.0</b>
Title: <b>Independent Assessment of the Backshell Pressure Field for MEDLI2</b>			Page #: 20 of 74

The two pieces were held together with six socket head cap screws. Two kidney-shaped caps, visible in Figure 7.1.3-3(a), cover the screws. The caps were held in place with set screws. Figure 7.1.3-3(b) shows the forebody of the model.



**Figure 7.1.3-2. Model Assembly Components and Instrumentation**




**a. Screw covers on model**

**b. Model forebody**

**Figure 7.1.3-3. Example of As-built Model (#2)**



	<b>NASA Engineering and Safety Center Technical Assessment Report</b>	Document #: <b>NESC-RP-14-00965</b>	Version: <b>1.0</b>
Title: <b>Independent Assessment of the Backshell Pressure Field for MEDLI2</b>			Page #: 21 of 74


The pressure transducers were mounted to the instrumentation circuit board (noted in Figure 7.1.3-2). The electronics board contained data-recording electronics and the solid-state memory with development instrumentation (magnetometers and accelerometers) added by the USARL to test the response of new components at flight-like conditions. The additional instrumentation was not intended to be used by the MEDLI2 project and was added to the models at no cost to NASA.

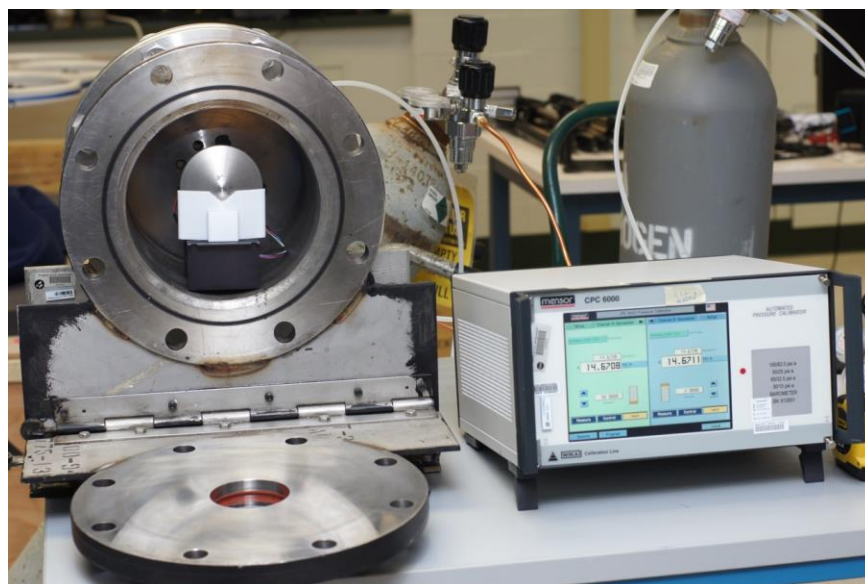
Prior use of similar instrumentation for previous blunt-body USARL testing showed that the ballistic range shadowgraphs provided significantly more accurate attitude information than onboard sensors. The NESC assessment team assessed the raw data from the development instrumentation and the data quality was again judged to be poor compared with the shadowgraph data. No development instrumentation data were used in the data reduction process for this task.

The nose pressure port was customized in an attempt to create a mechanism for clearing debris from the pneumatic path from the model surface to the transducer. It was expected that the port would be fouled by catcher material (e.g., plywood, Homasote®, and cardboard) upon impact as it struck the catcher box at the end of the range. A 4-40 cap screw, with a 1.02-mm (0.040-inch) diameter hole drilled down its axis, was threaded into the nose. The screw sealed in place with an O-ring between the screw and a cavity just upstream of the transducer face. The screw could be removed to clear debris. The local geometric complexity at the model surface, where the cap screw threads into a counter-bore, is a deviation from the MSL/Mars 2020 geometry. As this is in the stagnation region, it was assumed that surface irregularities would not significantly affect the vehicle aerodynamics or the pressure measurements. For each model tested, upon impact the catcher material passed through the cap screw hole, damaging the transducers. No forebody port survived to record valid data for a second flight.

#### **7.1.4 Pressure Transducer Calibration**

As part of model construction, the Kulite® pressure transducers were installed, connected to the electronics board, and potted. Model assembly was completed at the USARL with pressure calibration at NASA LaRC. Each model was calibrated individually in a pressure chamber. The calibration was conducted by the Aeronautics Systems Engineering Branch. USARL personnel brought the equipment required to communicate to the models (i.e., to command data recording to commence and retrieve the data) during transducer calibration. The models were connected to the USARL data system via a dedicated cable that passed through the pressure chamber. The pressure in the chamber was controlled by a Mensor® CPC6000. A nitrogen bottle supplied gas to the chamber, and the controller regulated the pressure to a set of calibration points to 1.0 MPa (150 psi). The maximum pressure was determined by the rating of the available pressure vessel. The pressure was automatically regulated to the prescribed data points. Each point was set at the target pressure to an accuracy of  $\pm 0.34$  Pa (0.00005 psi). The calibration setup is shown in Figure 7.1.4-1.

	<b>NASA Engineering and Safety Center Technical Assessment Report</b>	Document #: <b>NESC-RP- 14-00965</b>	Version: <b>1.0</b>
Title: <b>Independent Assessment of the Backshell Pressure Field for MEDLI2</b>			Page #: 22 of 74



***Figure 7.1.4-1. Model-Installed Pressure Transducer Calibration Setup (pressure chamber cover is removed to show model)***

Once the Mensor<sup>®</sup> controller settled at a prescribed data point, the USARL engineer commanded the ballistic range model to record 1 second (s) of data. The raw bits recorded from each transducer were averaged and used to determine the coefficients of a linear model. The full-scale range of the backshell transducers was 172.4 KPa (25 psi), so they saturated as the chamber pressure exceeded that range. The transducers saw much higher pressures within the gun barrel when shot down the range. This overpressure was done to provide calibration points for the forebody transducer and to assess whether the backshell transducers saw any hysteresis when overpressurized. The data indicated no significant hysteresis in any of the transducers. The pressure calibration points (psi) were as follows (in sequence):


Pressure calibration points (kPa):

3.446, 6.895, 13.790, 27.579, 41.369, 55.158, 68.948, 82.737, 103.421,  
172.369, 344.738, 517.107, 689.476, 861.845, 1034.214, 861.845, 689.476,  
517.107, 344.738, 172. 369, 103.421, 68.948, 41.369, 13.790, 6.895,  
Ambient

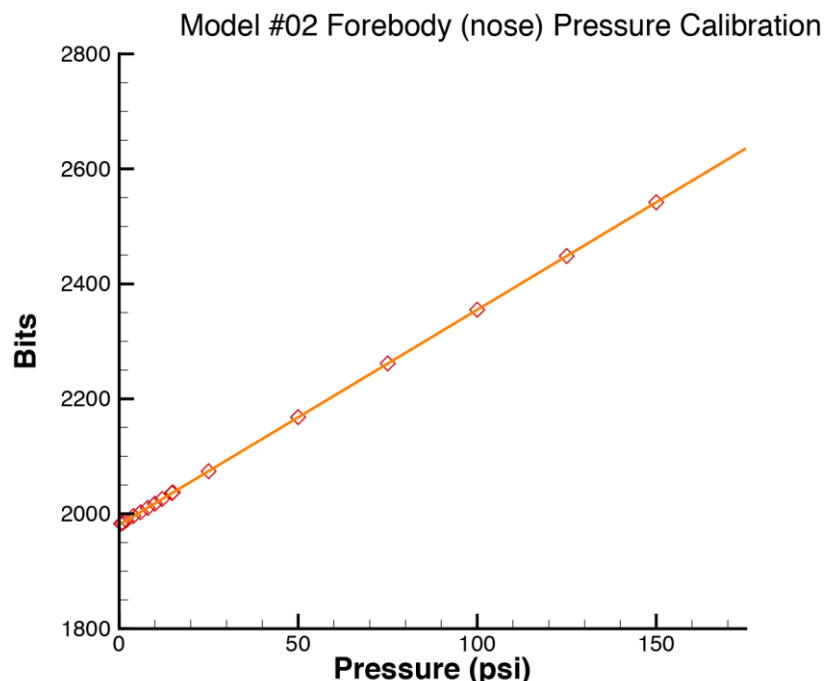
Pressure calibration points (psi):

0.4998, 1.0, 2.0, 4.0, 6.0, 8.0, 10.0, 12.0, 15.0, 25.0, 50.0, 75.0, 100.0, 125.0,  
150.0, 125.0, 100.0, 75.0, 50.0, 25.0, 15.0, 10.0, 6.0, 2.0, 1.0, Ambient


Examples of the linear fits through the calibration data are presented in Figures 7.1.4-2 and 7.1.4-3. Data from Model #2 forebody (nose) transducer data are plotted in Figure 7.1.4-2, and the backshell transducer data are plotted in Figure 7.1.4-3. The curves for the three backshell

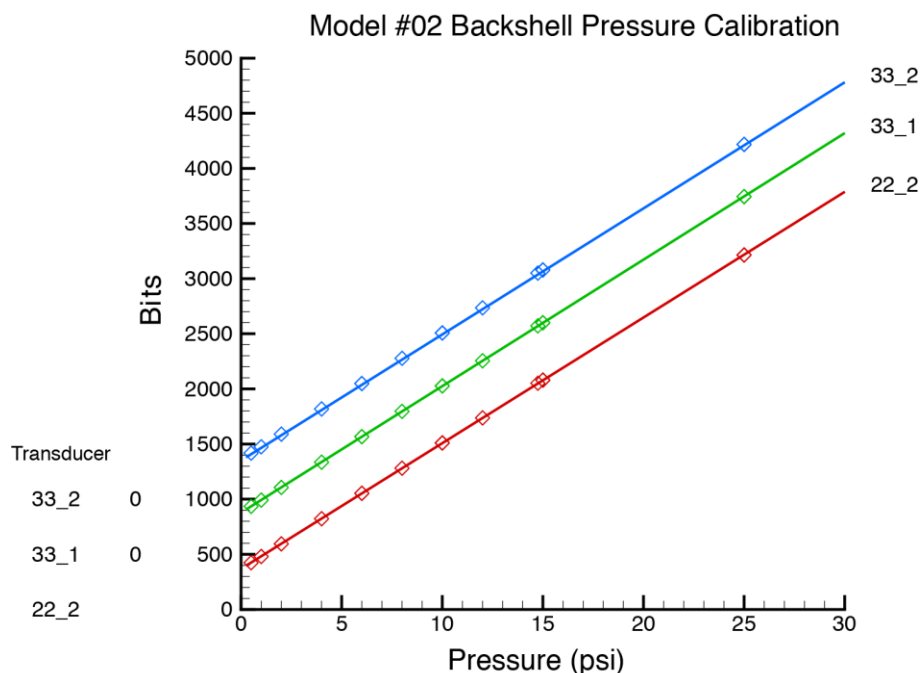
	<b>NASA Engineering and Safety Center Technical Assessment Report</b>	Document #: <b>NESC-RP-14-00965</b>	Version: <b>1.0</b>
Title: <b>Independent Assessment of the Backshell Pressure Field for MEDLI2</b>			Page #: 23 of 74

transducers are offset by 500-bit increments so the curves and data points do not overlap. The residual errors from these calibrations make negligible contributions to reconstructed parameters compared with other sources of error (e.g., model attitude and position measurements from shadowgraphs and transducer error sources specified by the vendor, such as temperature sensitivity). The vendor product specifications for the pressure transducers indicate that sensitivity to temperature should be less than 1 percent of full scale (quoted  $\pm 1$  percent/100 degrees Fahrenheit for the zero offset and sensitivity). Measurements of the ambient pressure in the gun barrel before launch provided a check that the transducers were operating nominally and provided some information about the health of the transducers after recovery from a prior shot. There are two instances where a model was shot in succession and pressure transducers survived to at least record ambient pressure while sitting in the gun barrel. Model #3 was fired twice (Shots 40017 and 40018) on March 3 and April 4, 2016, and pressure transducer 33-2 recorded valid data from both shots. The ambient pressure in the range was recorded for each shot, which was used as the free-stream pressure for data reduction. The ambient pressure measured by 33-2 prior to flight read 101.66 KPa (14.745), 1.3 percent lower than the range pressure (i.e., 102.98 KPa (14.936 psi)). Transducer 33-2 read 0.2 percent higher than the range pressure for Shot 40018 (i.e., 33-2: 101.43 KPa (14.711 psi); range: 101.22 KPa (14.681 psi)).



**Figure 7.1.4-2. Model #2 Linear Model Fit through Calibration Points (forebody transducer)**


	<b>NASA Engineering and Safety Center</b> <b>Technical Assessment Report</b>	Document #: <b>NESC-RP-14-00965</b>	Version: <b>1.0</b>
Title: <b>Independent Assessment of the Backshell Pressure Field for MEDLI2</b>			Page #: 24 of 74



**Figure 7.1.4-3. Model #2 Linear Model Fit through Calibration Points (backshell transducers)**

Model #1 was also fired twice in succession (i.e., Shots 40021 and 40022) on April 5 and 6, 2016. Ports 22-2 and 33-2 both survived Shot 40021 to record pressure while sitting in the barrel before Shot 40022, but both failed during their second launch. The range pressure recorded for Shot 40021 was 102.71 KPa (14.897 psi). Ports 22-2 and 33-2 in model #1 recorded pressures of 102.75 and 102.81 KPa (14.903 and 14.912 psi), respectively. These pressures were higher than the range pressure by only 0.04 and 0.1 percent, respectively. The next day, the range pressure for Shot 40022 was 102.78 KPa (14.907 psi). Ports 22-2 and 33-2 recorded pressures in the barrel of 102.62 and 102.09 KPa (14.884 and 14.807 psi), respectively. These differences were 0.15 and 0.5 percent lower than the range pressure.

This is believed to be the first time that NASA instrumented ballistic range models have been recovered with functional transducers. The models each experience over 10,000 G during launch. There is no practical pretest method to realistically simulate the duration and magnitude of launch accelerations. For other test programs, ground-based impulse shock testing of sample transducers suggested that pressure measurements should not be affected significantly by launch. The Kulite® product specifications indicate the transducers should work in this application. The data from these subsequent ballistic range shots are corroborative. The three pressure transducers that survived to provide nominal data after one shot showed agreement with the range pressure. Essentially, the transducers were “good” after a shot with similar accuracy, or they failed and provided no useful data. Based on the pretest calibration data and the shot-to-shot comparison of the ports that survived Shots 40017 and 40021, it is estimated that the

	<b>NASA Engineering and Safety Center Technical Assessment Report</b>	Document #: <b>NESC-RP-14-00965</b>	Version: <b>1.0</b>
Title: <b>Independent Assessment of the Backshell Pressure Field for MEDLI2</b>			Page #: 25 of 74


backshell transducer measurements are accurate to better than  $\pm 3.45$  KPa ( $\pm 0.5$  psi). A more detailed uncertainty quantification program was beyond the scope of this test program. This conservative accuracy estimate is adequate for the objectives of the test.

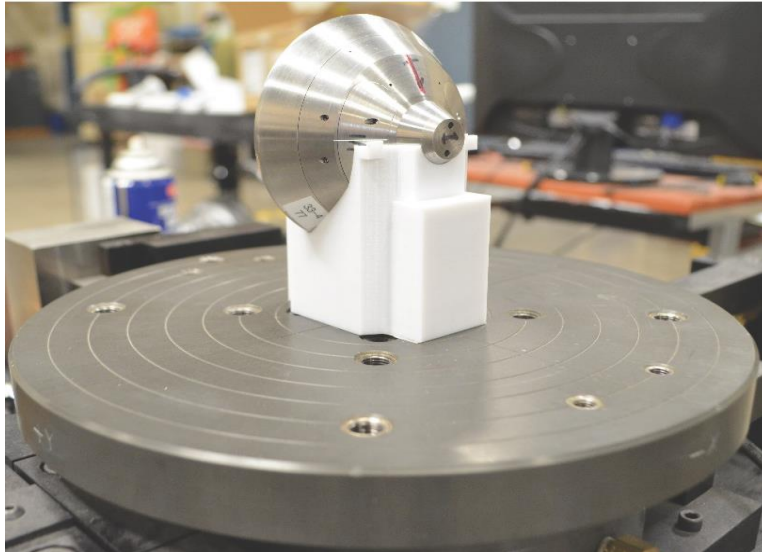
### 7.1.5 Mass Properties Measurements

Historically, the as-built mass properties of uninstrumented ballistic range models have been in close agreement with the design values provided by a computer-aided design (CAD) model. This is especially true if there is a measured density of the material(s) used to fabricate the models. The instrumented ballistic range models used in this test contain electronics boards, batteries, transducers, potting material, and other components whose exact mass were difficult to model and whose installed locations within the model could not be measured in the final assembly. Compared with the model body constructed of steel and tungsten, these components represented a small portion of the total mass. It was thought that any small errors in fabrication and installation of each component would result in small deviations from the design mass properties. However, it was critical that these models be recovered to download the recorded pressure histories. Preflight testing of uninstrumented models that were shot the full length of the TEF showed that small fabrication errors could result in the models swerving significantly and missing the catcher assembly. Following those early uninstrumented tests, it was determined the catcher would be placed between TEF pits 3 and 4. This would help mitigate the catch/recovery problem due to excessive swerve, while covering the desired Mach range and providing sufficient data points for reconstructing the trajectory. Analysis showed (see Appendix B) the model CGs had to be within 0.079 mm (0.003 inch) of the forebody 70-degree cone centerline axis. The NESC assessment team decided to use Space Electronics LLC, which specializes in mass property measurements to confirm that the model CG was within the offset limit to an accuracy of 0.025 mm (0.001 inch).

Mass-property measurements were made by Space Electronics LLC in Berlin, Connecticut. The development of the measurement procedures was complicated due to the model OML shape. The vendor and NASA worked together to develop fixtures the matrix of measurement points to achieve the necessary accuracy. As any CG offset was to be measured away from the axis of the forebody cone (i.e., the dominant aerodynamic surface that determined the model's trim angle of attack), the CG measurements had to be aligned to that axis. It proved difficult to hold the model with that axis aligned or perpendicular to the moment of inertia (MOI) measurement machine spin axis with any measurable accuracy. Ultimately, a polycarbonate fused deposition modeling fixture was designed by the NESC assessment team to match the model OML. The fixture was fabricated by NASA to hold the model at a fixed location and orientation with acceptable repeatability. Figure 7.1.5-1 shows the model seated in the fixture and installed in the Space Electronics LLC MOI measurement machine.




	<b>NASA Engineering and Safety Center Technical Assessment Report</b>	Document #: <b>NESC-RP-14-00965</b>	Version: <b>1.0</b>
Title: <b>Independent Assessment of the Backshell Pressure Field for MEDLI2</b>			Page #: 26 of 74

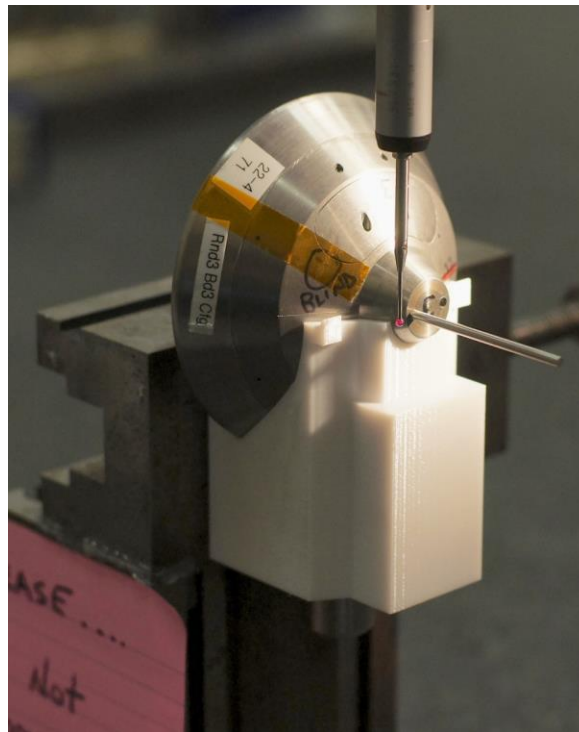


***Figure 7.1.5-1. Model Installed in Longitudinal MOI Measurement Fixture at Space Electronics LLC***

The LaRC QA lab performed extensive measurements to determine the model orientation in the fixture relative to the rotational axis of the measurement machine. One of the models being measured in the QA lab is shown in Figure 7.1.5-2. The QA lab measured the shape of each model OML to verify that it was machined to specified tolerances. This included measuring the location of the roll pins and pressure ports relative to axes scribed on the models. The model orientation, when seated in the MOI fixture, was measured so that each would return to a repeatable position when removed and resealed. The critical radial-offset CG measurements were made four times with the model installed in the fixture in four different positions, oriented at 0, 90, 180, and 270 degrees as defined by the scribed axes. This provided mirrored pairs of measurements of the longitudinal MOI y and z axes, and CG location along the y and z axes. The difference in CG position between the two mirrored pairs was used to determine the radial CG offset and the model's spin axis bias offset from the MOI measurement machine rotational axis. The CG offsets along the two longitudinal axes were used to determine the total radial offset for each model. These total offsets are given in Table 7.1.5-1. The measurements showed that the CG location of each model was within the radial offset limit of 0.076 mm (0.003 inch) and was acceptable for test. Pretest analysis predicted that a 0.076-mm (0.003-inch) radial CG offset would result in a 1-m swerve from a ballistic trajectory at the downrange station of the catcher boxes.

The MOI measurements were validated when the test was conducted. For each shot, the distance from the impact point to the bore-sighted target point of each model was within the predicted 1-m value. The test design and verification and validation (V&V) process used to ensure model recovery developed for this test proved highly successful and could be used for future tests when model recovery is critical.


	<b>NASA Engineering and Safety Center Technical Assessment Report</b>	Document #: <b>NESC-RP-14-00965</b>	Version: <b>1.0</b>
Title: <b>Independent Assessment of the Backshell Pressure Field for MEDLI2</b>			Page #: 27 of 74



**Figure 7.1.5-2. Model Orientation Measurements in NASA LaRC QA Lab**

**Table 7.1.5-1. Mass Properties of Models for Each Data Shot**

	Shot Number						
	40017	40018	40019	40021	40022	40023	40024
<b>NASA P-OBR#</b>	3	3	5	1	1	2	3
<b>length (mm)</b>	57.5	57.5	57.5	57.5	57.5	57.5	57.5
<b>diam (mm)</b>	90	90	90	90	90	90	90
<b>mass (kg)</b>	1.3307	1.3307	1.3398	1.3343	1.3343	1.3434	1.3307
<b>X CG (mm)</b>	28.32	28.32	28.44	28.29	28.29	28.36	28.32
<b>total radial offset (mm (in))</b>	0.00635 (0.00025)	0.00635 (0.00025)	0.04115 (0.00162)	0.02743 (0.00108)	0.02743 (0.00108)	0.04318 (0.00170)	0.00635 (0.00025)
<b>Y CG (mm)</b>	-0.00508	-0.00508	-0.02286	-0.03429	-0.03429	-0.04191	-0.00508

	<b>NASA Engineering and Safety Center Technical Assessment Report</b>	Document #: <b>NESC-RP-14-00965</b>	Version: <b>1.0</b>
Title: <b>Independent Assessment of the Backshell Pressure Field for MEDLI2</b>			Page #: 28 of 74


Shot Number							
	40017	40018	40019	40021	40022	40023	40024
<b>Z CG (mm)</b>	0.00381	0.00381	0.03429	0.02286	0.02286	-0.01016	0.00381
<b>Ixx (kgm^2)</b>	0.000884951	0.000884951	0.000889634	0.000890804	0.000890804	0.000894901	0.000884951
<b>Iyy (kgm^2)</b>	0.000598454	0.000598454	0.000606941	0.000629474	0.000629474	0.000630938	0.000598454
<b>Izz (kgm^2)</b>	0.000572994	0.000572994	0.000582359	0.000607234	0.000607234	0.000609721	0.000572994

### 7.1.6 Test Matrix

The test matrix for all the instrumented shots is listed in Table 7.1.6-1. The intended initial barrel exit velocity for each shot was 1,000 m/s (approximately Mach 3.0). This value was selected so that the Mach number at station #1 was near Mach 2.5. The Mach number history of the capsule through the range would be relevant to the flight conditions at which MEDLI2 was attempting to measure backshell pressures. This was close to the minimum initial Mach number at which the measured data would be useful to the MEDLI2 project. The minimum Mach number was chosen to minimize the penetration depth and deceleration loads in the catcher boxes to improve the chances that the models would survive flight and recovery so that data could be downloaded.

Development ballistic range shots conducted prior to the instrumented test campaign were used to determine empirically the target initial velocity for sizing gun propellant charges. An initial barrel exit velocity of 1,000 meters per second (m/s) or Mach 2.94 was selected for each shot based on the development shots and the observed velocities within the range. There is inherent variability in the exit velocity of sabot-launched projectiles even when the propellant mass is identical for each. The propellant ignition is not uniform or perfectly repeatable, and launch gases can pass around the sabot within the gun depending on how well the sabot seals against the gun barrel wall. Measured muzzle exit velocities varied from 915 to 1008 m/s or Mach 2.7 to 2.94, as shown in Table 7.1.6-1. The three key data shots saw muzzle exit velocities of 915 m/s (Shot 40018), 991 m/s (Shot 40021), and 992 m/s (Shot 40023).




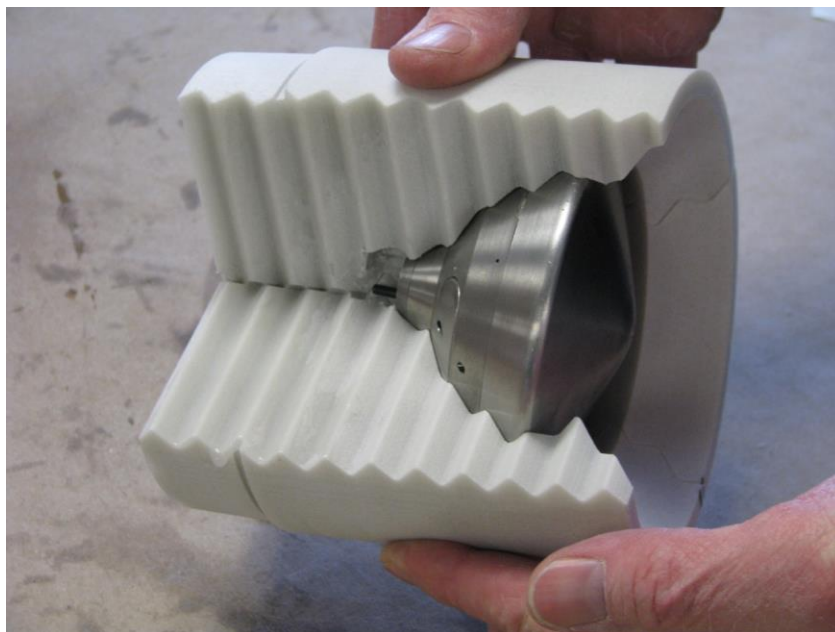
	<b>NASA Engineering and Safety Center Technical Assessment Report</b>	Document #: <b>NESC-RP-14-00965</b>	Version: <b>1.0</b>
Title: <b>Independent Assessment of the Backshell Pressure Field for MEDLI2</b>			Page #: 29 of 74

*Table 7.1.6-1. Ballistic Range Test Matrix*

Date	Shot	Model	V initial (m/s)	Sabot model cant angle (deg)	Notes
3/30/16	40015	Warmer 1	937	0	Uninstrumented
3/31/16	40016	Warmer 4	980	0	Uninstrumented
3/31/16	40017	#3	958	0	Good data up to breakscreen
4/4/16	40018	#3	915	0	1 wake pressure recorded to catcher
4/4/16	40019	#5	998	0	No communication after recovery
4/5/16	40020	Warmer 6	945	10	Uninstrumented
4/5/16	40021	#1	991	10	Good data up to breakscreen
4/6/16	40022	#1	1008	0	1 good wake pressure failed in gun
4/6/16	40023	#2	992	10	Complete data recorded to catcher
4/6/16	40024	#3	998	10	No communication after recovery

Two sabot designs were used to provide 0 and 10 degrees initial total angle of attack. The model cavity within the sabots was fabricated to support the model with the spin axis parallel to the sabot spin axis for the 0-degree sabots. For the 10-degree sabots, the axis of the model cavity was canted 10 degrees relative to the sabot axis. For the 10-degree angle of attack shots, the sabots were inserted as close as possible to purely nose-up or nose-down orientations in the gun. This was an attempt to observe pitch oscillations in the “hall” shadowgraph images, although each model did leave the smooth-bore barrel with some roll rate. The model cant orientation was selected so that any aerodynamic jump caused by sabot separation would result in deviations from the desired impact point at the catcher box to be oriented vertically rather than laterally. The catcher box arrangement was designed to accommodate greater vertical impact location variations. For the 10-degree angle of attack shots, models were launched in either pin-up or pin-down orientations, which roughly aligned the backshell ports with the pitch plane so they would observe the wake pressure variations due to the pitch oscillations induced by the sabot. For 0-degree angle of attack shots, the models were launched in pin-up or pin-down orientations to maintain a consistent procedure when arming the data recording system, loading the model in the sabot, and handing off the projectile to the gun operators who loaded the projectiles and propellant in the gun. An example of a model sitting in a 10-degree angle of attack sabot is shown in Figure 7.1.6-1. In this instance, the model is nose-down and the roll pin is aligned in the pitch plane in a pin-down orientation.

	<b>NASA Engineering and Safety Center Technical Assessment Report</b>	Document #: <b>NESC-RP- 14-00965</b>	Version: <b>1.0</b>
Title: <b>Independent Assessment of the Backshell Pressure Field for MEDLI2</b>			Page #: 30 of 74



**Figure 7.1.6-1. Loading Instrumented Model in 10-degree Sabot (3 of 4 petals shown)**


For reference, the ambient pressure within the range for each shot is listed in Table 7.1.6-2. The USARL TEF reported measured pressures in inches of mercury (Hg), temperatures in degrees Fahrenheit, and relative humidity (RH) in percent. Conversions to the International System of Units (SI units) are provided. The measured RH can be used to determine a correction to the ambient pressure and density. The effect was small and neglected for this assessment. The measured pressures and temperatures were used for all data reductions presented in this document and for all conditions provided for CFD runs.

**Table 7.1.6-2. Ambient Conditions for Ballistic Range Shots**

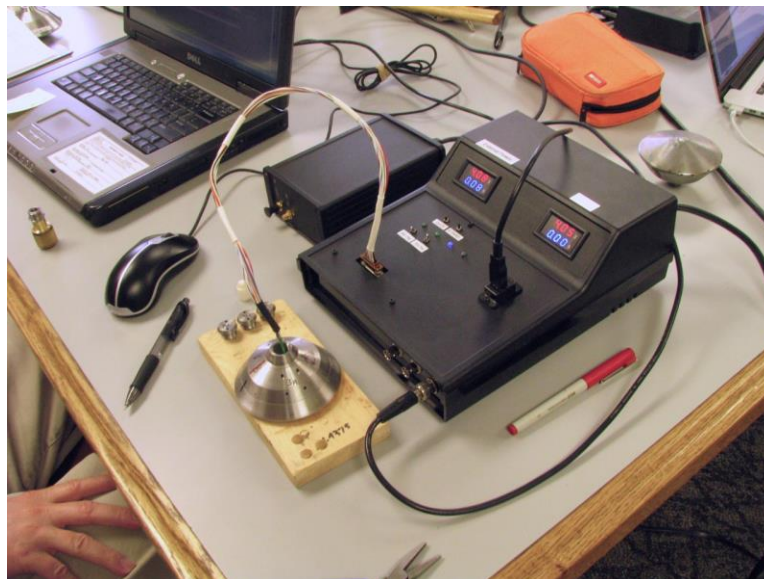
	40017	40018	40019	40021	40022	40023	40024
<b>Model Number</b>	3	3	5	1	1	2	3
<b><math>p_{\infty}</math> (in Hg)</b>	30.41	29.89	29.7	30.33	30.35	30.35	30.35
<b><math>p_{\infty}</math> (kPa)</b>	102.98	101.22	100.58	102.71	102.78	102.78	102.78
<b><math>T_{\infty}</math> (°F)</b>	53	51	52	43	41	43	45
<b><math>T_{\infty}</math> (K)</b>	284.82	283.71	284.26	279.26	278.15	279.26	280.37
<b>RH (percent)</b>	80	71	68	59	64	63	62

### 7.1.7 Data Recording

Pressure data were recorded at 62.5 kilohertz (kHz). The models were powered on and an onboard 10-minute timer commanded to start just prior to giving the models to the gun operators. While the timer was counting, the onboard data system would not record. This allowed the

	<b>NASA Engineering and Safety Center Technical Assessment Report</b>	Document #: <b>NESC-RP-14-00965</b>	Version: <b>1.0</b>
Title: <b>Independent Assessment of the Backshell Pressure Field for MEDLI2</b>			Page #: 31 of 74

models to be loaded with no fear that any impacts during loading could trigger data recording. After the 10-minute keep-out window expired, the data system used an onboard accelerometer to detect launch and start data recording. The system would nominally record 2 s of data to nonvolatile memory. Some important anomalies with this process were encountered, which are discussed in Section 7.2.1. The data interface equipment connected to a model is shown in Figure 7.1.7-1.




**Figure 7.1.7-1. Setup for Onboard Data Recording Initiation and Download**

### **7.1.8 Data Reduction**

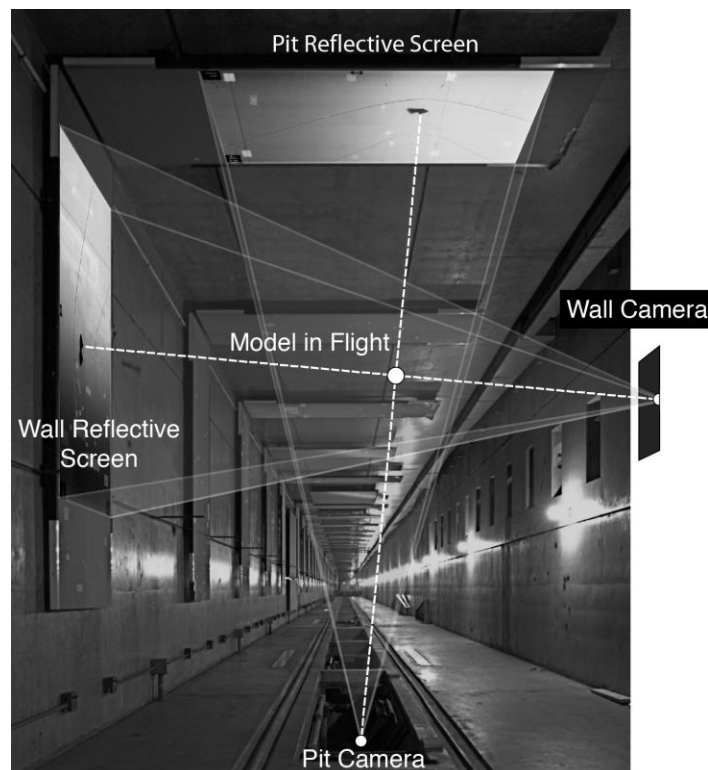
Fifteen shadowgraph image pairs from wall and pit views were captured for each shot. However, the model was not always imaged successfully in both shadowgraphs at each station. Only stations with clear images of the model in both the pit and wall shadowgraphs provide explicit position and orientation data for trajectory reconstruction.

Frequently, ballistic range testing seeks to determine aerodynamic coefficients by fitting 6-DOF trajectories through shadowgraph position/orientation data. The Mars Exploration Rover (MER) and MSL missions used this approach to measure the dynamic stability of their entry vehicles [refs. 2 and 3]. For blunt bodies with nonlinear pitch damping characteristics, this test technique requires numerous shots with more data stations (e.g., the Eglin Aeroballistic Test and Evaluation Facility (ATEF) used for MER and MSL had 50 data stations). For the MEDLI2 test program, the MSL ballistic range test program aerodynamic coefficients were used. The MSL models were geometrically similar to the Mars 2020 models. The MSL models were 65 mm in diameter. Prior to this test, MSL models were tested in the TEF with uninstrumented 90-mm Mars 2020 models. These tests showed that data from the TEF range were comparable to the ATEF range, and the Reynolds number differences due to different model sizes were small.

	<b>NASA Engineering and Safety Center Technical Assessment Report</b>	Document #: <b>NESC-RP-14-00965</b>	Version: <b>1.0</b>
Title: <b>Independent Assessment of the Backshell Pressure Field for MEDLI2</b>			Page #: 32 of 74

These pretest data indicated the MSL aerodynamic coefficients could be used to fit trajectories through the more limited data sets from the instrumented MEDLI2 shots.


Model position and orientation are determined from shadowgraph pairs at each station. Figure 7.1.8-1 is an annotated image of a representative ballistic range to show how this is achieved. In this case, the image shows a data station in the Eglin ATEF, but the concept is identical for the stations within the TEF. The shadow of the model in flight is produced by spark sources at each camera. In the TEF, the spark sources are triggered by infrared light sheets at the uprange end of each five-station pit. The spark sources at each pit camera are fired in succession using delays determined by pretest simulations, and refined using test shots of uninstrumented models. Fiducial markers in the shadowgraph images (i.e., beads strung on wires at known locations in front of each screen) provide reference points that locate the model in space. Image post-processing used the model silhouette, including the roll pin in this case, to determine orientation. Through these data points, a 6-DOF trajectory was fit to interpolate the model velocity and orientation history for comparison with the onboard pressure data.



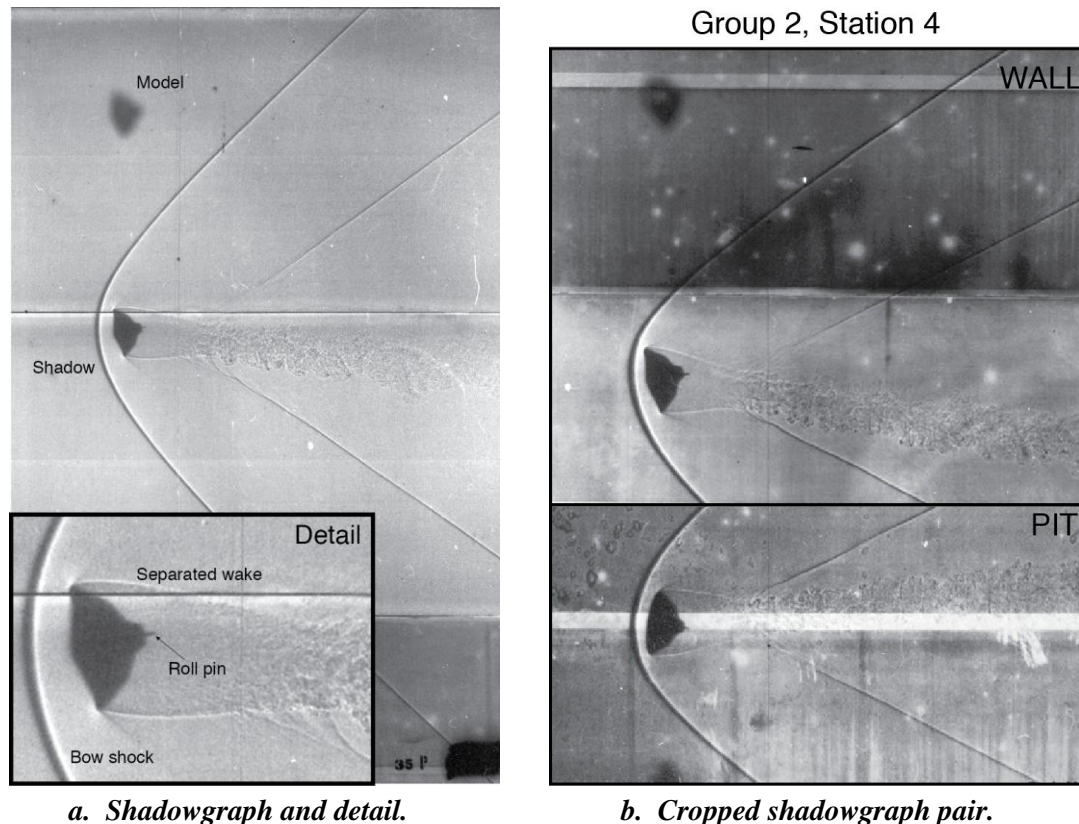
**Figure 7.1.8-1. Shadowgraph Geometry for Model Position/Orientation Measurement (Eglin ATEF ballistic range)**

Examples of the shadowgraph images are shown in Figure 7.1.8-2. The model in flight and the shadow on the reflective screen are shown in Figure 7.1.8-2(a). The detail insert shows the flow




	<b>NASA Engineering and Safety Center Technical Assessment Report</b>	Document #: <b>NESC-RP-14-00965</b>	Version: <b>1.0</b>
Title: <b>Independent Assessment of the Backshell Pressure Field for MEDLI2</b>			Page #: 33 of 74

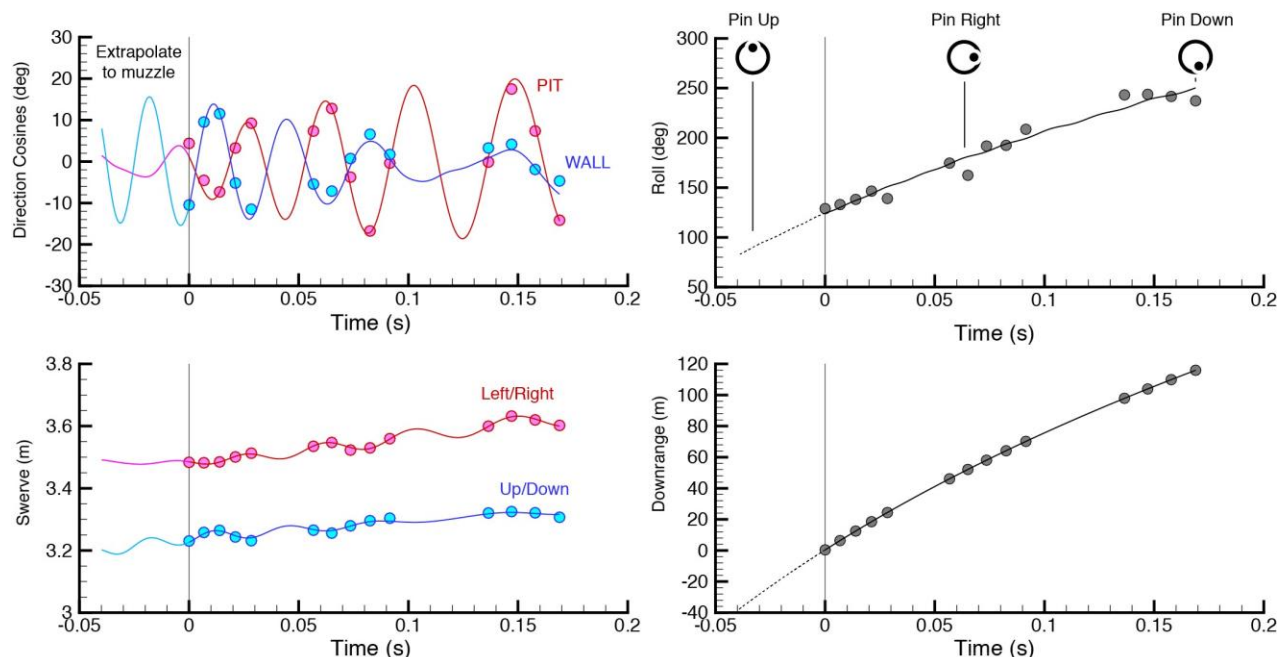
features around the model and the roll pin used to determine the model roll orientation. An example of two orthogonal shadowgraphs from station #4 in Group 2 is shown in Figure 7.1.8-2(b). From these two silhouettes and the fiducial markers visible in the full images, the position, orientation, and roll can be determined.



**Figure 7.1.8-2. Examples of Ballistic Range Shadowgraphs**

The raw data with the ambient air density and temperature conditions and the MSL aerodynamic model were used to fit 6-DOF trajectories to determine the velocity, position, and attitude history down the range. An example of trajectory reconstruction results is shown in Figure 7.1.8-3. The angles of attack, sideslip, roll orientation, and position history along the three range coordinate axes down the range are shown. Overall, the trajectories fit well to the data and provide useful information to which the pressure histories recorded onboard can be correlated. The roll data will allow the pressure ports to be located in the angle-of-attack/sideslip coordinate frame. This will be determined in subsequent analysis, which is beyond the scope of the NESC effort. For this assessment, pressure variations are correlated with total angle-of-attack variations.

	<b>NASA Engineering and Safety Center Technical Assessment Report</b>	Document #: <b>NESC-RP-14-00965</b>	Version: <b>1.0</b>
Title: <b>Independent Assessment of the Backshell Pressure Field for MEDLI2</b>			Page #: 34 of 74



**Figure 7.1.8-3. Examples of Ballistic Range Shadowgraphs (Shot 40021)**


## 7.2 Results

The plots shown in this section are representative of the pressure histories recorded during flight. Data are plotted against time or Mach number and the total angle of attack history is plotted to correlate with the pressure histories. Comparisons of the different pressure port measurements show that the total angle of attack is sufficient to assess the variations of the backshell pressures for the purpose of port selection. The near-uniform variation of pressure with capsule oscillation, correlated with the total angle of attack history, provided sufficient information to select the MEADS2 port location.

Follow-on analysis, which is beyond the scope of this assessment effort, will attempt to incorporate roll orientation data with the angle of attack and sideslip histories to determine the incidence angle of each port with time. That analysis may provide information about the unsteady variations of pressure as the capsule oscillates. This data may provide new insight into the mechanisms driving blunt body dynamic instabilities. However, the focus of the MEDLI2 test was to look for any evidence of flow attachment or other phenomena that would produce significant local deviations from the roughly uniform backshell pressure. The variation with total angle of attack proved sufficient for this assessment.

### 7.2.1 Data-recording Anomalies


The NESC assessment team encountered three data-recording anomalies that reduced the amount of acceptable information collected from the test campaign. The first was the loss of data

	<b>NASA Engineering and Safety Center Technical Assessment Report</b>	Document #: <b>NESC-RP- 14-00965</b>	Version: <b>1.0</b>
Title: <b>Independent Assessment of the Backshell Pressure Field for MEDLI2</b>			Page #: 35 of 74

channels after a model's first flight. The "catch" event resulted in pressure ports being fouled or circuits or electronic components being damaged. Therefore, reuse of a model that survived to download data was typically impaired to varying extents as pressure ports were lost. The second type of anomaly was a variation on the first: some models were damaged during the catch event such that the data computer could not download the onboard information. Data from Model #5 (Shot 40019) was not recovered. However, data were recovered from Model #2 (Shot 40023) even though the computer could not talk to the onboard data system after recovery. USARL engineers and technicians were able to obtain direct access to the nonvolatile memory and download a nearly complete data set, albeit almost 4 months after the test campaign was completed.

The third type of anomaly was an abrupt termination of the data recording during flight. This anomaly was puzzling to the NESC assessment team. It is now believed to have been a systematic problem with the test procedure, although detecting a root cause was complicated by the first two types of anomalies. Two shots (40017 and 40021) saw their recorded data files both stop at a point consistent with entry to the range. As part of the nominal test procedure, a break screen was placed in the path of the model that provided a timestamp for entry into the range. The break screen is a sheet of paper with a metallic circuit printed on it. A voltage is passed through the metallic circuit and screen. When the model passes through the screen, the severed connection time is recorded as the range entry point. It was first thought that the voltage passed through the screen was somehow causing the data recorder to stop. Shot 40018 used Model #3, which was reused after shot 40017. After Shot 40018, the model flew through the break screen and returned data along most of the range. This complicated the team's interpretation of what might be causing the data dropout. After Shot 40021, the break screen was removed. However, it was not until data were downloaded from Shot 40023 that the team confirmed that data would be successfully recorded down the range when no break screen was present. Both Shot 40018 (which survived flight through a break screen and kept recording) and Shot 40023 (which did not use a break screen) appeared to stop recording data upon impact with the catcher box. This was not expected, as the data recorder was programmed to run for 2 s, well beyond the total flight time. The NESC assessment team's working hypothesis was that the models accumulate a large static charge during launch as the sabot travels down the gun barrel and then discharge to the first object with which they make physical contact (i.e., either the break screen or the catcher box). This hypothesis has yet to be confirmed. Future analysis and testing is required to resolve this problem to ensure data are recorded during each flight and the models are not damaged by electrostatic discharge, thus preventing reflight.

The USARL have used sabot designs in the past with metallic "whiskers" built in each petal. The whiskers make an electrical connection between the projectile and the gun barrel. The phenomena for which these whiskers are used are not related to the onboard data recording problems encountered during this test program. It is believed that this is the first test that the USARL has conducted where data are recorded onboard and the projectiles make physical contact

	<b>NASA Engineering and Safety Center Technical Assessment Report</b>	Document #: <b>NESC-RP- 14-00965</b>	Version: <b>1.0</b>
Title: <b>Independent Assessment of the Backshell Pressure Field for MEDLI2</b>			Page #: 36 of 74

with an object during flight. The USARL engineers on the NESC assessment team suggested that whiskered sabots might be applied to this new problem.

## 7.2.2 Pressure Histories


The key data from successful shots are presented in the following sections. The most informative data came from Shot 40023, which was launched in a 10-degree (projectile cant-angle) sabot, experienced oscillations above 20 degrees, and recorded data from all transducers until catcher impact. Shot 40023 provided sufficient data to select the backshell port location. Data from the other shots provided information at low and intermediate angles of attack.

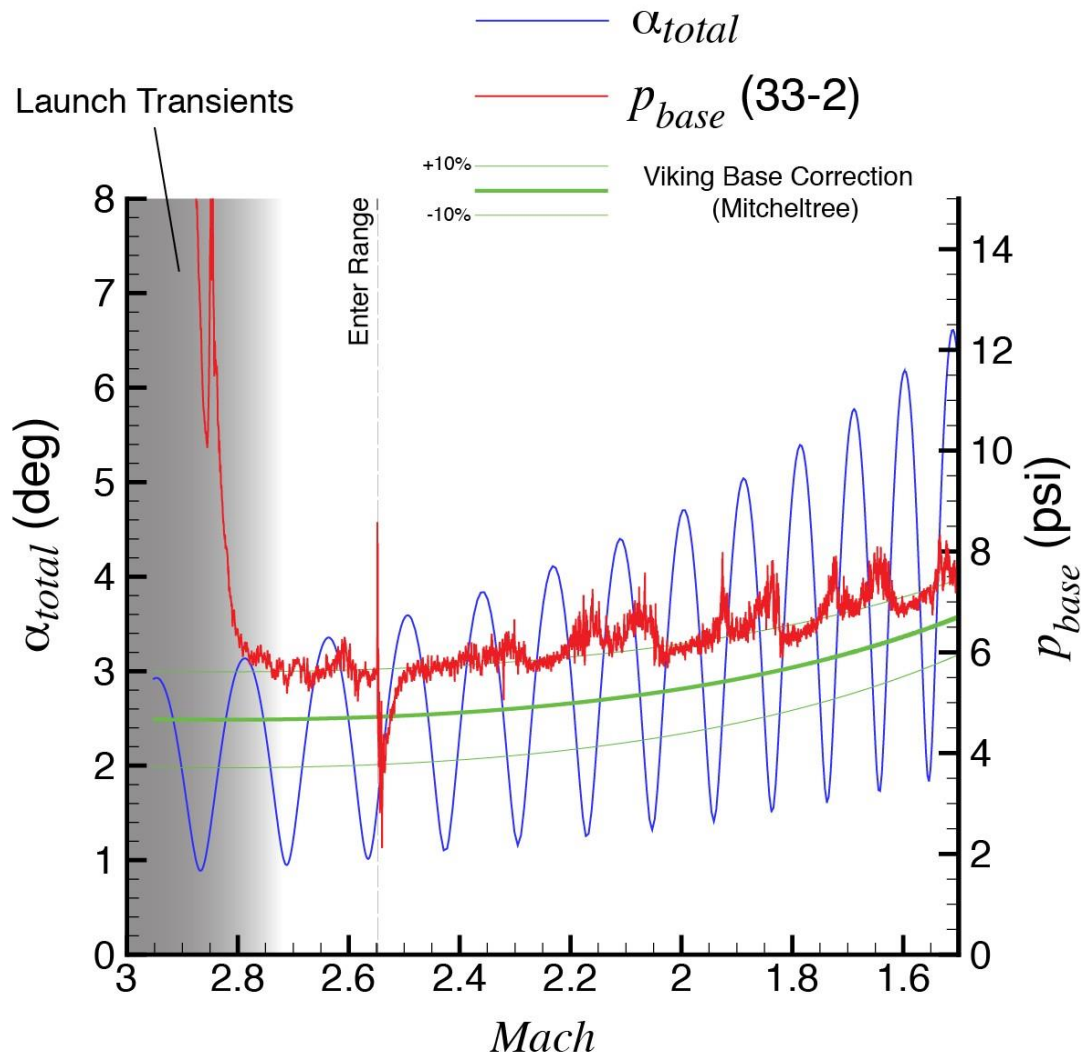
Pressure data from Shot 40018 are shown in Figure 7.2.2-1. The model was launched in a 0-degree sabot. This was a reflight of Model #3; only the backshell pressure port 33-2 was functional for the second shot. The backshell pressure is compared with the wake pressure model created by Mitcheltree [ref. 4], which has been used by all recent NASA Mars entry capsules to predict the supersonic wake pressure. This model was developed from wake pressure data measured by the two Viking entry vehicles that flew to Mars in 1976. The pressure data from Shot 40018 follow the Viking model with Mach number, but the data appear to be offset to the upper dispersion values. The pressure variations correlate angle-of-attack oscillations and are on the order of the uncertainty band used with the Viking models. This suggests that angle of attack has a first-order effect on the wake pressure. The Viking entry capsules trimmed near 11 degrees. Shot 40018 does not reach that total angle of attack. However, the variations with angle of attack suggest that the wake pressures should be lower at greater angles of attack. This would be in better agreement with the nominal Viking model at angles closer to the Viking trim angle. Subsequent shots also support the conclusion that wake pressure varies primarily with angle of attack and show trends consistent with the Viking wake model.

Note the gray area on the left side of the data plot Figure 7.2.2-1. This gray region indicates an estimate of where pressure measurements are recovering from the high pressures encountered during launch. The model is propelled by launch gases that easily over-range the 172.4 kPa (25 psi) full-scale backshell transducers. Upon exit from the gun, the model is flying through high-pressure gases before emerging into free-stream flow where the sabot petals peel away and free flight begins.

An additional feature in this figure is the pressure spike near Mach 2.55. This spike correlates with the model passage through the TEF aperture. For the shots where data were collected through the entire range, this pressure spike was used to synchronize the pressure and attitude histories.




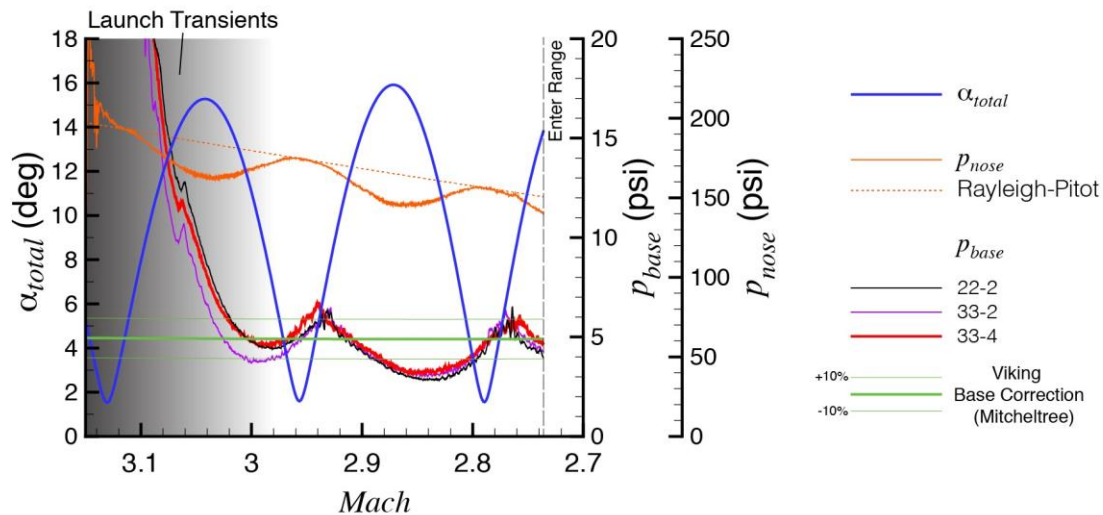
	<b>NASA Engineering and Safety Center</b> <b>Technical Assessment Report</b>	Document #: <b>NESC-RP-14-00965</b>	Version: <b>1.0</b>
Title: <b>Independent Assessment of the Backshell Pressure Field for MEDLI2</b>			Page #: 37 of 74



**Figure 7.2.2-1. Pressure History from Shot 40018**

Pressure data from Shot 40021 is plotted in Figure 7.2.2-2. This data set is an example where the onboard recorder stopped at or near the TEF break screen contact. Prior to this point, data from the three backshell and the stagnation ports were recorded. This model was launched at a 10-degree total angle of attack. Sabot separation appears to have tipped the model to approximately a 17-degree total angle of attack. The gray shaded area is used to mark the estimated region where launch pressures are decreasing and the model is emerging into unperturbed, quiescent atmosphere. Data were recorded for a little over one-half cycle of oscillation in the unperturbed atmosphere. The measured stagnation pressure was compared with the predicted stagnation pressure calculated using the Rayleigh-Pitot equation and the Mach number history derived from the ballistic range trajectory reconstruction results.

	<b>NASA Engineering and Safety Center</b> <b>Technical Assessment Report</b>	Document #: <b>NESC-RP-14-00965</b>	Version: <b>1.0</b>
Title: <b>Independent Assessment of the Backshell Pressure Field for MEDLI2</b>			Page #: 38 of 74




**Figure 7.2.2-2. Pressure History from Shot 40021**

Note that the total angle-of-attack history was determined by extrapolating upstream from the trajectory fit obtained using the TEF shadowgraph data. The extrapolated data are shown in Figure 7.1.8-3. Compared with the segment of data within the range, the distance uprange that the trajectory was extrapolated is small. The initial roll angle, angle of attack, and angle of sideslip are close to the model orientation within the sabot, as installed in the gun. This close agreement suggests that this extrapolation is accurate. The uncertainties on the extrapolated attitude history are greater than for the segment of data within the range, but the oscillation frequency and total amplitude are useful for comparison with the pressure history.


The measured forebody pressure drops when the stagnation point moves away from the nose as the capsule pitches to large total angles. However, when the model is at small total angles of attack there is agreement with the predicted stagnation pressure. This suggests that the reconstructed trajectory is good and the stagnation transducer was behaving as expected. The three wake pressures vary in a similar manner. Differences between three backshell pressures appear small after the model has passed the launch transients. The wake pressure data compare favorably with the Viking wake pressure model. The variation of all three ports with angle of attack was greater than the dispersions carried on the Viking wake pressure model. This suggests that the wake pressure is reasonably uniform over the backshell at angles to 17 or 18 degrees, and varies with total angle of attack. This finding is important and suggests the Viking model is only valid at its trim angle. It further suggests that for total angle of attack below 18 degrees, the pressure port location is not critical. From the limited available data, there is no strong evidence of flow attachment, which would first be expected to be detected by the outermost ports (i.e., 33-2 and 33-4) when those ports are most windward.

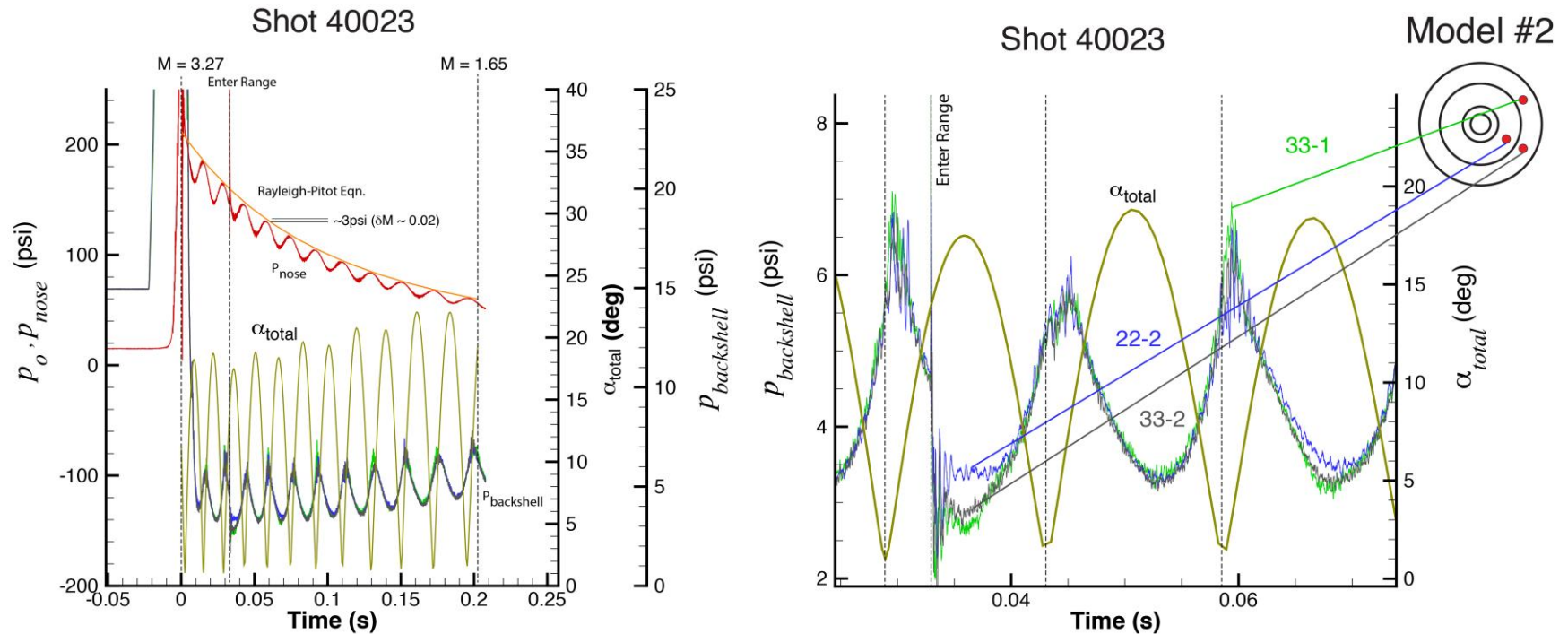
The pressure histories from Shot 40023 are shown in Figure 7.2.2-3. These data were recovered from Model #2 approximately 4 months after the test program was complete. The nose pressure


	<b>NASA Engineering and Safety Center Technical Assessment Report</b>	Document #: <b>NESC-RP- 14-00965</b>	Version: <b>1.0</b>
Title: <b>Independent Assessment of the Backshell Pressure Field for MEDLI2</b>			Page #: 39 of 74

and three wake pressure channels appear to have recorded pressures nominally. The data are consistent with those measured in Shot 40021 and can be correlated with the interpolated trajectory determined from shadowgraph data. Shot 40023 met the key test objectives of the test program. One of the objectives was to measure pressures at a total angle of attack greater than the Mars 2020 supersonic trim angle,  $\alpha_{trim} = 20$  degrees. The observed pressure variations of the wake transducers are similar, varying to first order with total angle of attack. There are small port-to-port deviations that might be related to reattachment or proximity to the parachute closeout cone (PCC), the aft-most, truncated cone section on the backshell. The nose pressure again varies with total angle of attack and is in closest agreement with the Rayleigh-Pitot model when the total angle is at a minimum. The data suggest good correlation between the recorded pressures and the reconstructed trajectory for Mach and total angle of attack. Shot 40023 indicates the pressure remains reasonably uniform beyond the angles seen in Shot 40021 to a total angle of attack slightly greater than 20 degrees.

The detail plot in Figure 7.2.2-3 shows port 22-2 deviating from the other wake pressures at ~0.035 and ~0.068 s. The Mach numbers at these two conditions are approximately 2.8 and 2.5, respectively. These are the largest port-to-port deviations observed in any of the wake pressure data. The deviation at 0.034 to 0.04 s immediately follows entry into the range where reflected shocks and other flow phenomena could be corrupting that data. OVERFLOW CFD results presented in Section 7.4.2 suggest the difference between ports 22-2 and 33-1/33-2 may be due to flow attachment on the first cone (i.e., measured by ports 33-1 and 33-2) at large angles of attack (near 20 degrees). This will be discussed in Section 7.6. The deviation persists as the capsule completes a full pitch oscillation but becomes less pronounced as the capsule decelerates and increases in amplitude. The data from all three backshell ports are in closer agreement after the first full oscillation past the range entry point.

	<b>NASA Engineering and Safety Center Technical Assessment Report</b>	Document #: <b>NESC-RP- 14-00965</b>	Version: <b>1.0</b>
Title: <b>Independent Assessment of the Backshell Pressure Field for MEDLI2 (Mars 2020)</b>			Page #: 40 of 74



	<b>NASA Engineering and Safety Center Technical Assessment Report</b>	Document #: <b>NESC-RP- 14-00965</b>	Version: <b>1.0</b>
Title: <b>Independent Assessment of the Backshell Pressure Field for MEDLI2 (Mars 2020)</b>			Page #: 41 of 74

### 7.3 Pretest CFD Summary

Prior to the ballistic range test, the NESC assessment team assessed the capabilities of the NASA's flow solvers, US3D and OVERFLOW, for application to ongoing ballistic range tests in support of MEADS II development. A detailed comparison of free to pitch simulations was provided in reference 5. This section will include only a summary of the two flow solvers and the approach to moving mesh simulations.

The computational analysis was added to this assessment in an attempt to compare experimental data with the current state-of-the-practice CFD codes being used by NASA for supersonic unsteady flows around blunt bodies. The intent was not to use CFD exclusively. There was no expectation that there would be good agreement, and the selection of the MEADS backshell port was not contingent on the NESC activity achieving a cohesive story with the experimental and computational data. Additionally, the time and personnel resources assigned to the CFD analysis limited the computational investigation to cases run at one Mach number. Regardless, the CFD results are in good agreement with the experimental data. The CFD can be used to interpret the experimental data. However, these comparisons raised more questions with regard to unsteady effects. This type of instrumented ballistic range testing may be an outstanding source of validation data to help develop blunt-body dynamic stability prediction tools.

#### 7.3.1 US3D


US3D is an unstructured, three-dimensional, finite-volume, parallel, implicit Navier-Stokes solver developed at the University of Minnesota. It can be considered the unstructured descendent of the Data Parallel Line Relaxation code, in use at NASA, academia, and industry. Originally developed for simulating hypersonic flow with thermochemical non-equilibrium, it has recently been applied to the high-resolution simulation of massively separated flows, such as that found in the wake of a blunt-body capsule. This increased usage was due to the implementation of low-dissipation numerical fluxes.

##### 7.3.1.1 Grid Generation

One of the critical differences between US3D and OVERFLOW is that US3D exclusively uses body-fitted meshes. In practice, this means that much of the user's time is spent generating a high-quality mesh to provide adequate resolution of critical flow features. This is in contrast to OVERFLOW, which uses overset grid techniques, thereby allowing increased grid-generation automation.

For the simulations in this assessment, the same grid was used for all cases. The grid was generated using the commercial package GridPro™. Because the same grid was used for a range of Mach numbers and pitch angles, refinements were added to accommodate complicated flow forward and aft of the body. Additionally, in performing dynamic simulations, it was desirable to have greater distance between the body and domain boundaries than would ordinarily be required. This is to accommodate the grid deformation that is used in US3D to perform rigid-



	<b>NASA Engineering and Safety Center Technical Assessment Report</b>	Document #: <b>NESC-RP- 14-00965</b>	Version: <b>1.0</b>
Title: <b>Independent Assessment of the Backshell Pressure Field for MEDLI2</b>			Page #: 42 of 74


body dynamic simulations. The grid used for these simulations was comprised of approximately 20 million cells. Typical grid spacing in the wake was approximately 2 mm. The first cell wall spacing was set to be 1  $\mu\text{m}$ , which resulted in a  $y^+ < 1$  for the entire vehicle surface.

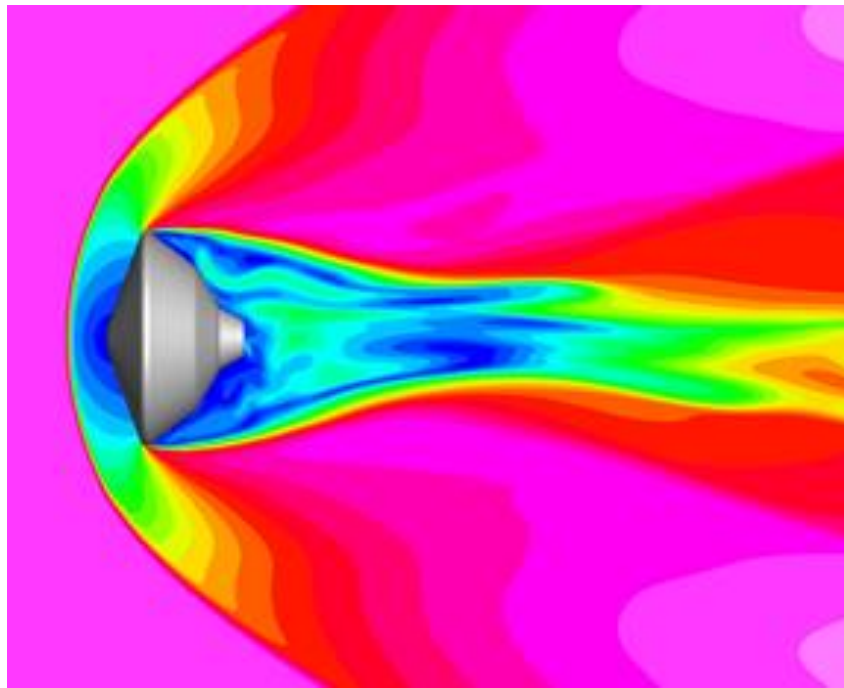
### 7.3.1.2 Numerical Methods

For this assessment, the second-order Kinetic Energy Consistent low-dissipation flux scheme was used, with the modified Steger-Warming flux-vector splitting scheme used for the dissipative portion of the flux. A Monotone Upwind Scheme for Conservation Laws extrapolation was used to achieve second-order reconstruction of the conserved variables at the faces in regions without a discontinuity. Time integration was performed using the Full Matrix Data-Parallel Method point implicit method. The global Courant–Friedrichs–Lewy (CFL) number for this scheme was set such that a local CFL number in the unsteady wake of approximate unity was achieved, which resulted in an average time step of approximately 1.25  $\mu\text{s}$ . Additionally, the flow in all cases was assumed to be fully turbulent, with the turbulent transport coefficient modeled using detached eddy simulation (DES). Finally, the Spalart–Allmaras one-equation model with the Catris-Aupoix compressibility correction was used to account for turbulent diffusion at subgrid scales.

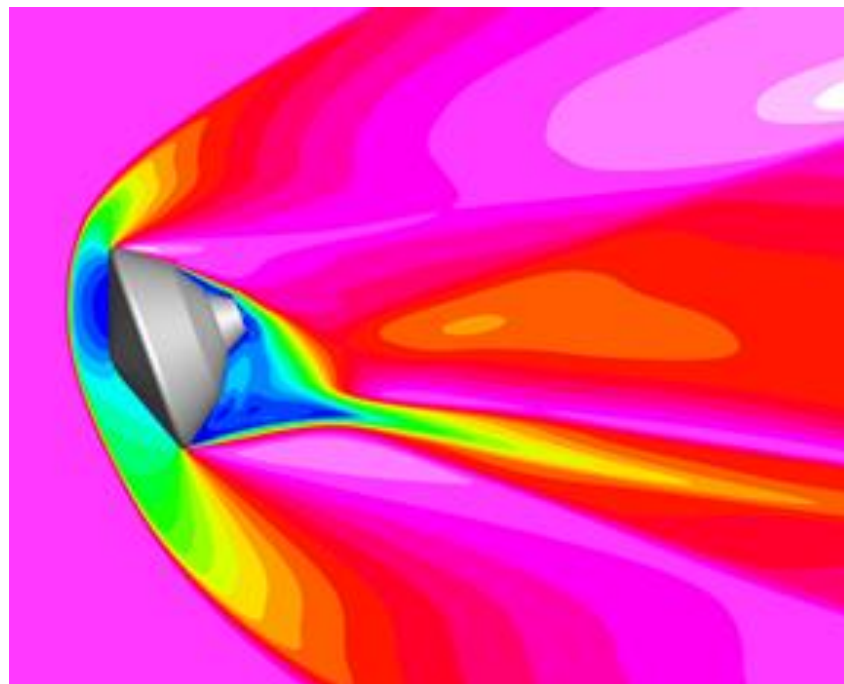
### 7.3.1.3 Moving Mesh Approach using US3D

The US3D flow solver uses body-fitted unstructured grids. Therefore, to accommodate a moving body the grid must be deformed in the simulation. The approach taken for deforming the mesh was to define a rigid sphere encapsulating the vehicle. Beyond this spherical region, a portion of the grid was allowed to deform as the vehicle rotated. Further, there was another rigid region between the flexible region and the mesh outer boundary where the grid points are held fixed. This approach is illustrated in Figures 7.3.1.3-1 through 7.3.1.3-4 for the Mars 2020 ballistic range model. Typically, the nominal mesh is generated for the trim angle of attack, in this case 0 degrees, as seen in Figures 7.3.1.3-1 and 7.3.1.3-3.

	<b>NASA Engineering and Safety Center Technical Assessment Report</b>	Document #: <b>NESC-RP- 14-00965</b>	Version: <b>1.0</b>
Title: <b>Independent Assessment of the Backshell Pressure Field for MEDLI2</b>			Page #: 43 of 74




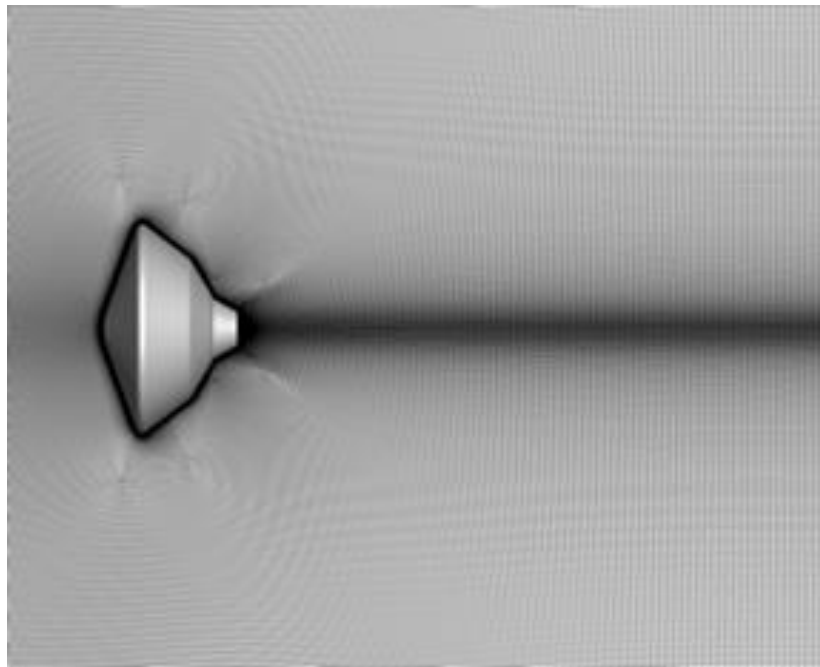
*Figure 7.3.1.3-1. Mach Contours, 0-degree Angle of Attack*



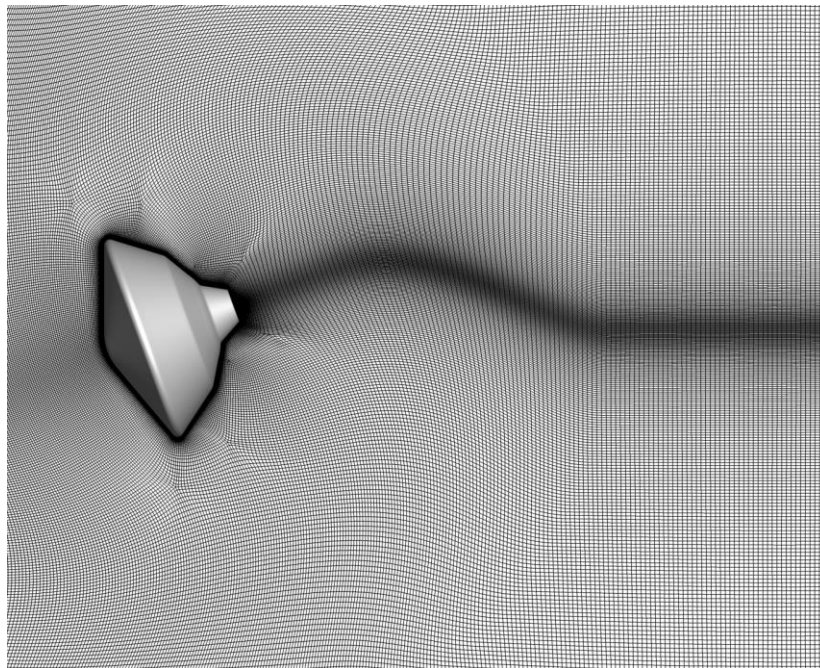
*Figure 7.3.1.3-2. Mach Contours, 20-degree Angle of Attack*




	<b>NASA Engineering and Safety Center Technical Assessment Report</b>	Document #: <b>NESC-RP- 14-00965</b>	Version: <b>1.0</b>
Title:	<b>Independent Assessment of the Backshell Pressure Field for MEDLI2</b>		
			Page #: 44 of 74



*Figure 7.3.1.3-3. Nominal Mesh, 0-degree Angle of Attack*



*Figure 7.3.1.3-4. Deformed Mesh, 20-degree Angle of Attack*

	<b>NASA Engineering and Safety Center Technical Assessment Report</b>	Document #: <b>NESC-RP- 14-00965</b>	Version: <b>1.0</b>
Title: <b>Independent Assessment of the Backshell Pressure Field for MEDLI2</b>			Page #: 45 of 74

For a given time step, the vehicle angular and translational accelerations were determined by the aerodynamic loads. The node displacements within the mesh were determined by the vehicle rotation and the node to the vehicle CG distance. The nodes in the near-body region were rotated with the body, while the nodes in the region extending the domain boundary remained static. The nodes in the interstitial deformable region simply undergo a weighted rotation based on their position between the inner and outer shells.

A limitation of this approach is that it cannot accommodate unlimited deflections. As the grid is moved further from trim, grid cells within the flexible layer become more skewed, which adversely affects the quality of the solution. Since entry vehicles are designed such that there should not be large excursions from trim during the decent phase, this is typically not a concern. Translational degrees of freedom are handled using a reference frame velocity that modifies the fluxes in the finite volume scheme.

### 7.3.2 OVERFLOW


OVERFLOW is a 3D, finite-difference, parallel, implicit Navier-Stokes solver capable of using overset grid topologies. It was originally developed at NASA ARC and is currently maintained by NASA LaRC. For moving-body simulations, it uses the Geometry Manipulation Protocol tool to modify the relative positions of the computational grids and allow for constrained or unconstrained motion.

#### 7.3.2.1 Grid Generation

Structured, overset grids of the capsule and the surrounding domain were generated with the Chimera Grid Tools (CGT). CGT allows for the creation of grid scripts for parametrically controlled grids for complex shapes. The script system fixes the surface and volume spacing, ensures bounded and consistent grid stretching ratios, and allows for rapid remeshing with updated inputs.

OVERFLOW's built-in Domain Connectivity Function (DCF) was utilized to perform hole cutting and calculation of interpolation stencils between overset grids. Regions of the overlapping grids were blanked due to intersection with solid bodies (i.e., the MSL capsule) and in regions of transition between body-fitted and off-body grids. Manual and automatically generated box grids were used for this analysis. The manual box grids include a shock box to capture the shock and near-body flow, and a wake box grid designed to contain the capsule's subsonic wake. The automatic box grids encapsulate the body-fitted and manual box grids, which extend into the far field.

By using the OVERFLOW DCF capabilities, the system component grids can be arbitrarily translated and rotated prior to hole cutting. This is useful for creating grids with the capsule at different angles of attack and is required to model motion during a simulation. Capsule motion is modeled by body-fitted grid motion inside the manual box grids, which remain oriented with the free-stream flow.

	<b>NASA Engineering and Safety Center Technical Assessment Report</b>	Document #: <b>NESC-RP- 14-00965</b>	Version: <b>1.0</b>
Title: <b>Independent Assessment of the Backshell Pressure Field for MEDLI2</b>			Page #: 46 of 74

With respect to grid spacing, the wake box uses a constant spacing at its core of  $0.017 D_o$  (normalized to the MSL diameter  $D_o$ ). The shock box is finer with its core of Cartesian cells having an isotropic spacing one-third of that in the wake box. The entire grid system has a total of 36 million points in the manual boxes and body-fitted grids, and an additional 200,000 points in the automatic off-body box grids.

### 7.3.2.2 Numerical Methods

For this assessment, the solver was run in a time-accurate mode with five Newton subiterations per time step. The Harten–Lax–van Leer–Einfeldt upwind scheme was used for discretization of the advective terms. Implicit time advancement used the symmetric successive over-relaxation algorithm. This work employed a hybrid DES model based on the two-equation shear stress transport turbulence model by Menter. The flow field was assumed to be fully turbulent.


Three levels of full-multigrid were used for flow-field initialization. Once a steady-state solution was reached, the simulation was run in a time-accurate mode to resolve unsteadiness. Similar to the US3D solutions, dynamic simulations begin with a statistically converged static simulation.

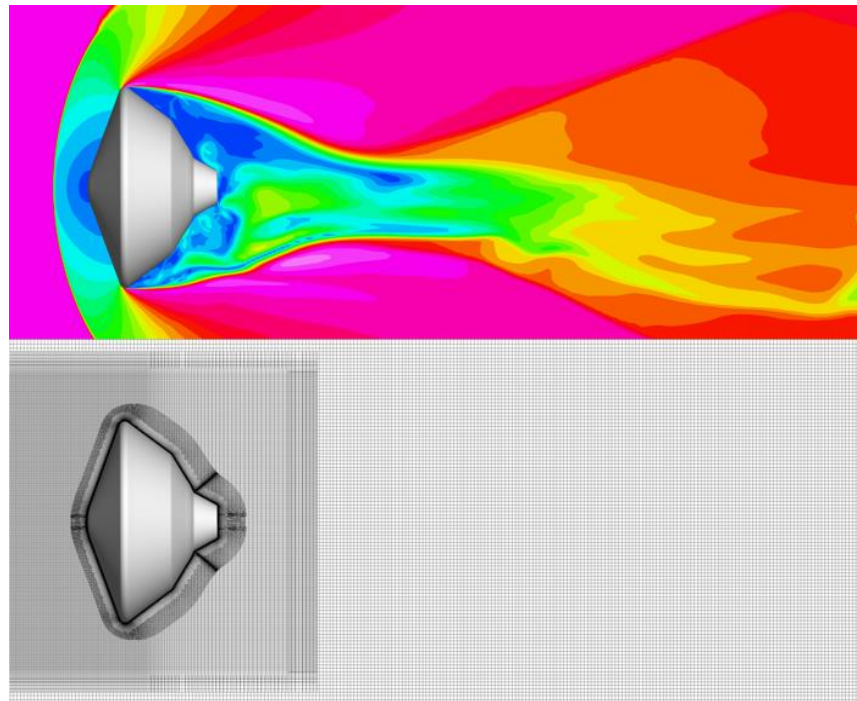
The NESC assessment team found that a normalized time step of  $0.01 \left( \frac{\Delta t V_\infty}{D_o} \right)$  was sufficient to achieve temporally converged results for moving-body simulations with respect to integrated aerodynamics. This time step was used for the static and moving-body results shown in the following sections.

### 7.3.2.3 Moving Mesh Approach using OVERFLOW

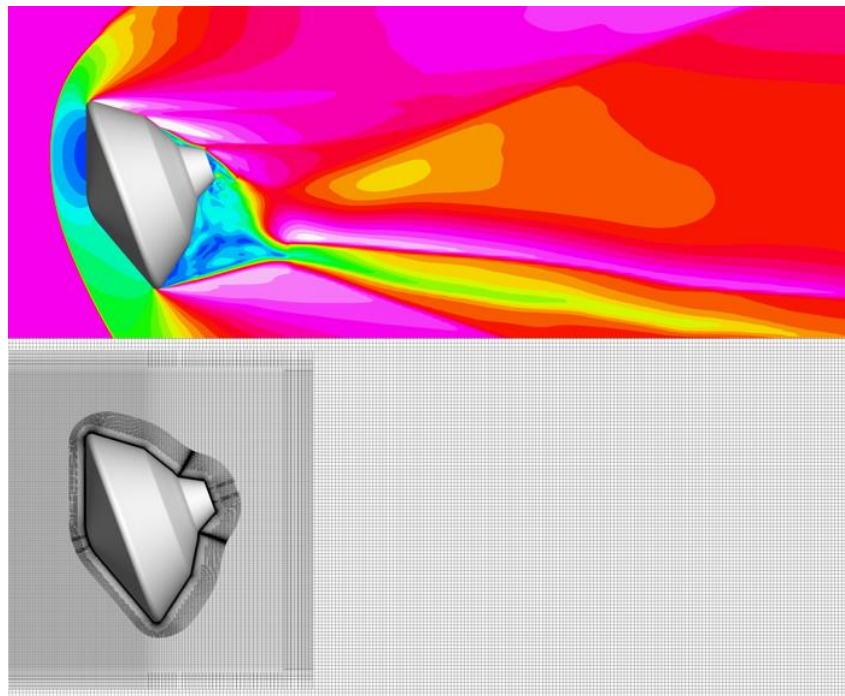
In OVERFLOW, the mechanics of the moving mesh allow for the capsule grids to rotate and translate independent of the background box grids. This provides flexibility in vehicle attitude without affecting the size or quality of the grid cells. For every time step, the solver recalculates overset boundaries and interpolation stencils based on the updated positions of all relevant components. Prior to this update, the vehicle integrated forces and moments dictate to the solver the accelerations to place on the capsule grids to update the position.

Figures 7.3.2.3-1 and 7.3.2.3-2 show an example of constrained pitch motion from a dynamic OVERFLOW solution. The initial capsule position was rotated to 30 degrees and allowed to freely pitch in a Mach 3.0 flow. Shown in these figures are the resulting grids and Mach contours of the flow at two instances of time: 1) when the capsule passes through a 0-degree angle of attack, and 2) when the capsule passes through a 20-degree angle of attack. The extent of the grid motion is limited to the capsule attitude with the surrounding box grids remaining fixed in space. For a solution involving capsule translation, the box grids translate with the body to track the movement.

	<b>NASA Engineering and Safety Center Technical Assessment Report</b>	Document #: <b>NESC-RP- 14-00965</b>	Version: <b>1.0</b>
Title: <b>Independent Assessment of the Backshell Pressure Field for MEDLI2</b>			Page #: 47 of 74




***Figure 7.3.2.3-1. Mach Contours and Mesh, 0-degree Angle of Attack***



***Figure 7.3.2.3-2. Mach Contours and Mesh, 20-degree Angle of Attack***



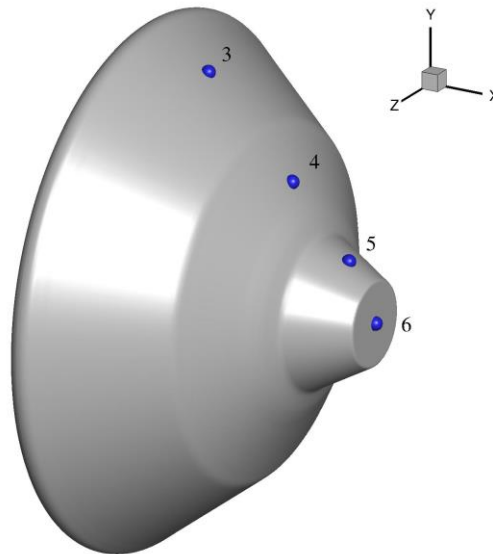
	<b>NASA Engineering and Safety Center Technical Assessment Report</b>	Document #: <b>NESC-RP-14-00965</b>	Version: <b>1.0</b>
Title: <b>Independent Assessment of the Backshell Pressure Field for MEDLI2</b>			Page #: 48 of 74

### 7.3.3 Pretest Dynamic CFD Analysis

Free-to-pitch simulations were run with the two flow solvers for Mach 3.0 and 1.5, and for initial angle-of-attack amplitudes of 30 and 5 degrees, to gain a better understanding of the expected flow field and surface pressures, and to identify differences between the flow solver predictions. This analysis is presented in greater detail in reference 5. The following is a summary of the findings from the pretest analysis.

#### 7.3.3.1 Backshell Pressure Traces

Pressures were taken during the simulations at the midpoint of each conic section on the backshell (see Figure 7.3.3.1-1 and Table 7.3.3.1-1).



**Figure 7.3.3.1-1. Pressure Measurement Locations from Pretest CFD**

**Table 7.3.3.1-1. Pressure Probe Locations with Origin at Nose of Model**

Probe	x (cm)	y (cm)
1	0.00	0.00
2	0.77	2.52
3	2.67	3.79
4	4.22	2.18
5	5.26	0.98
6	5.75	0.00

Pressures taken at location 4, which approximates the proposed flight instrument location for MEDLI2 during the free-to-pitch simulations can be seen in Figures 7.3.3.1-2 and 7.3.3.1-3.


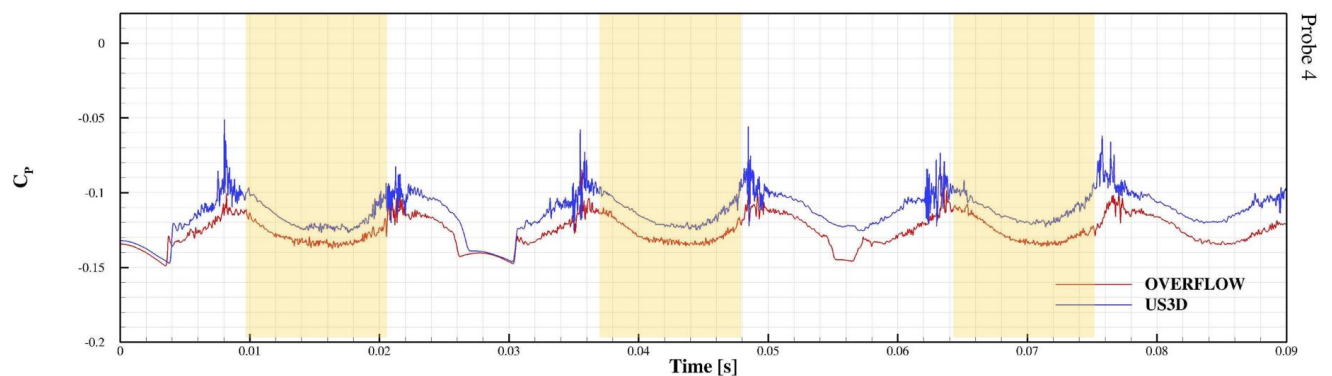
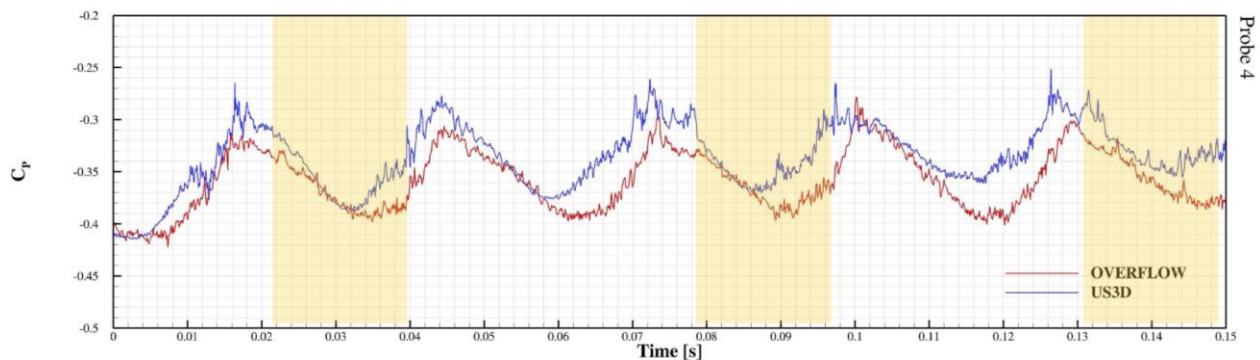
	<b>NASA Engineering and Safety Center</b> <b>Technical Assessment Report</b>	Document #: <b>NESC-RP-14-00965</b>	Version: <b>1.0</b>
Title: <b>Independent Assessment of the Backshell Pressure Field for MEDLI2</b>			Page #: 49 of 74

Figure 7.3.3.1-2 shows the computed backshell pressures for the Mach 3.0 case with 30-degree initial amplitude. This plot illustrates the separation and reattachment phenomena that occur on the backshell at high Mach numbers and angles of attack. When the model is released from 30 degrees, the pseudo-pressure probe is on the windward side, and in this trace a smooth pressure profile is indicative of an attached boundary layer. As the capsule pitches, the probe rotates to the leeward side, and a flat and “noisy” trace is observed, which is indicative of a fully separated wake. These portions of the trajectories are highlighted in yellow in the figures. Both solvers predict separated flow for the proposed flight instrument location. Similarly, the pressure at the same location for the Mach 1.5 and 30-degree initial amplitude case is shown in Figure 7.3.3.1-3. At this lower Mach number, the pressure trace is indicative of a fully separated flow at all angles of attack. However, for this case the boundary-layer attachment is not observed.




*Note: The yellow boxes highlight portions of trajectory where pressure measurement is on leeward side.*

**Figure 7.3.3.1-2. Computed Pressures on Second Backshell Conic for Free to Pitch Simulations having Initial Amplitude of 30 degrees and Mach 3**



*Note: The yellow boxes highlight portions of trajectory where pressure measurement is on leeward side.*

**Figure 7.3.3.1-3. Computed Pressures on Second Backshell Conic for Free to Pitch Simulations having Initial Amplitude of 30 degrees and Mach 1.5**

	<b>NASA Engineering and Safety Center Technical Assessment Report</b>	Document #: <b>NESC-RP-14-00965</b>	Version: <b>1.0</b>
Title: <b>Independent Assessment of the Backshell Pressure Field for MEDLI2</b>			Page #: 50 of 74

## 7.4 Posttest Results using OVERFLOW

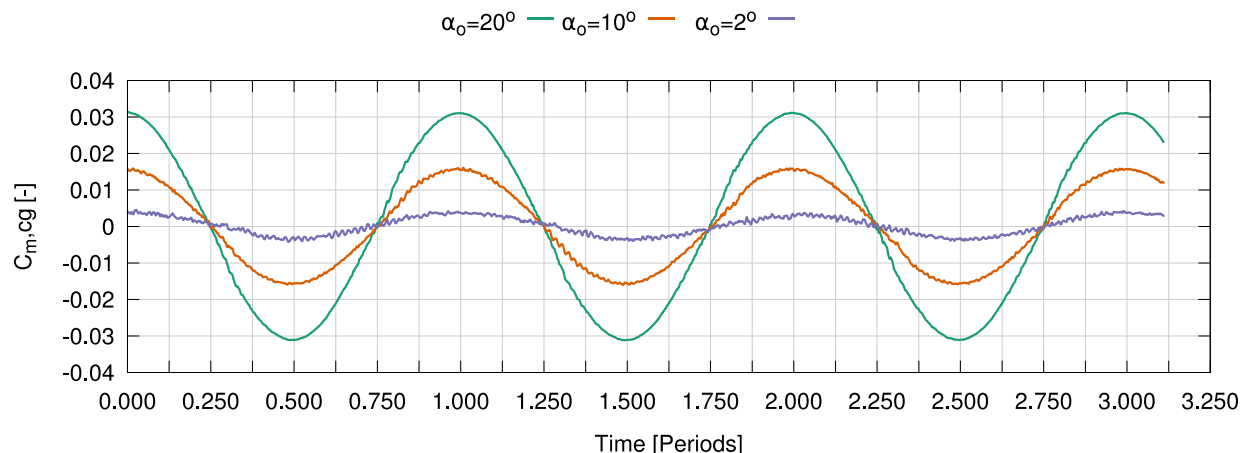
### 7.4.1 Posttest CFD Matrix

Following the ballistic range test, the NESC assessment team assembled a CFD matrix designed for comparison with the test data. This matrix consisted of a set of forced oscillation simulations at pitch amplitudes similar to what was observed in several shots. Also included were 6-DOF simulations initialized from the forced oscillation data.

Simulations were performed at Mach 2.8 with free-stream conditions consistent with Shot 40021. Forced oscillation simulations with pitch amplitudes of 2, 10, and 20 degrees were conducted. Six-DOF simulations for initial amplitudes of 2, 10, and 20 degrees were to be initialized from the forced oscillation results once startup transients were removed.


### 7.4.2 Forced Oscillation CFD Simulation Results

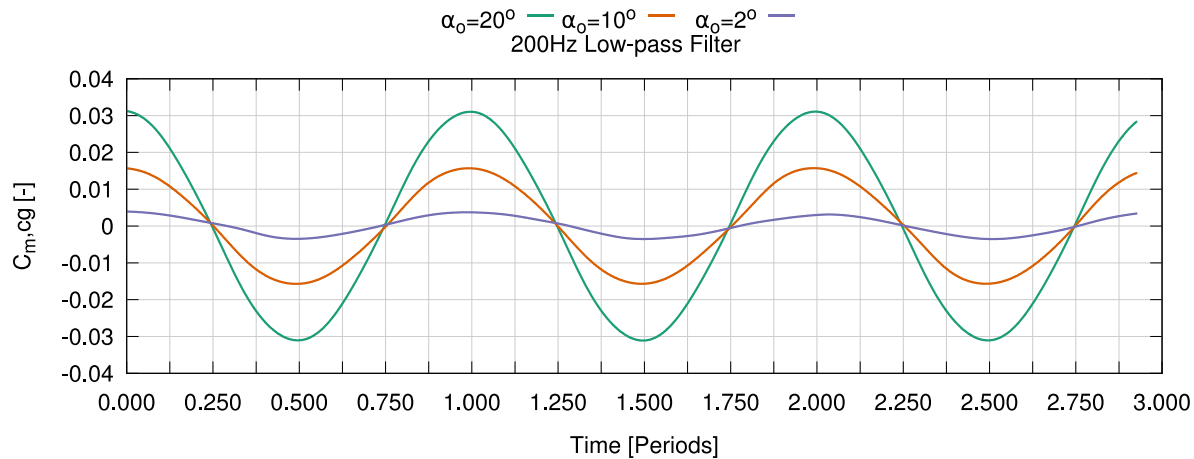
Three periods of forced oscillation at 36.797 (hertz) Hz was simulated using OVERFLOW. The data were reduced using the approach outlined in reference 5. To remove the high-frequency response in the data caused by the unsteadiness in the capsule wake and shear layer, the OVERFLOW output was passed through a 200-Hz low-pass filter. The pitching moment coefficient about the vehicle CG data before and after filtering is shown in Figures 7.4.2-1 and 7.4.2-2, respectively. The  $x$ -axis shows nondimensional time normalized by the period of the forced oscillation.



**Figure 7.4.2-1. Unfiltered Pitching Moment Coefficient from Forced Oscillation Simulations**



	<b>NASA Engineering and Safety Center</b> <b>Technical Assessment Report</b>	Document #: <b>NESC-RP-14-00965</b>	Version: <b>1.0</b>
Title: <b>Independent Assessment of the Backshell Pressure Field for MEDLI2</b>			Page #: 51 of 74

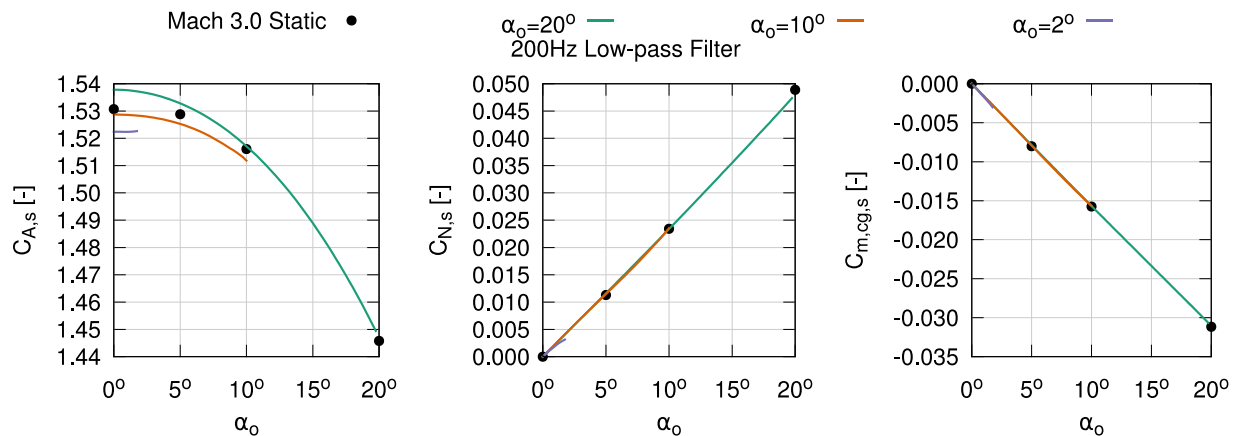


**Figure 7.4.2-2. Filtered Pitching Moment Coefficient from Forced Oscillation Simulations**


This work assumed a linear response in dynamic derivatives with respect to normalized pitch-rate  $\hat{q}$  and that the dynamic derivatives were only a function of angle of attack. The equation for a sample coefficient,  $C_\phi$ , is given as:

$$C_\phi = \underbrace{C_\phi(\alpha)}_{\text{static}} + \underbrace{C_{\phi,\hat{q}}(\alpha)}_{\text{dynamic}} \times \hat{q}$$

Using this approach, an estimate for the static and dynamic aerodynamic coefficients was obtained from the forced oscillation results. Figure 7.4.2-3 shows a comparison of the static aerodynamic estimations obtained from this technique at Mach 2.8 (i.e., lines) co-plotted with results from static pretest CFD simulations at Mach 3.0 (i.e., symbols).

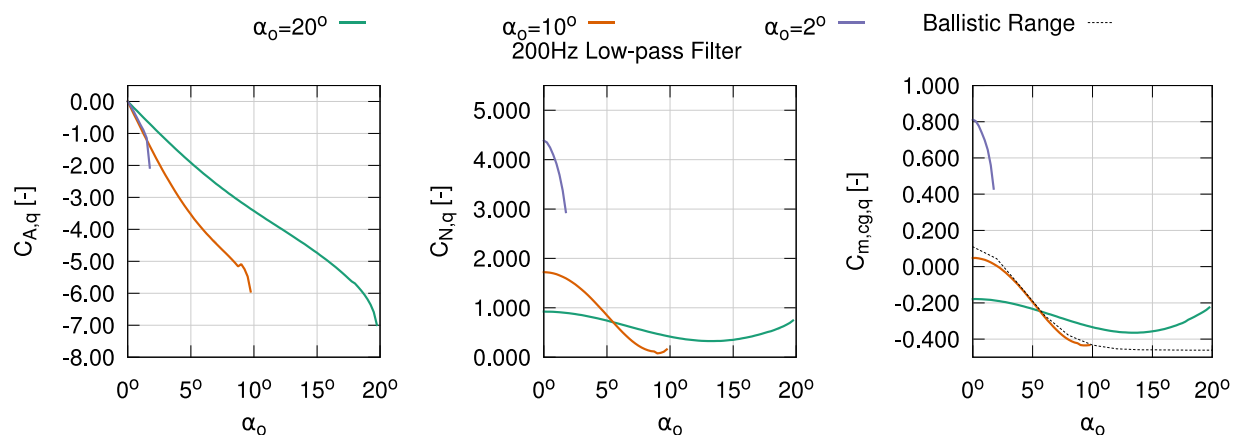


**Figure 7.4.2-3. Comparison of Static Aerodynamics between Forced Oscillations and Unmoving CFD**

	<b>NASA Engineering and Safety Center</b> <b>Technical Assessment Report</b>	Document #: <b>NESC-RP-14-00965</b>	Version: <b>1.0</b>
Title: <b>Independent Assessment of the Backshell Pressure Field for MEDLI2</b>			Page #: 52 of 74


The agreement was good, but there is noticeable variation in the  $C_A$  results. This could imply nonlinearity in the response for that coefficient, but the magnitudes of the discrepancies are within 1 to 2 percent. Some disagreement may be from the discrepancy in Mach number between the static and dynamic data. The agreement observed in the coefficients provides a high level of confidence in the simulations and the analysis technique.

To provide a similar comparison for the estimate for the dynamic coefficients, existing ballistic range data were used [ref. 3]. The data were obtained on a 65-mm MSL capsule and Mach and Reynolds numbers that were different from USARL TEF ballistic range conditions, but were assumed to be representative. Only an estimate of pitch damping coefficient was provided in the MSL ballistic range reference. Figure 7.4.2-4 shows three solid lines representing the OVERFLOW data and a dashed line for the MSL pitch damping curve.

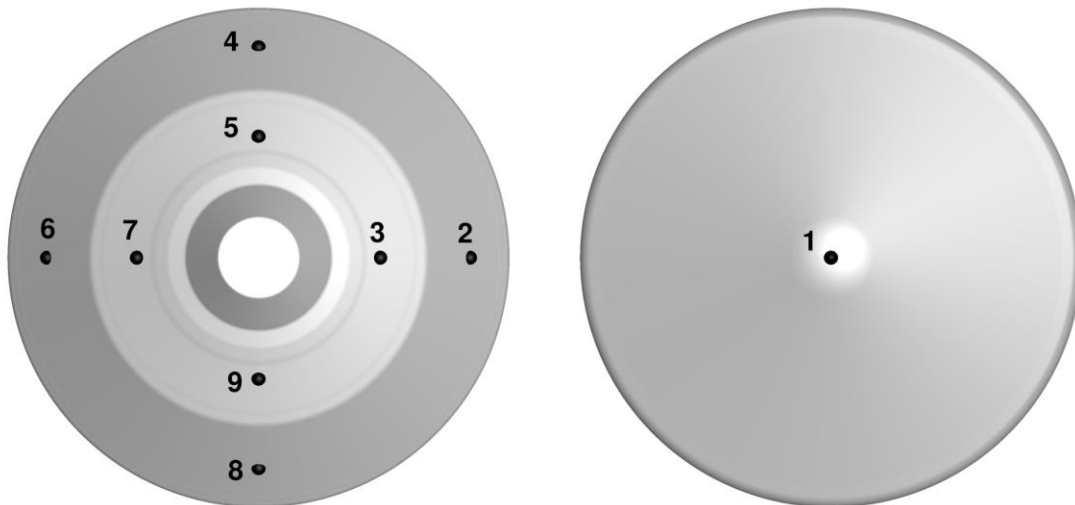


**Figure 7.4.2-4. Comparison of Dynamic Aerodynamic Coefficients between Forced Oscillation CFD and 65-mm Ballistic Range Data**

The agreement between the ballistic range data and the 10-degree simulations was impressive. It is difficult to obtain small-amplitude data in the ballistic range due to disturbances during launch and sabot separation. A large portion of the ballistic range data was obtained when the model was oscillating at moderate angles of attack (i.e., 5 to 15 degrees). It is not surprising that the pitch damping extracted from the 10-degree oscillating case agrees most closely with the ballistic range data. However, detailed analysis of the data reduction methods is required to make any quantitative comparisons between the OVERFLOW results and the ballistic range damping data. The undamped behavior at low angles of attack agrees with data from the MSL ballistic range test, as does the relatively damped behavior at high amplitudes. The CFD results look promising, but further analysis is required that is beyond the scope of this assessment. In the context of this assessment, the CFD and ballistic range damping results being in reasonable agreement is circumstantial evidence that the wake flow is being predicted accurately. Reasonable agreement was expected between the measured and the calculated wake pressures.

	<b>NASA Engineering and Safety Center Technical Assessment Report</b>	Document #: <b>NESC-RP- 14-00965</b>	Version: <b>1.0</b>
Title: <b>Independent Assessment of the Backshell Pressure Field for MEDLI2</b>			Page #: 53 of 74


Pressures were recorded at nine locations on the MSL capsule (see Figure 7.4.2-5 and Table 7.4.2-1). For this analysis, pressure monitors were added in the yaw plane to facilitate anticipated comparison between 6-DOF simulations and data from the experiment. The complete set of pressures is shown in Figures 7.4.2-6 through 7.4.2-8. Looking at the 20- and 10-degree amplitude oscillation cases, the behavior in the heatshield and backshell pressure traces shows the typical phase lag in the response between the two portions of the vehicle. Depending on which side of the backshell is advancing or retreating, a subset of the pressures shows a noticeable lag. The 2-degree amplitude oscillation simulation does not have a strong character in the backshell measurements.

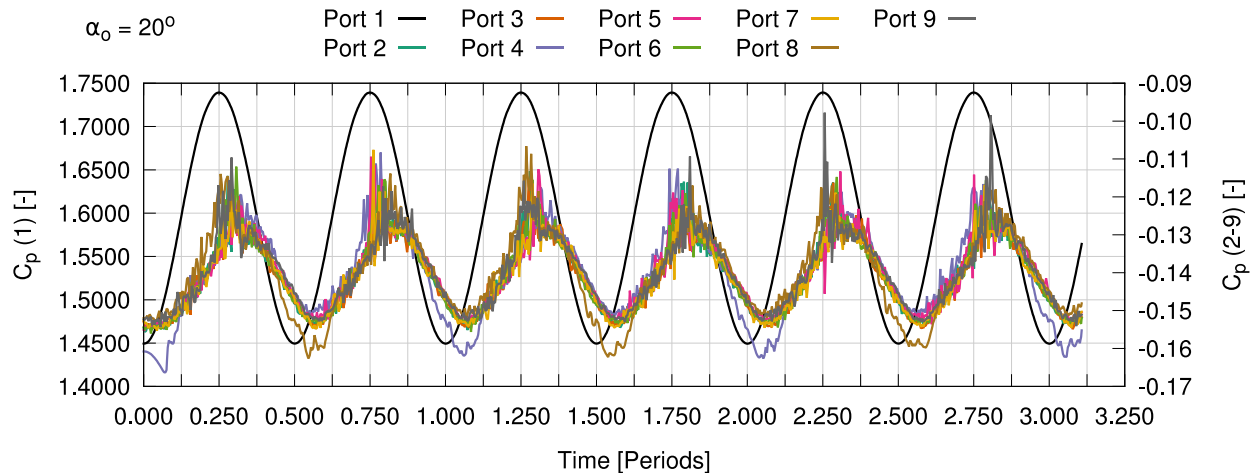


**Figure 7.4.2-5. Pressure Measurement Location for CFD Simulations**

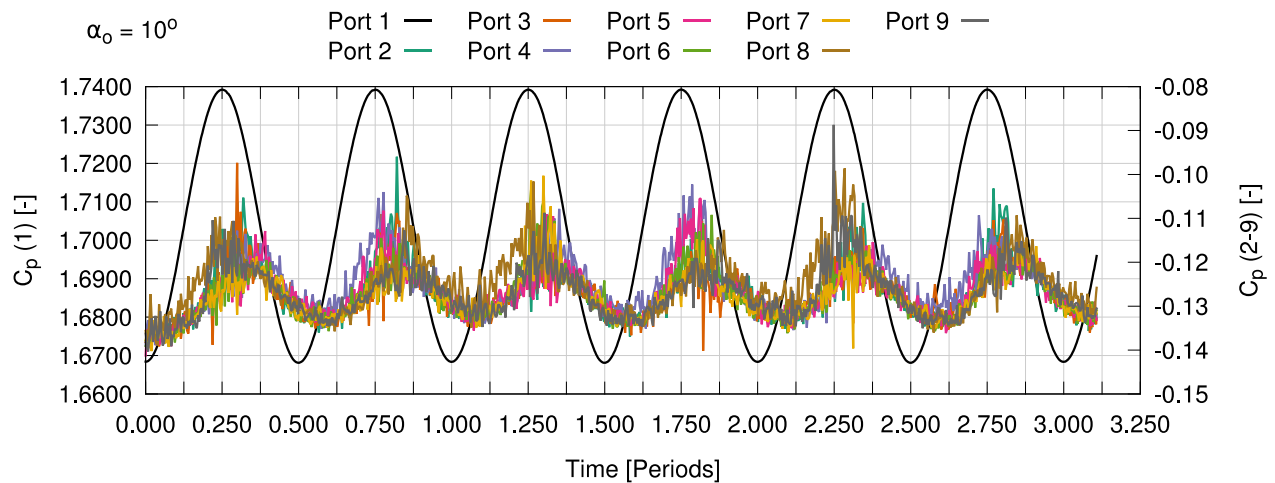
**Table 7.4.2-1. Pressure Probe Locations with Origin at Nose of Model**

Probe	x (cm)	y (cm)	z (cm)
1	0.00	0.00	0.00
2	2.67	0.00	3.79
3	4.22	0.00	2.18
4	2.67	3.79	0.00
5	4.22	2.18	0.00
6	2.67	0.00	-3.79
7	4.22	0.00	-2.18
8	2.67	-3.79	0.00
9	4.22	-2.18	0.00


	<b>NASA Engineering and Safety Center</b> <b>Technical Assessment Report</b>	Document #: <b>NESC-RP-14-00965</b>	Version: <b>1.0</b>
Title: <b>Independent Assessment of the Backshell Pressure Field for MEDLI2</b>			Page #: 54 of 74

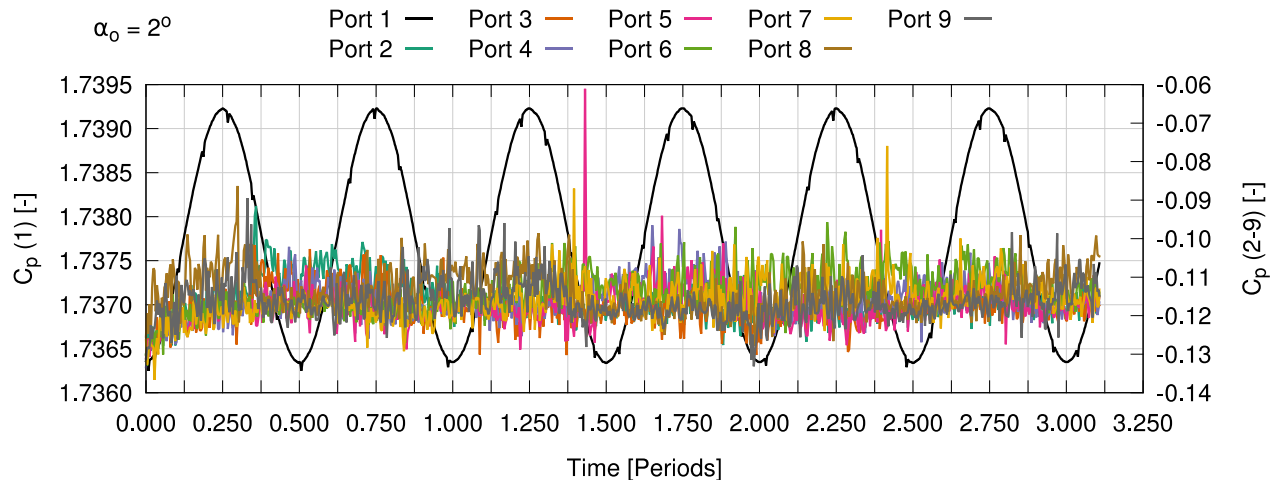


**Figure 7.4.2-6. Pressure Measurements from 20-degree Pitch Amplitude Simulation**



**Figure 7.4.2-7. Pressure Measurements from 10-degree Pitch Amplitude Simulation**

	<b>NASA Engineering and Safety Center</b> <b>Technical Assessment Report</b>	Document #: <b>NESC-RP-14-00965</b>	Version: <b>1.0</b>
Title: <b>Independent Assessment of the Backshell Pressure Field for MEDLI2</b>			Page #: 55 of 74



**Figure 7.4.2-8. Pressure Measurements from 2-degree Pitch Amplitude Simulation**

### 7.4.3 6-DOF CFD Simulation Results

Preliminary results for 6-DOF simulations are shown with the forced oscillation data. Only simulations for the 2- and 10-degree amplitude cases were completed. Qualitative comparisons to the current ballistic range data are provided.

Three significant improvements were made to the data reduction scripts to enable analysis of the 6-DOF simulations:

1. Capsule attitude must be augmented to account for vehicle motion. With a fixed rotation point and no vehicle velocity, the body rotation rate in the pitch plane is  $\dot{\alpha}$ . Rotation coupled with vehicle motion means that the body rotation rate  $\hat{q}$  and  $\dot{\alpha}$  are similar, but not identical.
2. The aerodynamic linear model assumed nondimensional  $q$  was an important parameter. This model now reads the average of  $\hat{q}$  and  $\dot{\alpha}$ .

$$C_{\phi} = \underbrace{C_{\phi}(\alpha)}_{static} + \underbrace{C_{\phi,\hat{q}}(\alpha)}_{dynamic} \times \tilde{q}, \text{ where } \tilde{q} = \frac{\hat{q} + \dot{\alpha}}{2}$$

3. Force, moment, and pressure coefficients were nondimensionalized to a dynamic pressure from the initial Mach 2.8 free stream. After the effective Mach number was calculated due to vehicle motion, these nondimensionalizations required recalculation.

Simulations were allowed to transition to 6-DOF after three periods of forced oscillation. This means that the initial conditions were  $\alpha = \alpha_o$ ,  $\beta = 0$  degrees. No attempt was made to match a specific ballistic range condition. Cases were continued for roughly three periods of free oscillation. The natural period was somewhat larger than that used for the forced oscillation simulations. The 2- and 10-degree cases were undamped.


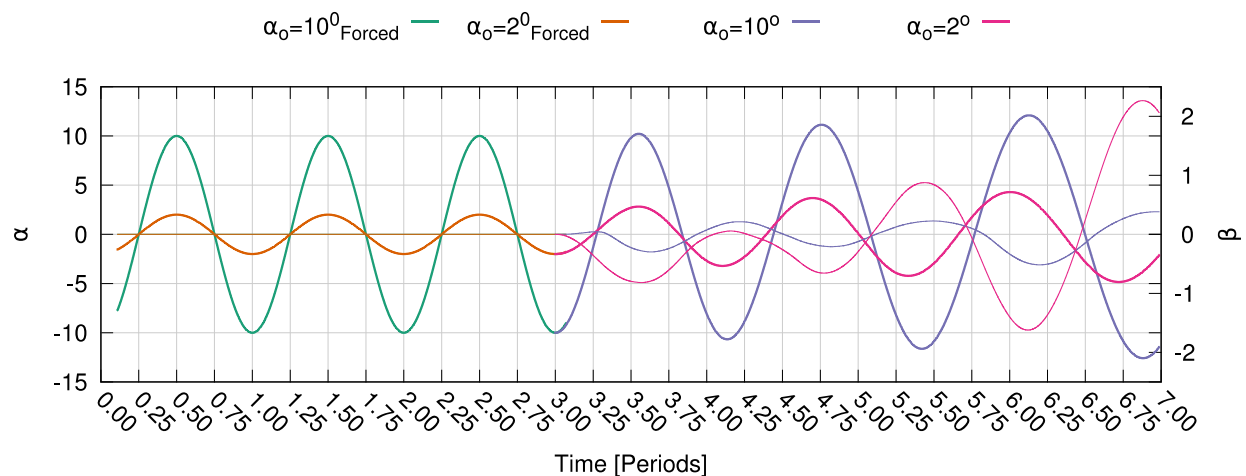
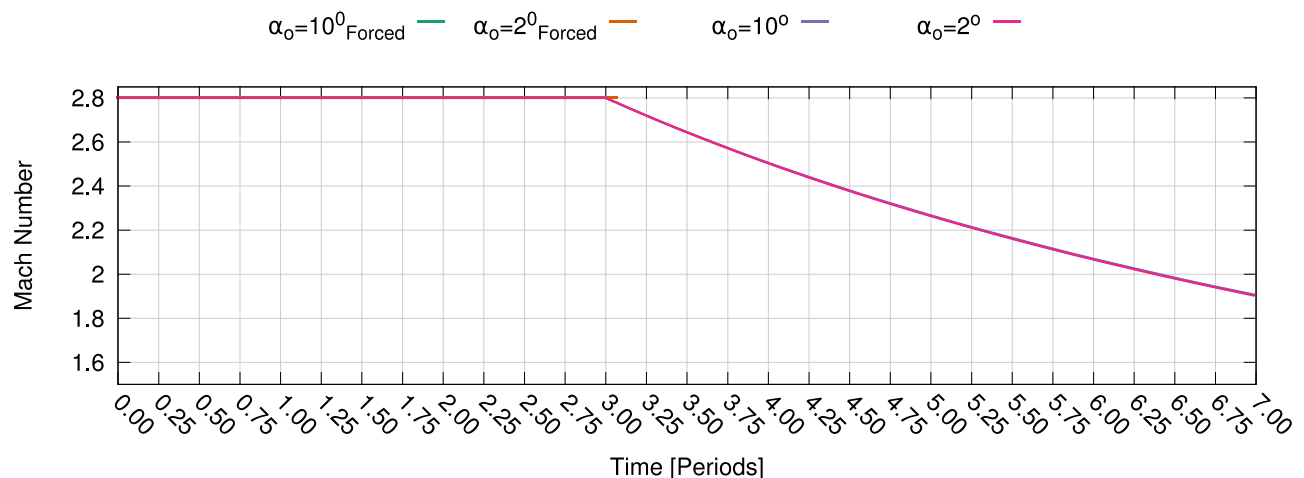
	<b>NASA Engineering and Safety Center</b> <b>Technical Assessment Report</b>	Document #: <b>NESC-RP-14-00965</b>	Version: <b>1.0</b>
Title: <b>Independent Assessment of the Backshell Pressure Field for MEDLI2</b>			Page #: 56 of 74

Figure 7.4.2-9 shows  $\alpha$  (i.e., left-hand axis, bold lines) and  $\beta$  (i.e., right-hand axis, thin lines) for the two 6-DOF simulations. Prior to three periods on the  $x$ -axis is the forced oscillation data. After three periods (i.e., normalized to the forced oscillation frequency) are the 6-DOF results. Once the CFD solution is switched to 6-DOF, the capsule starts oscillating in sideslip  $\beta$ , and the  $\alpha$  amplitude grows to larger amplitudes than that prescribed in the forced oscillation segment of the simulation. As mentioned, the period of oscillation changes, which is evidenced by the periods no longer aligning with the normalized time on the  $x$ -axis.




**Figure 7.4.2-9.  $\alpha$  and  $\beta$  for 6-DOF Simulations**

Figure 7.4.2-10 shows the capsule deceleration by the changing Mach number. For the 2- and 10-degree cases, the behavior is nearly identical following the beginning of 6-DOF motion at a time of three periods. After a time of seven normalized periods, both cases have decelerated to about Mach 1.8.

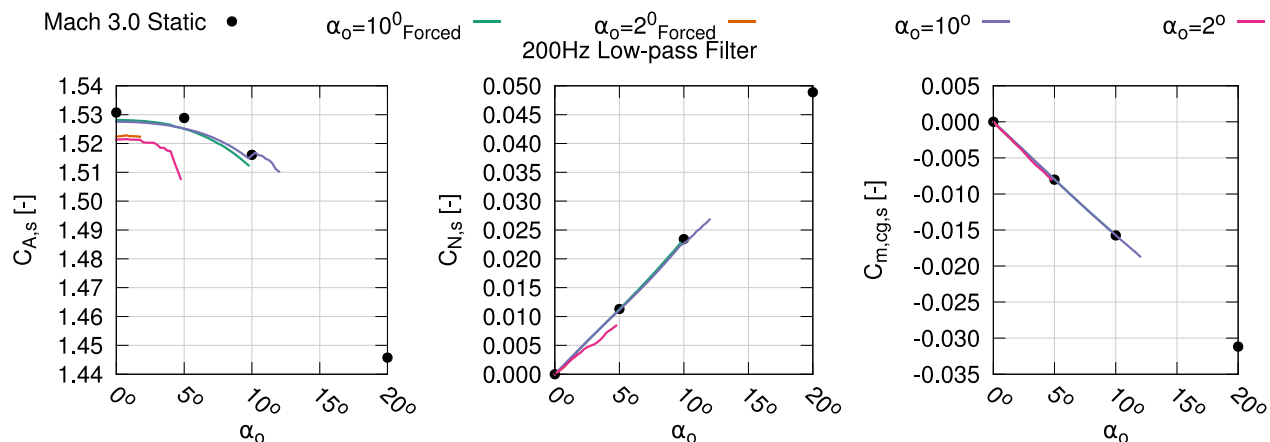


**Figure 7.4.2-10. Mach-number Variation during 6-DOF Simulations**



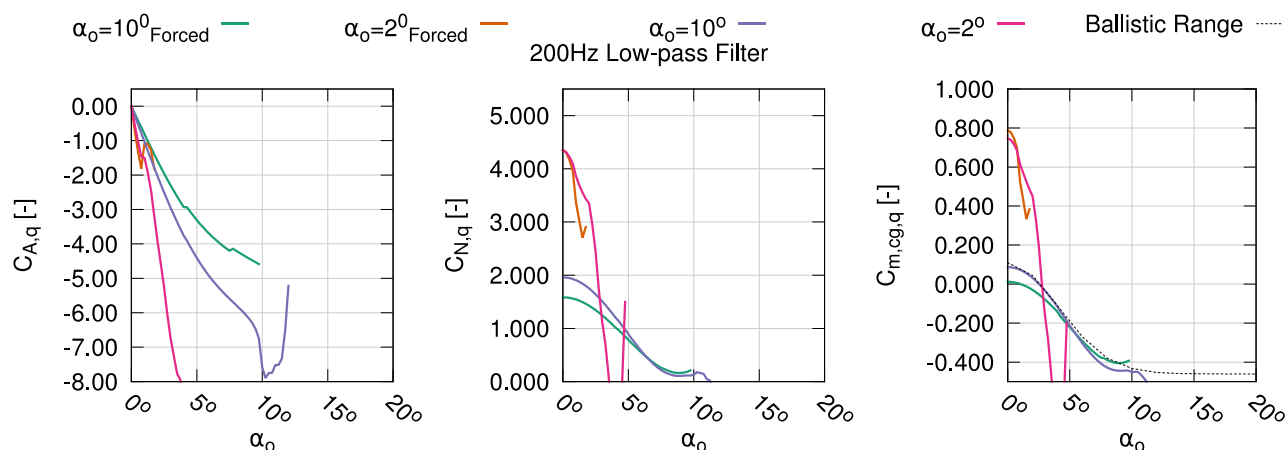
	<b>NASA Engineering and Safety Center</b> <b>Technical Assessment Report</b>	Document #: <b>NESC-RP-14-00965</b>	Version: <b>1.0</b>
Title: <b>Independent Assessment of the Backshell Pressure Field for MEDLI2</b>			Page #: 57 of 74

Computed static and dynamic coefficients are compared with the forced oscillation results. In Figure 7.4.2-11, the static coefficients show agreement to the initial angle of the forced oscillation data. For attitudes greater than the initial amplitude, less data are available (i.e., the amplitude is growing from period to period) and the behavior is more erratic.




**Figure 7.4.2-11. Comparison of Static Aerodynamics between Fixed, Forced Oscillation, and 6-DOF CFD Simulations**

The dynamic coefficients are shown in Figure 7.4.2-12. The 65-mm ballistic range data were included for the pitching moment coefficient as a reference. The 10-degree data continues to show agreement with the range data. However, note the range data are for Mach 3.0, while the CFD data included data from Mach 1.8 through 2.8, as shown in Figure 7.4.2-10.



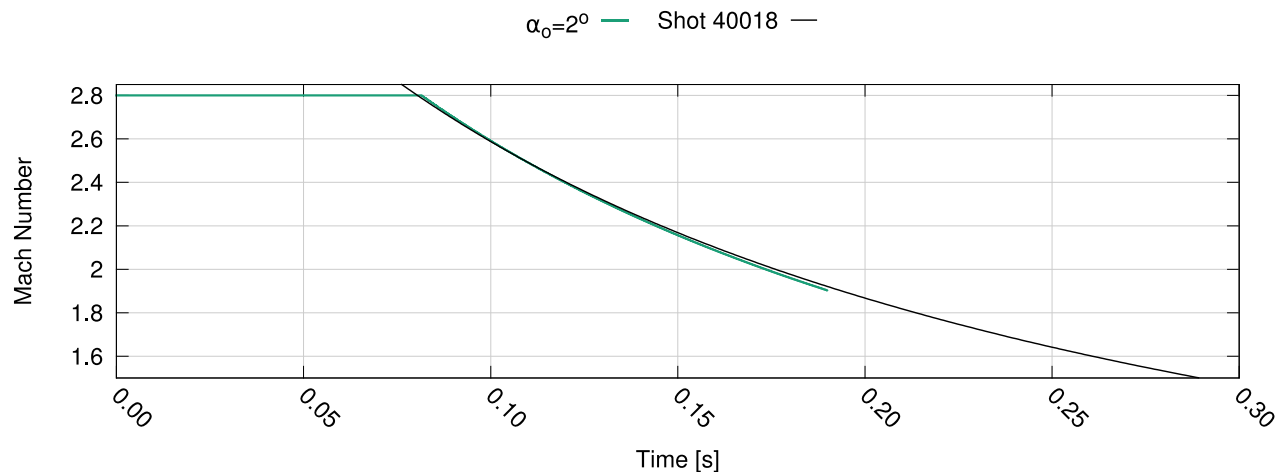
**Figure 7.4.2-12. Comparison of Dynamic Aerodynamic Coefficients between Forced Oscillation CFD, 6-DOF CFD, and 65-mm Ballistic Range Data**

	<b>NASA Engineering and Safety Center Technical Assessment Report</b>	Document #: <b>NESC-RP-14-00965</b>	Version: <b>1.0</b>
Title: <b>Independent Assessment of the Backshell Pressure Field for MEDLI2</b>			Page #: 58 of 74

Three preliminary comparisons were made to the ballistic range data and the OVERFLOW 6-DOF simulations. Shot 40018 had an initial Mach number and  $\alpha_{Total}$  amplitude similar to that of the 2-degree 6-DOF simulation. Notable differences between the 6-DOF simulations and Shot 40018 were:


- Gravity was not included in the CFD, making the  $z$ -position/velocity difficult to compare.
- The 6-DOF simulations used MOI and the vehicle mass consistent with Shot 40021, which was different than the model for Shot 40018.
- For comparison, the data were shifted in time to match initial conditions. Each comparison used a different shift since the 6-DOF simulations were not initialized to the same conditions as any one shot.

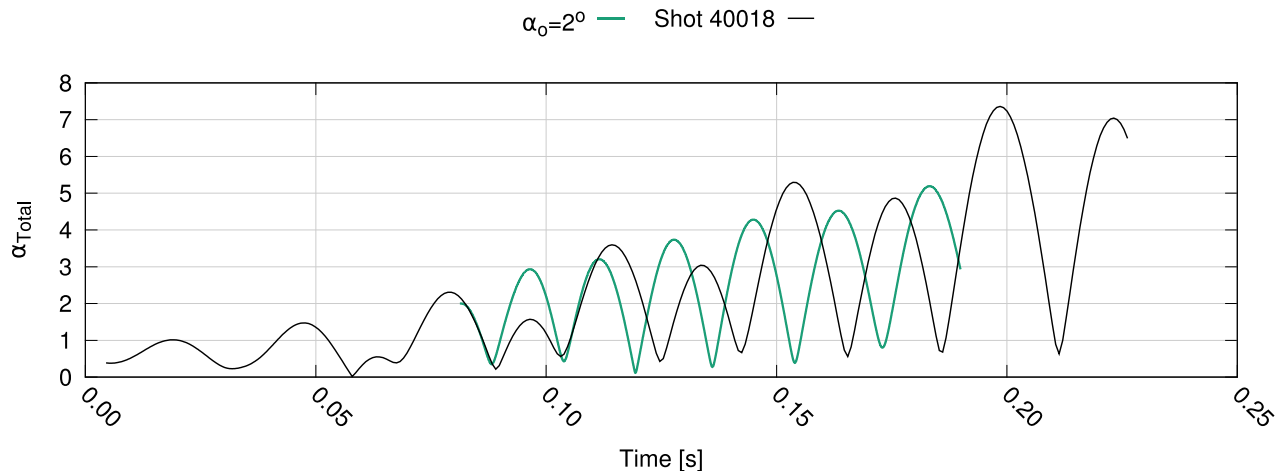
Figure 7.4.2-13 shows capsule Mach number as a function of time for the 2-degree 6-DOF simulation (i.e., colored line) and Shot 40018 (i.e., black line). The Mach number decay is more pronounced in the CFD analysis than in the reconstructed data. This is not surprising since drag on a bluff body can be difficult to match using CFD. Further, the two vehicles have different oscillation character, which can contribute to a change in the net drag force on the capsule.



**Figure 7.4.2-13. Mach-number Variation in CFD versus Shot 40018**

Figure 7.4.2-14 shows the  $\alpha_{Total}$  as a function of time for the two data sets. The peaks in the ballistic range data (i.e., black line) alternate in their magnitude, which is not seen in the CFD data (i.e., colored line). Both data sets show undamped oscillations, but the ballistic range data have more pronounced growth. By the end of the trace, the  $\alpha_{Total}$  for Shot 40018 is greater than 7 degrees.

	<b>NASA Engineering and Safety Center Technical Assessment Report</b>	Document #: <b>NESC-RP- 14-00965</b>	Version: <b>1.0</b>
Title: <b>Independent Assessment of the Backshell Pressure Field for MEDLI2</b>			Page #: 59 of 74



**Figure 7.4.2-14.  $\alpha_{Total}$  Growth in CFD versus Shot 40018**

## 7.5 Posttest Results using US3D

### 7.5.1 Posttest CFD Matrix


Forced oscillation cases using the US3D code were run to compare with the OVERFLOW results. US3D allows cases to be run simulating Mars conditions.

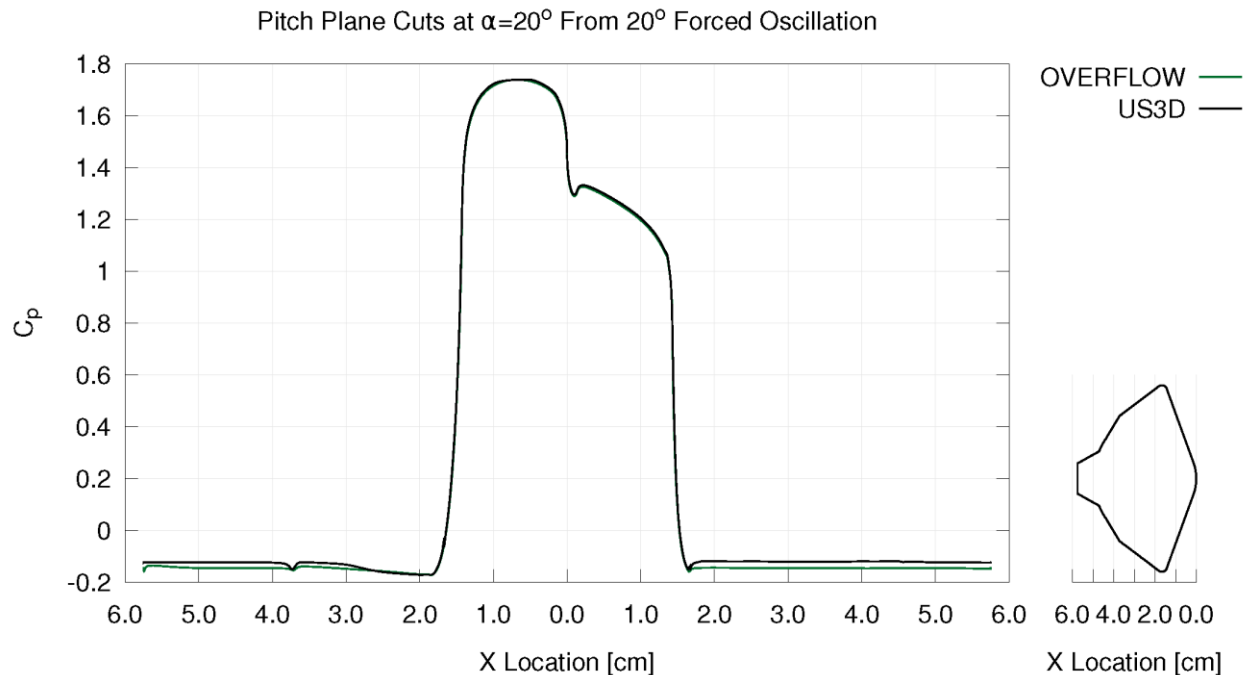
The US3D posttest simulation was run at Mach 2.8 with free-stream conditions consistent with Shot 40021. A forced oscillation simulation with a pitch amplitude of 20 degrees was run to model the wake flow to angles of attack expected during Mars 2020 flight and bounding those observed in Shot 40021.

A similar forced oscillation case at Mars conditions was run. The results of the Mars and Earth cases were compared to look for wake behavior at Mars conditions that would affect any interpretation of the ballistic range results for the MEADS port location on the Mars 2020 backshell.

### 7.5.2 Comparison of US3D and OVERFLOW, Mach = 2.8, 20-degree Forced Oscillation


Comparable US3D and OVERFLOW cases were run at Mach 2.8 and a forced pitching oscillation with an amplitude of 20 degrees. Pressure variations along the capsule OML where the pitch plane intersects the body are shown in Figure 7.5.2-1. Pressures were extracted at an instant when the model was at its peak amplitude (i.e., 20 degrees) during the CFD runs. Overall agreement was good. Forebody pressures continuing around the capsule shoulders (i.e.,  $x = 0$  to  $\sim 1.75$  cm) were in good agreement. The wake pressures were different. Subsequent figures show the wake pressures in more detail.

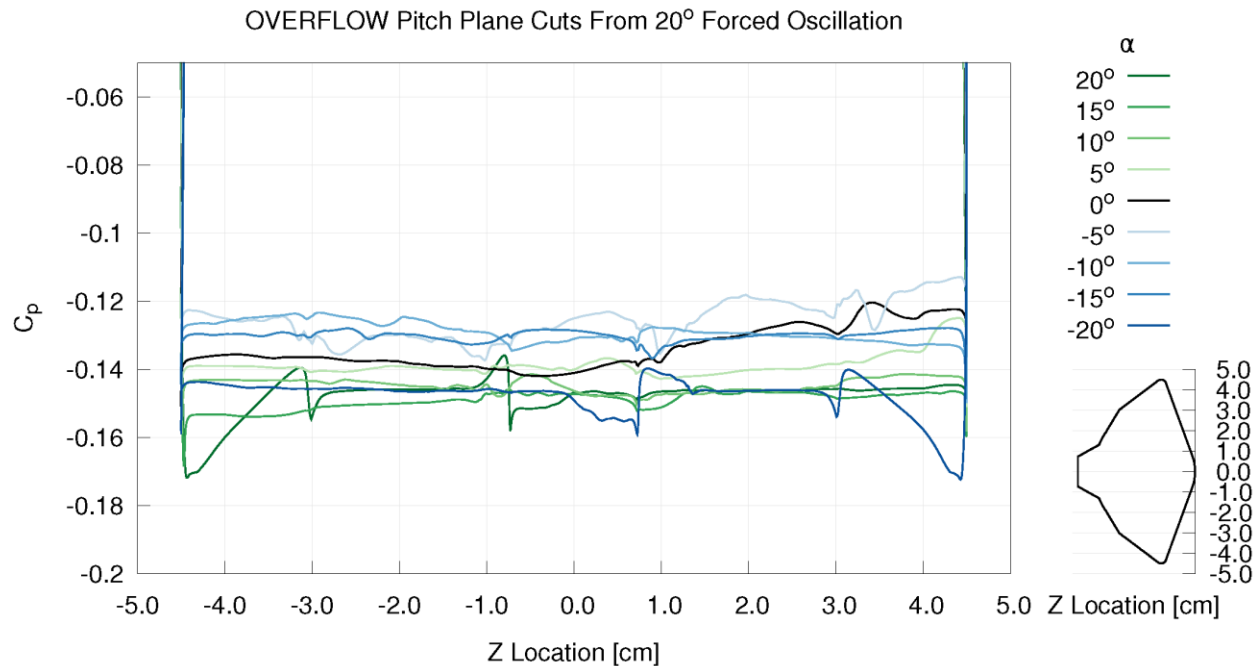
	<b>NASA Engineering and Safety Center Technical Assessment Report</b>	Document #: <b>NESC-RP-14-00965</b>	Version: <b>1.0</b>
Title: <b>Independent Assessment of the Backshell Pressure Field for MEDLI2</b>			Page #: 60 of 74



**Figure 7.5.2-1. OVERFLOW and US3D Pressure Coefficient Contours along Pitch Plane, 20-degree Angle of Attack**

Figure 7.5.2-2 shows a number of wake pressure contours from the OVERFLOW 20-degree forced oscillation simulation taken as the model swept through a number of positive and negative pitch angles. The +20 and -20-degree contours show local variations on the backshell to be symmetric. At +20 degrees, OVERFLOW appears to show flow reattachment on the first backshell cone (i.e.,  $|z| > 3$  cm) and local recompression on the third cone (i.e.,  $|z| \sim 0.75$  cm). At smaller angles, the wake pressure is more constant over the entire backshell, rising and falling as with angle of attack. The 0-degree angle of attack curve shows a pronounced asymmetry between the positive and negative sides of the model. Unsteady aerodynamics suggest there should be a lag of the pressure behind the instantaneous attitude of the model. There are likely other variations that would average out by taking multiple plane cuts from subsequent oscillations. For the MEADS2 project, the results from these plane cuts show results similar to the ballistic range data (i.e., roughly constant pressure, rising and falling with angle of attack). At the peak amplitude, it appears the flow starts to reattach. This will be considered when comparing the ballistic range data with the CFD results.

	<b>NASA Engineering and Safety Center Technical Assessment Report</b>	Document #: <b>NESC-RP- 14-00965</b>	Version: <b>1.0</b>
Title: <b>Independent Assessment of the Backshell Pressure Field for MEDLI2</b>			Page #: 61 of 74




**Figure 7.5.2-2. OVERFLOW Wake Pressure along Pitch Plane, Captured at Different Angles of Attack**

Comparisons of the wake pressures predicted by US3D and OVERFLOW are plotted in Figures 7.5.2-3 and 7.5.2-4. Both pressure curves were taken from Mach-2.8 forced-oscillation cases as the model passed through the peak amplitude of +20 degrees. Both sets of CFD results show approximately constant pressures to the first cone (i.e.,  $|z| > 3$  cm), although they differ by a roughly constant offset. Both codes see a disturbance near  $z = 3$  cm, with pressure decreasing on the first cone, suggesting reattached flow. The US3D results do not show the recompression feature on the PCC. In the US3D solution, there appears to be a pressure change at  $z = +1.75$  cm, near the junction between the PCC and the second cone. This is emphasized in Figure 7.5.2-4, where the vertical axis of the graph has been stretched. However, that variation is small compared with the differences between the two codes. Both codes suggest the first cone windward area ( $z < -3$  cm) can see reattachment when the model is at a 20-degree angle of attack. Both codes show roughly constant pressure at other model locations.

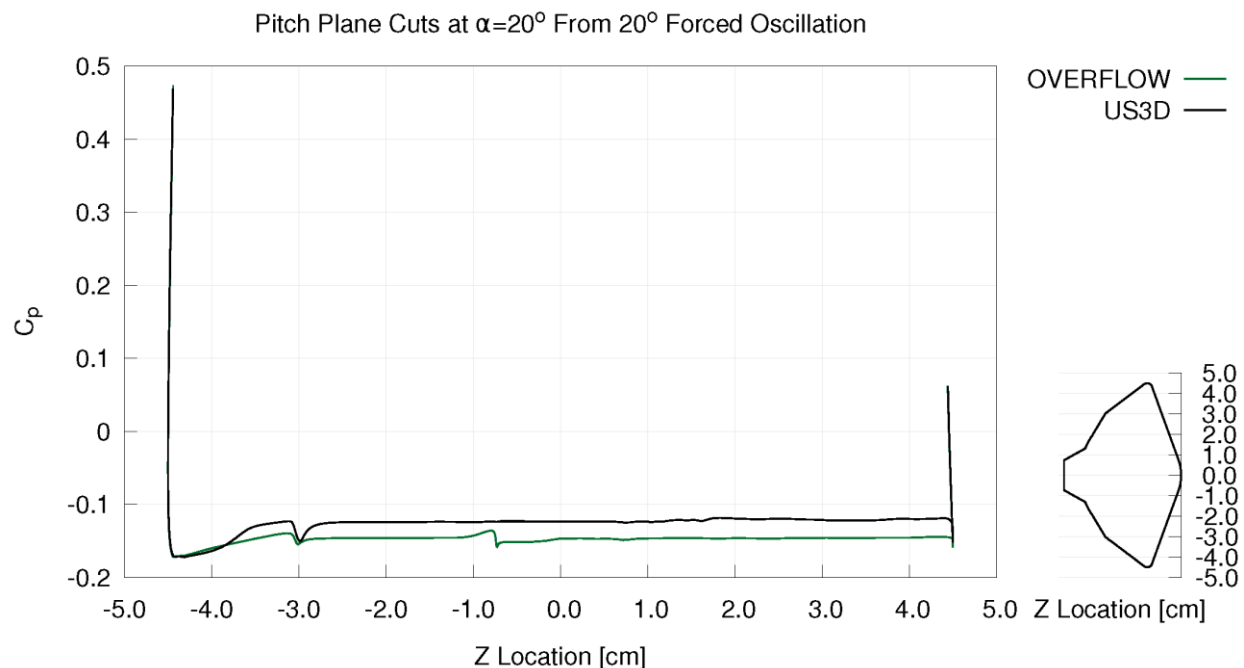
The code-to-code differences suggest further investigation, but this is outside the assessment scope. The pretest CFD work showed disagreement in the  $C_A$  at Mach-3.0 conditions consistent with the wake pressure differences shown. Possible disagreement sources include:

- Differences in the separation behavior between the two turbulence models (i.e., shear stress transport in OVERFLOW and Spalart-Allmaras in US3D).

	<b>NASA Engineering and Safety Center Technical Assessment Report</b>	Document #: <b>NESC-RP-14-00965</b>	Version: <b>1.0</b>
Title: <b>Independent Assessment of the Backshell Pressure Field for MEDLI2</b>			Page #: 62 of 74


- Variable capsule resolution and immediate volume grid between the two solvers.
- Variation in grid resolution at 20 degrees (i.e., OVERFLOW includes moving overset boundaries, and US3D includes deformation due to capsule rotation).
- Differences in the accuracy of the numerics.

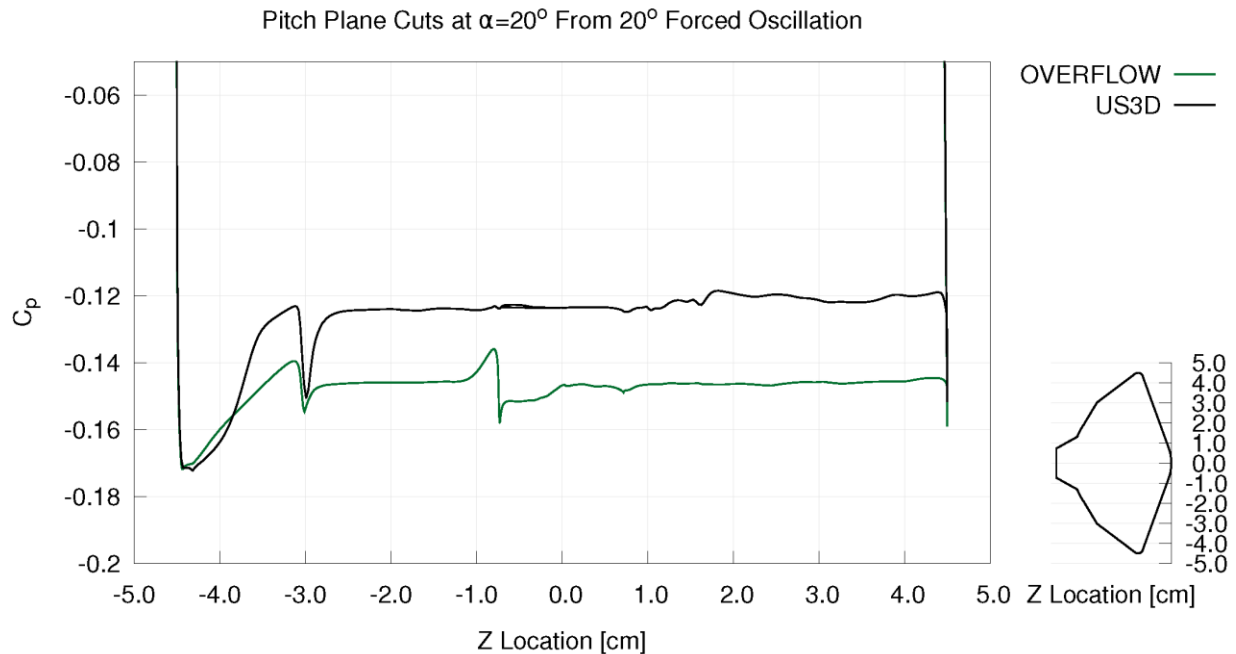
Regardless of the source, the code differences are in quantifying the wake pressure. Both solvers predict attached flow on the first windward conic and identify the leeward side as being a preferred candidate for wake pressure measurement.



**Figure 7.5.2-3. Comparison OVERFLOW and US3D Predictions of Wake Pressure Coefficient along Pitch Plane**




	<b>NASA Engineering and Safety Center Technical Assessment Report</b>	Document #: <b>NESC-RP-14-00965</b>	Version: <b>1.0</b>
Title: <b>Independent Assessment of the Backshell Pressure Field for MEDLI2</b>			Page #: 63 of 74



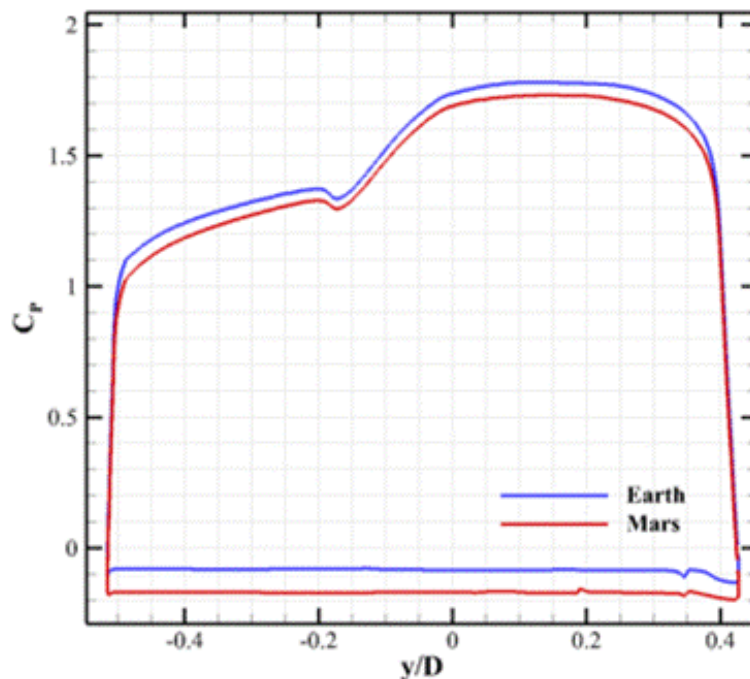
**Figure 7.5.2-4. OVERFLOW/US3D Wake Pressure Coefficient Comparison, Stretched Vertical Axis**

### 7.5.3 Effect of Atmosphere on the Backshell Pressure Profile


The analysis in the previous section used air as the gas to emulate the environment of the ballistic range test. US3D has the capability to run a simulation with a carbon dioxide atmosphere, as would be experienced on Mars. A Mars simulation was run to investigate whether there are substantive differences due to the atmosphere composition that would affect pressure port placement. Such a comparison is not practical in available wind tunnel or ballistic range facilities. To that end, the ballistic range configuration was scaled to a 4.5-m diameter and simulated using US3D in Martian atmosphere at the free-stream conditions where the predicted MSL trajectory passed through Mach 2.8. This corresponds to a free-stream velocity of 640.57 m/s (i.e., Mach 1.87), a free-stream density of 0.0046 kg/m<sup>3</sup>, and a free-stream temperature of 228.8 K. Figure 7.5.3-1 shows the comparison of the nondimensional pressure coefficient for the two atmospheres. Overall, the profiles appear similar, with the Martian result experiencing lower compression. This effect is owed to the gamma dependence in the Rankine-Hugoniot jump conditions. Figure 7.5.3-2 shows a closer view of the backshell portion of the previous figure. The leeward portion of the second conic is highlighted in yellow. For both atmospheres, a flat profile on the leeward side is indicative of a fully separated flow; therefore, it can be concluded that the atmospheric composition does not impact the viability of the proposed instrument location. The somewhat smoother profile seen in the Mars simulation is likely due to the effect of the significantly lower Reynolds number at Mars conditions. On the windward side, there is a small disturbance on the second cone. This disturbance is similar to, but less

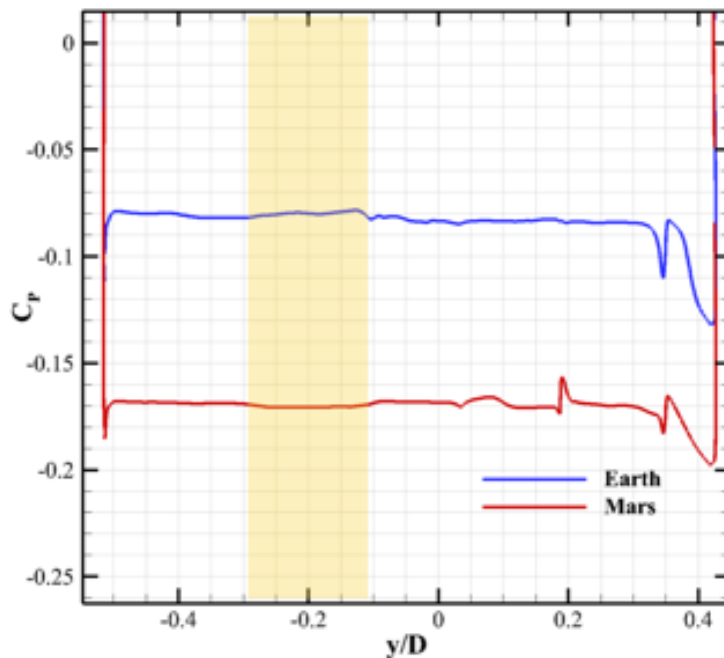
	<b>NASA Engineering and Safety Center</b> <b>Technical Assessment Report</b>	Document #: <b>NESC-RP-14-00965</b>	Version: <b>1.0</b>
Title: <b>Independent Assessment of the Backshell Pressure Field for MEDLI2</b>			Page #: 64 of 74

pronounced than, the disturbance on the first cone predicted at ballistic range conditions. The wake structure at Mars conditions may be more susceptible to local reattachment flow features over a larger portion of the windward side of the capsule backshell. The details of the local pressure variations should be studied in more detail. The backshell surface pressures predicted at Mars conditions are further evidence that the port should be located on the leeward side. It also suggests that additional transducers located on the windward side could be helpful in understanding the backshell contribution to the drag characteristics of the Mars 2020 flight vehicle. The magnitude of the local pressure fluctuation is small but may be indicative of a region where more significant variations occur in flight. Additional CFD should be performed to compare Earth and Mars wake flows, and to prepare for interpreting MEDLI2 flight data.



**Figure 7.5.3-1. Comparison of Pressure Coefficient in Pitch Plane for Earth (Mach 2.8, 90-mm-diameter model at ballistic-range conditions) and Mars (Mach 2.8, 4.5-m diameter MSL capsule at reconstructed entry conditions) Atmospheres**

	<b>NASA Engineering and Safety Center Technical Assessment Report</b>	Document #: <b>NESC-RP-14-00965</b>	Version: <b>1.0</b>
Title: <b>Independent Assessment of the Backshell Pressure Field for MEDLI2</b>			Page #: 65 of 74




**Figure 7.5.3-2. Zoomed View of Pressure Coefficient on Backshell for Earth and Mars Atmospheres**

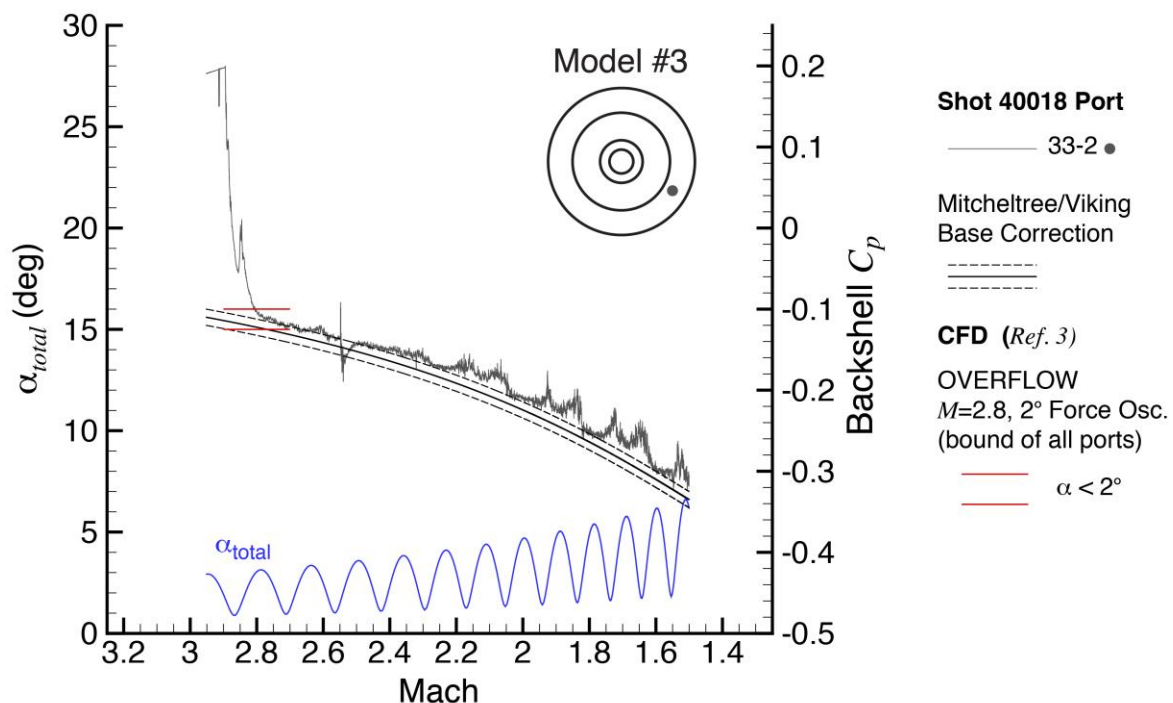
## 7.6 Comparison of Ballistic Range Data and CFD

The CFD and ballistic range data are combined in two comparison plots shown in Figures 7.6-1 and 7.6-2. These comparisons provide the best summation of the ballistic range data, the focused area where the CFD analysis was calculated, and how the CFD codes agree with the experimental data. For comparison with the CFD results presented, the pressure data from the ballistic range shots were nondimensionalized into pressure coefficients. The in-range free-stream pressures recorded by the USARL for each shot, with the reconstructed Mach number, were used to calculate the pressure coefficients.

As reported above, Shot 40018 provided a single backshell pressure measurement through the range as the model oscillated at small angles of attack. The pressure coefficient from port 33-2 is plotted against CFD results and the Mitcheltree base correction model in Figure 7.6-1. The reconstructed total angle of attack is plotted for reference. The pressure coefficient ( $C_p$ ) data show that the measured pressure is at or above the upper uncertainty bound of the Mitcheltree model, indicating higher wake pressures than for the model. The wake pressure coefficients calculated using the OVERFLOW CFD code are shown in Figure 7.6-1 as well. Two lines are plotted for the CFD results, representing the upper and lower bounds of the coefficients calculated. OVERFLOW was run at Mach 2.8, but the bounding lines span a Mach range from 2.9 to 2.7. The reconstructed Mach number has some uncertainty, so the exact condition to


	<b>NASA Engineering and Safety Center Technical Assessment Report</b>	Document #: <b>NESC-RP-14-00965</b>	Version: <b>1.0</b>
Title: <b>Independent Assessment of the Backshell Pressure Field for MEDLI2</b>			Page #: 66 of 74

compare the CFD and experimental data is not known. A conservative bound on the Mach number accuracy was assumed to be  $\pm 0.1$  Mach. The OVERFLOW  $C_p$  bounds were determined from the pressure coefficients calculated on the backshell first cone, as shown in Figure 7.4.2-8. Shot 40018 is exiting the region influenced by the launch gases at Mach 2.8. The backshell pressure is decreasing and starts to assume a nominal wake pressure. The model total oscillation amplitude is approximately 3 degrees at this point. The measured pressure approaches the upper bound of the Mitcheltree model. As discussed, this appears to be consistent with the model being at a smaller angle of attack than the Viking capsule, from which the base pressure model was derived. The OVERFLOW pressures appear to be higher than the wake model and bound the port 33-2 pressure data. The US3D pressures appear to agree well with the wake model.



**Figure 7.6-1. Shot 40018, Comparison of Measured Pressure Coefficients with CFD Calculations**


Data from the US3D and OVERFLOW 20-degree forced oscillation calculations are plotted in Figure 7.6-2 to compare with pressures recorded in Shot 40023. The OVERFLOW pressure coefficient bounds were determined from the results plotted in Figure 7.4.2-6. The red lines through the OVERFLOW data points approximate the region of comparison, reflecting uncertainty in the reconstructed Mach number. The US3D  $C_p$  points reflect the maximum and minimum coefficients observed on the pitch plane in the 20-degree forced oscillation solution plotted in Figures 7.5.2-1 through 7.5.2-4 at the maximum angle of 20 degrees. Initially, the OVERFLOW pressure variations agree with the pressure variations measured by the three backshell pressure ports on Model #2 during this shot. The wake pressure absolute magnitude

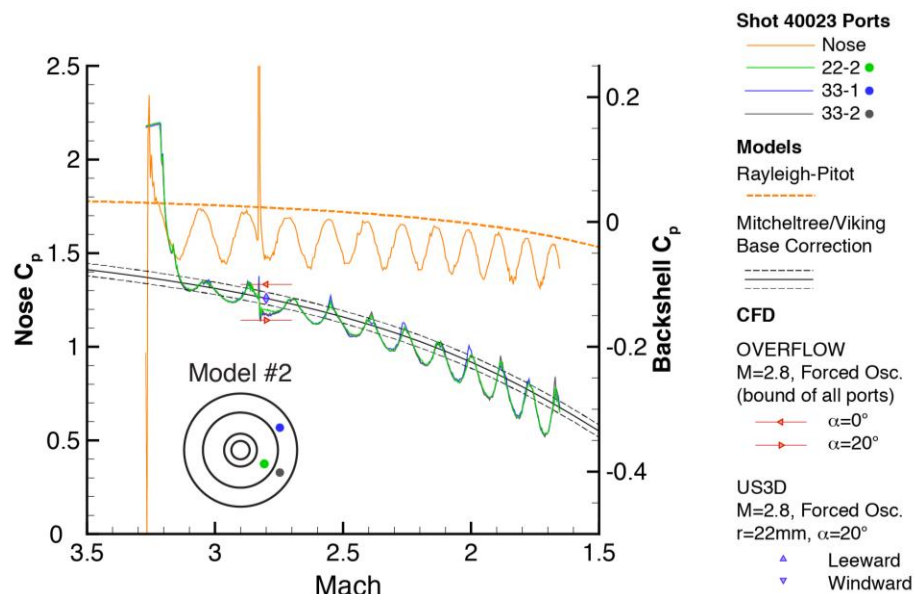
	<b>NASA Engineering and Safety Center Technical Assessment Report</b>	Document #: <b>NESC-RP-14-00965</b>	Version: <b>1.0</b>
Title: <b>Independent Assessment of the Backshell Pressure Field for MEDLI2</b>			Page #: 67 of 74

and angle of attack variation are closely predicted. Though at a constant Mach number, the wake pressures plotted in the OVERFLOW 20-degree forced oscillation solution (see Figure 7.4.2-6) vary in a similar manner to the wake pressures measured on the ballistic range model. For the CFD and the experimental data, the pressure variations appear to be driven by the total angle of attack regardless of port location. As noted, port 22-2 deviates from the other ports. This may be related to local flow phenomena near the PCC. However, in Figure 7.4.2-6, the OVERFLOW 20-degree forced oscillation results show the two most outboard ports (4 and 8) deviate from all other ports when the model is at peak amplitude. The departures of the pressure histories at ports 4 and 8 from the other pressure ports alternate when they are the most windward. The pressures measured by ports 33-1 and 33-2 appear to deviate only when they are most windward, but agree with port 22-2 when leeward. With supporting evidence from CFD, it is likely that Shot 40023 experienced flow attachment on the windward side of the first backshell cone at large angles of attack (i.e., total angle of attack > 20 degrees). There is a pressure history discontinuity as the model flies into the range. The observed deviation of port 22-2 occurs just after entry into the range and this disturbance. In addition to flow attachment (or alternatively), it is possible that the pressure deviations may be affected by flight through the range aperture.

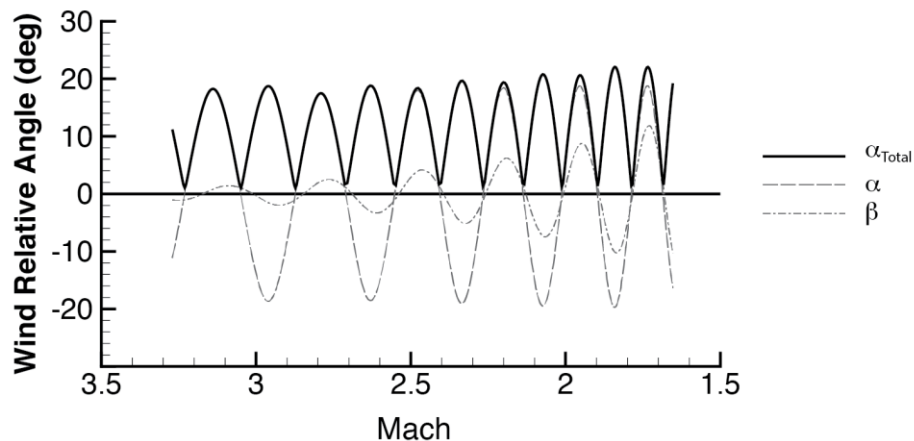
The US3D data points plotted in Figure 7.6-2 reflect the upper and lower bounds of the pressure coefficients on the second backshell cone on the pitch plane at a 20-degree angle of attack. In Figure 7.5.2-4, the US3D pressure coefficient becomes more negative on the windward side first cone. Near the capsule shoulder, US3D and OVERFLOW are in agreement. Inboard, the US3D data points are less negative than the 20-degree OVERFLOW point. The US3D wake pressure is higher (i.e., closer to the free stream) than the OVERFLOW prediction at 20 degrees. This is consistent with the comparisons described in Section 7.5.2. While the CFD solutions predict different separated wake pressures, both predict that the model will see attachment on the windward side of the first cone at large angles of attack. This attachment does appear to be present in the Shot 40023 pressure data.

The large wake pressure variation with angle of attack measured by the ballistic range model in Shot 40023, and the similar variation shown in the OVERFLOW results indicate that angle of attack is the primary determiner of the wake pressure. Pressure port location is less significant and there appears to be no critical area to avoid that might see significant local flow features that could confuse the interpretation of a single pressure measurement (especially on the second cone section). However, as both CFD codes and the pressure data from Shot 40023 suggest flow attachment occurs on the windward side of the model at large angles of attack (i.e.,  $\alpha > 20$  degrees), the preference is to locate the pressure port on the capsule leeward side. While the CFD and experimental data suggest that pressure changes due to flow attachment are a second-order effect, locating the MEADS2 port on the leeward side ensures that the measured pressures will always be in the separated region of the backshell. This will help with interpretation of the MEADS2 data and its use in corroborating the wake contribution to the reconstructed  $C_A$ .

	<b>NASA Engineering and Safety Center</b> <b>Technical Assessment Report</b>	Document #: <b>NESC-RP-14-00965</b>	Version: <b>1.0</b>
Title: <b>Independent Assessment of the Backshell Pressure Field for MEDLI2</b>			Page #: 68 of 74




*a) Pressure Coefficient Comparison*



*b) Reconstructed Attitude History*

**Figure 7.6-2. Shot 40023, Comparison of Measured Pressure Coefficients with CFD Calculations**




	<b>NASA Engineering and Safety Center Technical Assessment Report</b>	Document #: <b>NESC-RP-14-00965</b>	Version: <b>1.0</b>
Title: <b>Independent Assessment of the Backshell Pressure Field for MEDLI2</b>			Page #: 69 of 74

## 8.0 Findings, Observations, and NESC Recommendations

### 8.1 Findings

The following findings were identified:

- F-1.** Pretest analysis correctly determined lateral CG offset requirements for ballistic range models.
- F-2.** The USARL ballistic range onboard recorder (OBR) survived initial launch loads to record data during flight of the instrumented ballistic range models, except Model #5 on Shot 40019.
- F-3.** The test program demonstrated the correlation of recorded onboard wake pressure data with attitude and Mach number histories reconstructed from external TEF shadowgraph data.
- F-4.** Onboard data recording during Shots 40017 and 40021 stopped abruptly during flight in the vicinity of a break screen.
- F-5.** Trajectory reconstructions could be extrapolated to the gun barrel exit to correlate model attitude with pressures recorded before range entry.
- F-6.** Shot 40023 recorded pressure data from all transducers from launch to catcher box impact.
- F-7.** Ballistic range Shot 40018 recorded one backshell pressure at small total angles of attack as the model flew down the range until impact in the catcher box.
- F-8.** Shots 40021 and 40023 experienced oscillation amplitudes that bound the expected Mars 2020 capsule trim angle of attack.
- F-9.** Angle of attack was found to be the primary determiner of the wake pressure for a given Mach number. Pressure port location is a second-order effect.
  - The three backshell pressures recorded on Shot 40023 showed close agreement, varying primarily with total angle of attack.
  - Shot 40023 backshell pressure port showed the wake pressure coefficient varying with angle of attack with greater amplitude than the Viking base correction model uncertainty bounds, indicating that the base contribution to  $C_A$  (wake pressure) is a strong function of the trim angle of attack.
  - OVERFLOW and US3D results show nearly uniform wake pressure variation with angle of attack over the backshell with their amplitude variation of similar magnitude to the ballistic range data.
- F-10.** Shot 40018 backshell pressure measurements at low total angle of attack (i.e., 3 to 7 degrees) showed a wake pressure variation with Mach number that is consistent with


	<b>NASA Engineering and Safety Center Technical Assessment Report</b>	Document #: <b>NESC-RP-14-00965</b>	Version: <b>1.0</b>
Title: <b>Independent Assessment of the Backshell Pressure Field for MEDLI2</b>			Page #: 70 of 74

the Viking-derived base pressure correction used in Mars entry capsule aerodynamic databases.

- F-11.** US3D and OVERFLOW wake pressure predictions at a 20-degree angle of attack show a small but distinct difference (offset) in the near-constant wake pressure.
- F-12.** Ballistic range data and CFD predictions both show evidence of flow attachment on the first backshell cone at large angles of attack (at or near the Mars 2020 trim angle).
  - In the Shot 40023 data, a small pressure deviation was observed near Mach 2.8 between the second backshell cone port and the two first cone ports, which was greatest as the model swept through its peak amplitude.
  - US3D and OVERFLOW predictions of the ballistic range shots indicate flow reattachment on the first backshell cone at or near a 20-degree angle of attack.
- F-13.** US3D predictions at Mars flight conditions support ballistic range data to locate the backshell port on the capsule leeward side.
- F-14.** Small differences were observed between Mars CFD predictions and those run to predict the ballistic range cases. Differences included pressure variations on the second cone on the windward side of the backshell.

## 8.2 Observations

- O-1.** USARL personnel at the Aberdeen Proving Grounds provided outstanding support, analysis, and services in developing a new test technique to achieve the objectives of this effort, including retrieving critical data from Model #2 (Shot 40023) by machining into the model to get physical access to the onboard memory.
- O-2.** Smaller, second-order port-to-port wake pressure measurement variations showed unsteady effects.
- O-3.** The US3D and OVERFLOW did well predicting local surface pressure measurements from the ballistic range test with good agreement. However, when the codes were run in 6-DOF mode for this study, the simulated model trajectories did not match the observed capsule oscillation growth or even the oscillation frequency. Historically, codes predict more dynamic stability than is observed in ballistic range testing, which is consistent with numerical dissipation effects in the wake flows. The integrated effects on capsule dynamics must be incorrect for some unknown reason as the codes fail to replicate the free-flight trajectories recorded in ballistic range testing.

	<b>NASA Engineering and Safety Center Technical Assessment Report</b>	Document #: <b>NESC-RP-14-00965</b>	Version: <b>1.0</b>
Title: <b>Independent Assessment of the Backshell Pressure Field for MEDLI2</b>			Page #: 71 of 74

### 8.3 NESC Recommendations

The following NESC recommendations are directed toward the MEDLI2 project:

- R-1.** CFD and ballistic range data indicate that the mean backshell pressure is best measured on the leeward side of the Mars 2020 entry capsule where surface pressure varies with angle of attack and is close to invariant with location. Therefore, the single backshell port should be located on the second cone on the leeward side of the vehicle. The port should be located at or near the pitch plane of symmetry and at the same radial position as the baseline location (originally on the windward side). This location is in the middle of the desired surface pressure environment, and installation considerations are similar to the baseline location. Any additional deviations in location required for the accommodation of Mars 2020 hardware or systems is acceptable. *(F-9 through F-14)*
- R-2.** Perform additional CFD comparing wake flows for ballistic range and Mars flight conditions to understand the observed differences on the backshell windward side. *(F-14)*

### 9.0 Alternate Viewpoint

There were no alternate viewpoints identified during the course of this assessment by the NESC assessment team.


### 10.0 Other Deliverables

The raw ballistic range data will be delivered to the NRB for dissemination to any party interested in blunt body wake analysis. The data will include the following for each successful shot:

- The raw time, position, and orientation data obtained from the spark-shadowgraphs and chronometer.
- The best-fit 6-DOF trajectory data.
- The pressure history recorded by each transducer.
- Measured mass properties of each model and dimensioned drawings of the model.

### 11.0 Lessons Learned

No applicable lessons learned were identified for entry into the NASA Lessons Learned Information System (LLIS) as a result of this assessment.


	<b>NASA Engineering and Safety Center Technical Assessment Report</b>	Document #: <b>NESC-RP-14-00965</b>	Version: <b>1.0</b>
Title: <b>Independent Assessment of the Backshell Pressure Field for MEDLI2</b>			Page #: 72 of 74

## 12.0 Recommendations for NASA Standards and Specifications

No recommendations for NASA standards and specifications were identified as a result of this assessment.

## 13.0 Definition of Terms


Corrective Actions	Changes to design processes, work instructions, workmanship practices, training, inspections, tests, procedures, specifications, drawings, tools, equipment, facilities, resources, or material that result in preventing, minimizing, or limiting the potential for recurrence of a problem.
Finding	A relevant factual conclusion and/or issue that is within the assessment scope and that the team has rigorously based on data from their independent analyses, tests, inspections, and/or reviews of technical documentation.
Lessons Learned	Knowledge, understanding, or conclusive insight gained by experience that may benefit other current or future NASA programs and projects. The experience may be positive, as in a successful test or mission, or negative, as in a mishap or failure.
Observation	A noteworthy fact, issue, and/or risk, which may not be directly within the assessment scope, but could generate a separate issue or concern if not addressed. Alternatively, an observation can be a positive acknowledgement of a Center/Program/Project/Organization's operational structure, tools, and/or support provided.
Problem	The subject of the independent technical assessment.
Proximate Cause	The event(s) that occurred, including any condition(s) that existed immediately before the undesired outcome, directly resulted in its occurrence and, if eliminated or modified, would have prevented the undesired outcome.
Recommendation	A proposed measurable stakeholder action directly supported by specific Finding(s) and/or Observation(s) that will correct or mitigate an identified issue or risk.
Root Cause	One of multiple factors (events, conditions, or organizational factors) that contributed to or created the proximate cause and subsequent undesired outcome and, if eliminated or modified, would have prevented the undesired outcome. Typically, multiple root causes contribute to an undesired outcome.

	<b>NASA Engineering and Safety Center</b> <b>Technical Assessment Report</b>	Document #: <b>NESC-RP-14-00965</b>	Version: <b>1.0</b>
Title: <b>Independent Assessment of the Backshell Pressure Field for MEDLI2</b>			Page #: 73 of 74

**Supporting Narrative** A paragraph, or section, in an NESC final report that provides the detailed explanation of a succinctly worded finding or observation. For example, the logical deduction that led to a finding or observation; descriptions of assumptions, exceptions, clarifications, and boundary conditions. Avoid squeezing all of this information into a finding or observation

## 14.0 Acronym List

$\alpha$	Angle of Attack
$\alpha_{trim}$	Supersonic Trim Angle
$\beta$	Sideslip Angle
$C_A$	Axial Force Coefficient
$C_m$	Pitching Moment Coefficient
$C_p$	Pressure Coefficient, $(p-p_\infty)/q_\infty$
$p$	Pressure
$p_\infty$	Free-stream (ambient) Pressure
$q$	Body Pitch Rate
$q_\infty$	Dynamic Pressure
$\mu s$	microsecond
AMA	Analytical Mechanics Associates
ARC	Ames Research Center
CAD	Computer-aided Design
CFD	Computational Fluid Dynamics
CFL	Courant–Friedrichs–Lewy
CG	Center of Gravity
CGT	Chimera Grid Tools
DCF	Domain Connectivity Function
DES	Detached Eddy Simulation
DOF	Degree of Freedom
Hg	Mercury
Hz	hertz
IMU	Inertial Measurement Unit
JPL	Jet Propulsion Laboratory
kg	kilogram
kHz	kilohertz
LaRC	Langley Research Center
m	meter
MEADS	Mars Entry Air Data System
MEDLI2	Mars Entry, Descent, and Landing Instrumentation 2
MER	Mars Exploration Rover
mm	millimeter

	<b>NASA Engineering and Safety Center Technical Assessment Report</b>	Document #: <b>NESC-RP- 14-00965</b>	Version: <b>1.0</b>
Title: <b>Independent Assessment of the Backshell Pressure Field for MEDLI2</b>			Page #: 74 of 74

MOI	Moment of Inertia
m/s	meters per second
MSL	Mars Science Laboratory
MTSO	Management and Technical Support Office
NESC	NASA Engineering and Safety Center
NGC	Northrop Grumman Corporation
NIO	NESC Integration Office
OBR	Onboard Recorder
OML	Outer Mold Line
Pa	Pascal
PCC	Parachute Closeout Cone
psi	pounds per square inch
QA	Quality Assurance
s	second
SI	International System of Units
TEF	Transonic Experimental Facility
USARL	United States Army Research Laboratory
V&V	Verification and Validation

## 15.0 References

1. Schoenenberger, M., Van Norman, J., Karlgaard, C., Kutty, P., and Way, D., "Assessment of the Reconstructed Aerodynamics of the Mars Science Laboratory Entry Vehicle," *Journal of Spacecraft and Rockets*, Vol. 51, No. 4, 2014, pp. 1076–1093.
2. Schoenenberger, M., Hathaway, W., Yates, L., and Desai, P., "Ballistic Range Testing of the Mars Exploration Rover Entry Capsule," AIAA 2005-0055, January 2005.
3. Schoenenberger, M., Yates, L., and Hathaway, W., "Dynamic Stability Testing of the Mars Science Laboratory Entry Capsule," AIAA 2009-3917, 2009.
4. Dyakonov, A. A., Schoenenberger, M., and Van Norman, J. W., "Hypersonic and Supersonic Static Aerodynamics of Mars Science Laboratory Entry Vehicle," AIAA 2012-2999, 2012.
5. Stern, E., Schwing, A., Brock, J., and Schoenenberger, M., "Dynamic CFD Simulations of the MEADS II Ballistic Range Test Model," AIAA 2016-3243, 2016.

## 16.0 Appendices (separate volume)

- Appendix A. Technical Drawings for Ballistic Range Models and Uninstrumented Rounds  
Appendix B. Predicting Swerve of Blunt Body Ballistic Range Models with Small CG Offsets



REPORT DOCUMENTATION PAGE					Form Approved OMB No. 0704-0188	
<p>The public reporting burden for this collection of information is estimated to average 1 hour per response, including the time for reviewing instructions, searching existing data sources, gathering and maintaining the data needed, and completing and reviewing the collection of information. Send comments regarding this burden estimate or any other aspect of this collection of information, including suggestions for reducing the burden, to Department of Defense, Washington Headquarters Services, Directorate for Information Operations and Reports (0704-0188), 1215 Jefferson Davis Highway, Suite 1204, Arlington, VA 22202-4302. Respondents should be aware that notwithstanding any other provision of law, no person shall be subject to any penalty for failing to comply with a collection of information if it does not display a currently valid OMB control number.</p> <p><b>PLEASE DO NOT RETURN YOUR FORM TO THE ABOVE ADDRESS.</b></p>						
1. REPORT DATE (DD-MM-YYYY) 09/18/2017		2. REPORT TYPE Technical Memorandum			3. DATES COVERED (From - To)	
4. TITLE AND SUBTITLE Independent Assessment of the Backshell Pressure Field for Mars Entry, Descent, and Landing Instrumentation 2 (MEDLI2)				5a. CONTRACT NUMBER		
				5b. GRANT NUMBER		
				5c. PROGRAM ELEMENT NUMBER		
6. AUTHOR(S) Prince, Jill L.; Schoenenberger, Mark				5d. PROJECT NUMBER		
				5e. TASK NUMBER		
				5f. WORK UNIT NUMBER 869021.05.07.05.36		
7. PERFORMING ORGANIZATION NAME(S) AND ADDRESS(ES) NASA Langley Research Center Hampton, VA 23681-2199				8. PERFORMING ORGANIZATION REPORT NUMBER L-20877 NESC-RP-14-00965		
9. SPONSORING/MONITORING AGENCY NAME(S) AND ADDRESS(ES) National Aeronautics and Space Administration Washington, DC 20546-0001				10. SPONSOR/MONITOR'S ACRONYM(S) NASA		
				11. SPONSOR/MONITOR'S REPORT NUMBER(S) NASA/TM-2017-219666/Vol. I		
12. DISTRIBUTION/AVAILABILITY STATEMENT Unclassified - Unlimited Subject Category 16 Space Transportation and Safety Availability: NASA STI Program (757) 864-9658						
13. SUPPLEMENTARY NOTES						
14. ABSTRACT The Mars Entry, Descent, and Landing Instrumentation 2 (MEDLI2) project requested that the NASA Engineering and Safety Center (NESC) support a ballistic range test to measure backshell pressures on scale models of the Mars 2020 entry capsule. The MEDLI2 project needed the test to provide important dynamic pressure data to help select a backshell pressure port, quantify drag coefficient reconstruction uncertainties, and design the data acquisition hardware. This document contains the outcome of the NESC assessment.						
15. SUBJECT TERMS MEDLI2; NASA Engineering and Safety Center; Backshell Pressure; Mars 2020 entry capsule; Computational fluid dynamics						
16. SECURITY CLASSIFICATION OF:			17. LIMITATION OF ABSTRACT	18. NUMBER OF PAGES	19a. NAME OF RESPONSIBLE PERSON	
a. REPORT	b. ABSTRACT	c. THIS PAGE			STI Help Desk (email: help@sti.nasa.gov)	
U	U	U	UU	79	19b. TELEPHONE NUMBER (Include area code) (443) 757-5802	